Mechanically Storing Renewable Energy
at a Residential Scale

Integrated Product Design

Master Thesis by Stefan Lorist

Amstel Engineering

TU Delft

August 2019

Mechanically Storing Renewable Energy
at a Residential Scale

Stefan Henrico Lorist
stefanlorist@gmail.com
+31 6 83350531

Master Thesis, MSc Integrated Product Design
Faculty of Industrial Design Engineering
Delft University of Technology
Landbergstraat 5
2628 CE Delft

Supervisors
Dr. Ir. S.F.J. Flipsen
Ir. E.W. Thomassen

Amstel Engineering

TU Delft

Preface

This project was the final assessment of the master's degree Integrated Product Design, at the faculty of Industrial Design Engineering of the TU Delft. The graduation assignment is used to show my ability to run a design project individually. Being able to complete a project in a way that both the process and the final result are satisfactory to the company, is what I like to achieve when I finalize my studies. My skills as an Integrated Product designer are determined by the ability to conduct sufficient research and to apply this during the design process, resulting in a feasible product.

During the past years of studying and traveling, I have seen the world in all its beauty, but also its misery. Being a designer might offer me a chance to improve the bad things. In my opinion, contributing to a better world can be done by increasing awareness of social and environmental aspects in life. On the other hand, a better world is a place where people have all products they need to make it pleasant. This could include any product, from health care to pure luxury.
My bachelor's degree in Mechanical Engineering has taught me the technical skills needed to understand most practical phenomena, whereas a master's degree in Industrial Design Engineering provides me with the methods for concept development as well as embodiment into a feasible product.
The subject of this graduation assignment therefore suits my interests very well and has allowed me to work on something that, in my opinion, can really make a difference.

Requiring full focus and an extensive amount of energy, finally resulting in a satisfactory result, this project has been a worthy conclusion of my University studies.

Besides my personal efforts, I have been helped by a number of very nice and inspiring people.

I would like to thank my supervisory team, consisting of Bas Flipsen and Erik Thomassen, who have always provided me with useful insights during meetings. After leaving their office, it often felt like I was given a push in the right direction. Sometimes this was confirming the direction I was already heading, sometimes a stronger correction needed to be given.

At Amstel Engineering, both Robert de Graaff and Niels Defize have shown continuous interest in everything I was doing. There has been endless enthusiasm, from the small discoveries to the final result. I have always felt appreciated, even when their ideas were slightly different from mine. Eventually, I think we have been working towards a great outcome. Thank you for allowing me to work of this project, and supporting me this well.

I am grateful to my friends and roommates for listening to my endless considerations of every single step in the process. My girlfriend Lisa has been the best in supporting me through good and bad times, and my parents have been a source of comfort. Thank you all!

I am hoping this thesis will give you an idea of all the work I have done, and convince you of the effect it might have.

Stefan Lorist

LEFt

Leftover **E**nergy **F**lywheel **t**echnology
by **Amstel** Engineering

Executive summary

Today, more and more households are generating their own solar power. This helps us to come closer to a circular economy, since less fossil fuels are required to meet our energy needs. However, excessively generated energy is often wasted, since transporting or storing it for later use is challenging. Lithium ion batteries provide a solution, however their short lifespan and environmental problems that are caused during production make them far from green.

A mechanical storage system was proposed, minimizing the environmental problems of Li-ion while providing the household with a storage solution for excessively generated solar energy.

After exploring multiple energy storage methods and analyzing their potential suitability to residential energy supply & demand, Flywheel Energy Storage was chosen as the applied storage technology due to its high energy density and mainly mechanical components.

Script

Essential calculations were extended into a full simulation script, used to analyze different scenarios of use. It is capable of the following:

- Confirming chosen rotor dimensions
- Determining required rotational speed
- Characterization of rotor losses & spin-down times
- Characterization of torque losses
- Reading supply/demand data from external source
- Visualizing 24h supply/demand/storage profile

Prototype

The script was partially validated using a functional model and performing tests concerning spin-down times with two different rotors and vacuum levels.

LEFt

As a final deliverable, a full mechanical storage system was designed. LEFt, which stands for *Leftover Energy Flywheel technology*, is a mechanical battery that stores an excess of residential solar power in the form of kinetic energy by spinning a flywheel in a vacuum. It comes in three main form factors; Flat, Slender and Extra Slender. These types all suit different scenarios and therefore different households.

LEFt was designed using a subsystem approach to cope with all co-dependent aspects of the system. The most essential part, the flywheel rotor, was dimensioned according to the script.

Rotor

Different versions of LEFt include differently dimensioned rotors. A large height over radius ratio makes LEFt suitable for short term storage. It can be applied to store electricity that is generated during the afternoon for evening use.
Changing the application and storage limit result in different configurations and dimensions. A rotor with a small height over radius ratio can be suitable for longer term storage. A setup with a certain supply & demand makes this type potentially capable of 24h storage and might allow off-the-grid living in the future.

Suspension

The flywheel rotor is suspended nearly frictionless in the vacuum, by levitating it using a magnetic bearing system. The main vertical thrust is supplied by a Halbach Array of passive magnets, whereas radial displacement is corrected by two Active Magnetic Bearings that are handled by an advanced control system.

Motor/Generator

Driving the rotor and regenerating electricity is done by one machine; an electric motor that is positioned outside the vacuum. Using a single phase motor allows easy installation without the need for a transformer.

Magnetic coupler

To drive the rotor from outside the vacuum, a magnetic coupler was designed, making use of two discs with a pattern of passive magnets. A control system allows smart coupling and decoupling, resulting in a freely spinning rotor in idle situations.

Vacuum housing

Enclosing the flywheel rotor is done by a depressurized housing. This has proven to reduce resistances, increasing storage times and therefore the applicability to longer term storage.

Market implementation

Selling LEFt is done best by a lease plan, in collaboration with solar panel suppliers. The full retail price of over €10,000 will be too high for a one-time investment.

Sustainability assessment

The environmental impact of the design is done by comparing it to a competing lithium ion battery. The results of an Eco Audit show that the impact of LEFt is lower, but still significant because of the large amounts of steel that are needed.

Conclusion

A conceptual design for a flywheel energy storage system was proposed and partially validated. It was concluded to be a better alternative for lithium ion batteries in residential energy storage, since it minimizes social and environmental problems.
Further development and extensive analysis is required to fully validate and make the design ready for production.

Appendix Contents

Appendix A. Methods of Energy Storage (continued) 90

Appendix B. List of Requirements 98

Appendix C. Matlab Script FlywheelCalc 100

Appendix D. Morphological Chart 114

Appendix E. Technical Drawings Prototype 116

Appendix F. Cover Design Sketches 122

Appendix G. Cost Price Calculation 124

Appendix H. Bill of Materials 126

Appendix I. Sustainability Assessment 128

Appendix J. Project Brief 132

Contents

Executive Summary 7

Project Structure 10

1. Explorative analysis: Context 13

1.1 Context 14
- *1.1.1. Problem statement* 15
- *1.1.2. Issued assignment* 16
- *1.1.3. Scope* 17
- *1.1.4. Sustainable Storage* 18

1.2 Energy Supply & Demand 20
- *1.2.1. Supply data* 20
- *1.2.2. Demand data* 21
- *1.2.3. System power* 21

1.3 Methods for Energy Storage 22
- *1.3.1. Methods overview* 22
- *1.3.2. Rating by multiple aspects* 22

1.4 Choice of Storage Method 24
- *1.4.1. Rough comparison* 24
- *1.4.2. Narrowed down selection* 25
- *1.4.3. Harris Profile* 26

2. Technology Driven Design 29

2.1 Technical System Design 30
- *2.1.1. FESS characteristics* 30
- *2.1.2. Subsystems approach* 31

2.2 Subsystem Solutions 32
- *2.2.1. Subsystems overview* 32
- *2.2.2. Subsystem 1: Rotor* 33
- *2.2.3. Subsystem 2: Suspension* 35
- *2.2.4. Subsystem 3: Motor/Generator* 36
- *2.2.5. Subsystem 4: Housing* 37

2.3 Potential Systems 38

3. Embodiment 41

3.1 Technical Concept 42
- *3.1.1. Requirements* 42
- *3.1.2. Cross-influence of subsystems* 42
- *3.1.3. Multi-rotor advantage* 42
- *3.1.4. Rotor dimensions* 44
- *3.1.5. Validation of calculations* 45
- *3.1.6. Peak storage capabilities* 46

3.2 Scenario simulation; Embodiment phase I 48
- *3.2.1. Average daily energy profile* 48
- *3.2.2. Required vs available energy* 49
- *3.2.3. Scenario specific optimization* 50
- *3.2.4. Types of households* 50

3.3 Prototyping & validation; Embodiment phase II 52
- *3.3.1. Goal of the prototype* 52
- *3.3.2. Bearings* 52
- *3.3.3. Magnetic drive* 53
- *3.3.4. Vacuum: Scaling effects* 53
- *3.3.5. Structure of the model* 54
- *3.3.7. Unforeseen effects* 55
- *3.3.6. Validation* 56
- *3.3.8. Limitations by equipment* 59

4. Final Design 61

4.1 Final Design 62
- *4.1.1. Household applicability* 62
- *4.1.2. Communication to the user* 62
- *4.1.3. Components* 64
- *4.1.4. Technology readiness levels* 66
- *4.1.5. Number of rotors* 67

4.2 Market Strategy 68
- *4.2.1. LEFt configurator* 68
- *4.2.2. Cost & retail price* 70
- *4.2.3. Collaboration* 71

4.3 Sustainability Assessment 72
- *4.3.1. Li-ion problems* 72
- *4.3.2. Environmental impact* 74
- *4.3.3. Recommendations to design* 74
- *4.3.4. Eco Audit* 74
- *4.3.5. Uncertainties in analysis* 75

5. Conclusion, Recommendations & Reflection 77

5.1 Conclusion 78
- *5.1.1. Evaluation of requirements* 78
- *5.1.2. Overall design conclusion* 79
- *5.1.3. Adjusted requirements* 79
- *5.1.4. Answering research questions* 79

5.2 Recommendations 80
- *5.2.1. Development of subsystems* 80
- *5.2.2. Script & prototype* 81
- *5.2.3. Regeneration of electricity* 81
- *5.2.4. Future vision* 81

5.3 Personal Reflection 82
- *5.3.1. Project structure* 82
- *5.3.2. Mechanical vs Design* 82

References 86

Appendix 90

Project Structure

Before you start reading this thesis, the project structure is clarified on these pages. Throughout the document, references will be made to the steps in this design process that are taken.

1. Explorative analysis; context

Why was this project started? What is sustainable energy storage? Which methods exist and how can one of these be used at residential scale? These are questions that are answered in the first part of this thesis. This first phase is concluded with a choice of technology and sets the basis for further design.

2. Technology driven design

Before diving further into the embodiment phase, various possibilities for the system's technical specifications were explored. To get a clear overview of the parts to be taken into account, the system is split up into subsystems, which are then separately analyzed.

Subsystem design approach

Designing a Flywheel Energy Storage system is complicated, especially in terms of the influences between subsystems. Therefore, different solutions for each of the defined subsystem are evaluated and combined into technological solutions.

3. Embodiment

This phase of the project was split up in two, since these are parallel processes that have been done to get to a final result.

Simulation

In the first place, the most desirable technical product details were chosen by using the knowledge of and implementing this in a set of calculations; a Matlab-script. Thereafter, relevant scenarios are analyzed to test applicability of the system in various contexts.

Prototyping

Validation of the calculated flywheel behavior was done using a functional model; a prototype which is suitable for testing key functional features of the Matlab-script.

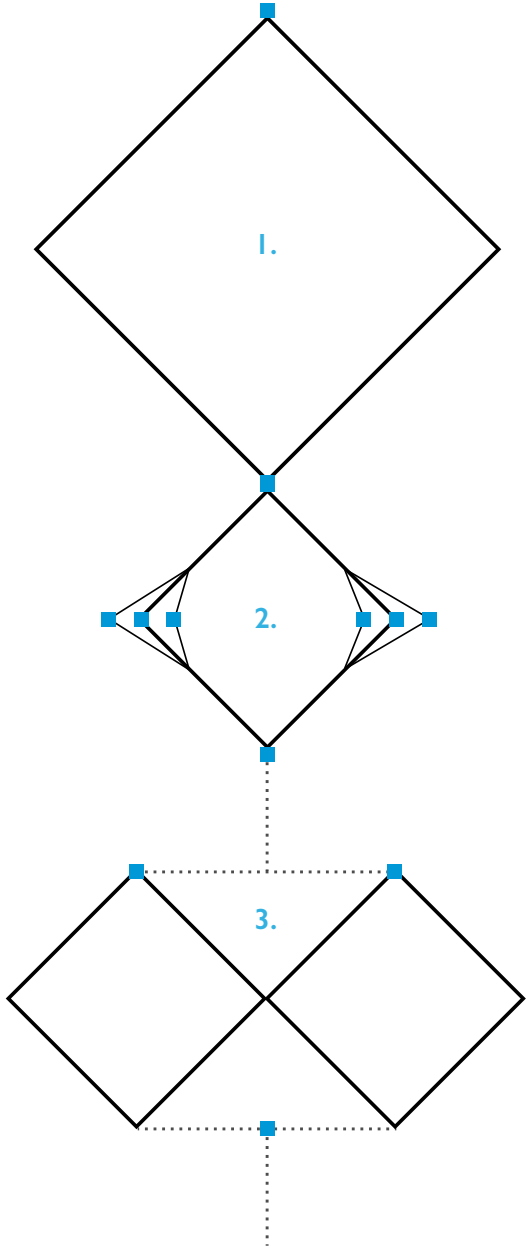

Figure 1: Diamond visualization of the project structure*

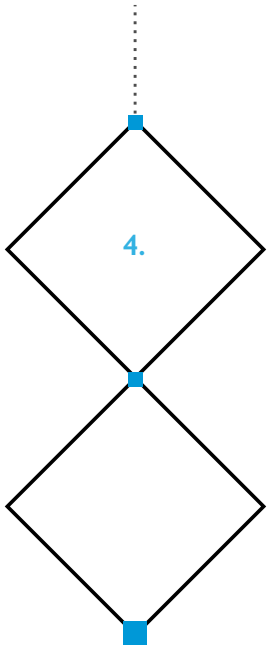

*Figure 1 displays the project structure in a visual way. It is used to show where the study is diverging and converging. Two diamonds show that some aspects of the project were done in parallel.

4. Final design

Combining all knowledge into a finished product that can be placed within the context. It is provided with visualizations of the product and context and a description of the product's configuration.

User-specific market positioning

Energy supply and demand varies significantly among households, this is why the design of the final product was aimed to be user-specific. This part is concluded with the design of a system configurator.

Cost- and sustainability analysis

Determining the feasibility of the concept requires a cost analysis, which resulted in a consumer price and market plan. In addition, to check whether the goal of reducing impact has been achieved, the sustainability of the concept was analyzed.

5. Conclusion & Recommendations

The concluding remarks for this design project, followed by recommendations for the related projects to come.

A. Appendix

Additional in-depth information to what is told in the main report can be found in the appendix.

Quick referencing

While reading this thesis, the phase of the project can always be referenced with the colored tab on the right hand side of the right page.
For digital readers: click to navigate!

Figure 2: Solar panel placement in the Netherlands. More and more households are generating their own renewable energy. (NOS, 2018)[1]

1. Explorative analysis: Context

Why was this project started? What is sustainable energy storage? Which methods exist and how can one of these be used at residential scale? These are questions that are answered in the first part of this thesis. This first phase is concluded with a choice of technology and sets the basis for further design.

1.1 Context

Vision

The world is a beautiful place, but studies have shown that we as its inhabitants are not treating it very well. With the ever-increasing population, technological developments and product oriented way of life, we are causing a level of pollution that is already resulting in serious health risks in some cities. People love to live a luxurious life, and as an industrial designer I like to support that. However, one should keep in mind the pitfalls. Fortunately, the awareness of consumption is a rising trend. Ecological food is available in more and more supermarkets and eco-labels for products and houses are becoming normal. Additionally, an increasing number of people provide their house with solar panels and generate a significant part of their energy in a sustainable way. All together, the perception of sustainable behavior is changing in a good way.

During the many projects at TU Delft, my interest for sustainability has increased to a level that is even higher than it was before. It occurred to me that I could really make a difference when implementing my sustainable vision in any kind of project.

Mission

With the increasing awareness and urge to change our electricity generation in an even more sustainable direction, I think interesting steps can be made at consumer level. Since individuals already invest in their own set of solar panels, there will be interest for an increase in efficiency. It is widely known that financial benefits increase motivation to undertake action, hence the increase of solar panels installed after introduction of subsidies. Additionally, net metering can drive down the energy bill and therefore looks more and more attractive to the average consumer.

The biggest downside is that the power net cannot store energy in any way, resulting in a loss of generated energy on sunny days. On cloudier days, which occur quite often in the Netherlands, the amount of solar energy that is generated is insufficient for powering the household.
Amstel Engineering has presented their capabilities and knowledge of electricity storage solutions in previous projects. A method to store electrical energy that makes use of compressed air has been conceptualized and delivered promising results. Combining this knowledge and drive for improvement with my personal vision, supported by the expertise of the Department of Design Engineering and the Section Design for Sustainability of the TU Delft, a difference can be made.

Goal

My ultimate goal for this project is the development of a high efficiency mechanical battery for household use, which will be sold alongside a set of solar panels. The system should avoid any unnecessary political, social and ecological impact. Making it the standard solution for households where a significant amount of electricity is lost because it is not being used immediately.

The final goal is to design a system that can compete with Tesla's Powerwall (introduced later in this thesis), being the sustainable alternative for storing electrical energy in households.
The envisioned final deliverable of the project is to develop a concept that consists of a detailed 3D model, a prototype that demonstrates the working principle and a product vision for implementation in the market.

1.1.1. Problem statement

In the Netherlands, generating energy is transitioning from fossil fuels towards sustainable sources. This transition has become a research topic that is gaining interest. Generation of sustainable energy has been developed for many years and will definitely continue in the foreseeable future.

With interesting tax benefits for placing photo-voltaic panels to one's home, the government successfully stimulated a large number of people choose to generate their own energy in this promising way.

In most areas in the Netherlands, the power grid is a trustworthy source of energy. Power cuts have been minimized and virtually everyone is connected.

However, there is no standard solution when it comes to the excess of renewable energy that is generated, particularly because of weather conditions. Strong winds are beneficial for windmills and sunny days result in more solar power being generated. Weather conditions can be forecast very well, making it possible to accurately determine when electricity can be generated from a renewable resource like the sun (Blanc et al., 2017)[2]. Unfortunately, supply and demand cannot be synchronized continuously. This is where losses occur and interesting possibilities arise. It causes the requirement of fossil power plants to produce the amount of energy that is utilized during the periods when renewable electricity is insufficient.

The excess of energy that is generated using residential solar panels can be fed back to the grid, resulting in a discount on the energy bill. Net metering, 'Salderen' in Dutch, as this is called, allows consumers who generate their own electricity to use it anytime, compared to only using it at the moment it is generated (Dutch Government, 1998)[3] . As the power grid does not have any possibilities for storing electricity, this is not entirely true. Net metering only transfers the electricity to another place where it is used immediately.

A number of companies have noticed this and have started developing storage systems for electric energy. Electric car company Tesla has developed the Powerwall (Tesla, 2019)[4] , which is a 13.5 KWh lithium ion battery providing a household with nearly two days' worth of electricity. The Powerwall is displayed in Figure 4.

Unfortunately, production of this type of batteries causes high emissions, and disposal is polluting since only limited recycling is possible (U.S. EPA, 2013)[5] . Political, social and ecological problems are being involved with mining certain materials like lithium. Certain lithium compounds are carcinogenic and teratogenic (Granta Design Limited, 2018)[6] and can cause health problems while handled. Socio-political instability of a country could disrupt supply of these materials (Olivetti et al., 2017)[7] , and classification as "critical material" of lithium and graphite (Erdmann & Graedel, 2011)[8] is concerning for continuity of production.

Methods like flywheels, redox flow batteries, saltwater storage and some other methods look promising (International Electrotechnical Commission, 2011)[9] , but none of these have resulted in a product that can be compared in terms of capacity and efficiency to a lithium ion battery pack (Chen et al., 2009)[10] and therefore are not ready to be used for storing electricity at a residential scale.

Figure 3: Pollution in the Kennemer Dunes, Holland.

Figure 4: Tesla Powerwall.
(Tesla, 2019)[12]

1.1.2. Issued assignment

Amstel Engineering BV, which is based in Amsterdam, is a multidisciplinary engineering company that works on end-to-end engineering projects and describes itself as "Engineers with passion for technology". Ideas around the topic of sustainability are taken very seriously and have already resulted in issuing an earlier graduation project for developing an energy storage system. To develop their sustainable vision, formulated as "upgrading the world by connecting the dots"[11] , into a feasible product for energy storage.

In Figure 5, the concept for a Compressed Air Energy Storage system is displayed. This system was developed by a previous graduation student at Amstel Engineering. Although the concept was promising, the company requested to take a step back, the system will be considered as an alternative for energy storage. Creating an overview of all potential methods for energy storage will be the starting point for this project, followed by the selection process that also considers the result of the previous graduation project.

The Project Brief, which can be found in Appendix J, describes the agreements that were made between me, the supervisory team and the company Amstel Engineering BV, before starting the project.

Figure 5: Compressed Air Energy Storage Concept.
(Amstel Engineering BV, 2018)[12]

1.1.3. Scope

Comparing different methods will be most useful after the scope has been set. The prospected use of a Dutch household in 2025 has been studied by Dobber (2018) and is estimated at 4800 kWh per year, which comes down to an average of 13.2 kWh per day. Considering the design goal of storing an amount of electrical energy which is equivalent to a household's use for one full day, the system should be able to store a minimum of 13.2 kWh of electricity. If the goal would be adjusted to be capable of peak shaving only, measurements and trend calculations have shown that a capacity of 7.7 kWh will be sufficient. Peak shaving is the process of storing electricity peaks for a short period, to be used soon after this period.
These capacities were determined for the average relatively sunny day, where the only period during which no solar power is being generated is nighttime. When considering a photovoltaic installation with a 2.087 kiloWatt peak generation, Dobber (2018) calculated the system should be able to store a maximum peak power of 1.733 kW.

This study will focus on finding the optimal storage method for a household with the described supply and demand. A consumer product will be designed with user experience kept in mind, but this part of the process will only start after the technological solution has been found and specified.

A broad scope was chosen for creation of the first overview of methods, but application to households was kept in mind. The system should be suitable for placement in a standard sized garage/storage room of 5 x 3 x 2.5 m. A full list of requirements was set up later and is availabel in Appendix B.

Lastly, for the scope of this project, focus lies on a mechanical solution. Amstel Engineering BV has been specialized in machine building and therefore a system that works mechanically rather than chemically or electrically is best suitable. The last rating is therefore called "AE suitability", and has been determined in discussion with employees of Amstel Engineering BV.

Conclusion

Considering the current state-of-the-art of sustainable storage and combining this with the analysis that was previously done at Amstel Engineering, the scope for the project has been set. From this, the two questions displayed below have arisen, these will be answered at the end of this project.

Can mechanical battery be a feasible alternative to lithium ion batteries, when using it to store an excess of sustainably generated energy, within the house?

&

How can an energy storage system be designed, that is suitable to the company Amstel Engineering BV and their expertise?

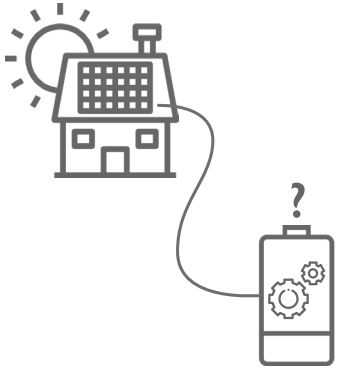

Amstel Engineering

1.1.4. Sustainable Storage

Off-peak electricity storage is gaining interest, which is driven by the fact that the use of renewable energy has been increasing over the past years (Aneke & Wang, 2016)[13] . It is widely known that certain types of sustainable energy are only generated in good weather conditions. While development of these types of electricity generation continues, optimization of every step of the process comes into play. Decades ago, the first energy storage plants have been built (Meyer, 2007)[14] , but only since fairly recently this development gained popularity. Startups building flywheels with the purpose of peak shaving (Amber Kinetics, 2019)[15] , liquid air energy storage plants to convert air from its gas to its liquid phase are amongst the past decade's advancements. Even institutions that are known for their use of fossil fuels like the Dutch Oil Company (NAM) are starting to show their engagement in sustainable technologies. A large challenge that was organized by NAM, the NAM70, recently rewarded €50,000 to an initiative by Storelectric (NAM, 2018)[16] . This company has been working on a compressed air energy storage plant and is looking to install one in the Netherlands.

Currently, a small number of power plants like wind farms are implementing off-peak storage systems. A large scale Compressed Air Energy Storage, which can deliver up to 290 MW over two hours, has been installed over 40 years ago in Huntorf, Germany and is still operational. (Meyer, 2007) Another system making use of this method is being utilized in McIntosh, USA. (Budt et al., 2016)[17]

Despite the promising efficiency and no use of fossil fuels, these are currently amongst the few plants that are currently active. The technology looks promising, but still only a handful of concrete plans exist that are seriously considering the possibility of using it. (Budt et al., 2016)

As mentioned before, over the past decade methods for storing electrical energy have kept developing and many promising alternatives have been studied. Most of these are applicable to large scale power plants, but might also be interesting for application to residential scale electricity generation, which makes it especially interesting for this project. Residential storage has gained interest over the years since more households have their own solar panels installed. Combining the home power plant with grid power and a battery requires a system similar to the one sketched by CleanTechnica[18] in Figure 6.

In chapter 1.4, the most promising methods is chosen. An overview and classification of conventional, as well as state-of-the-art methods has been made by Amstel Engineering before starting the current project (Dobber, 2018)[19]. This analysis of the many available energy storage methods was used as a starting point and extended by reading research papers and articles to build the comparison visualization on page 25.

The design of a storage solution will start after a well-founded comparison has helped choosing the method that is best applicable.

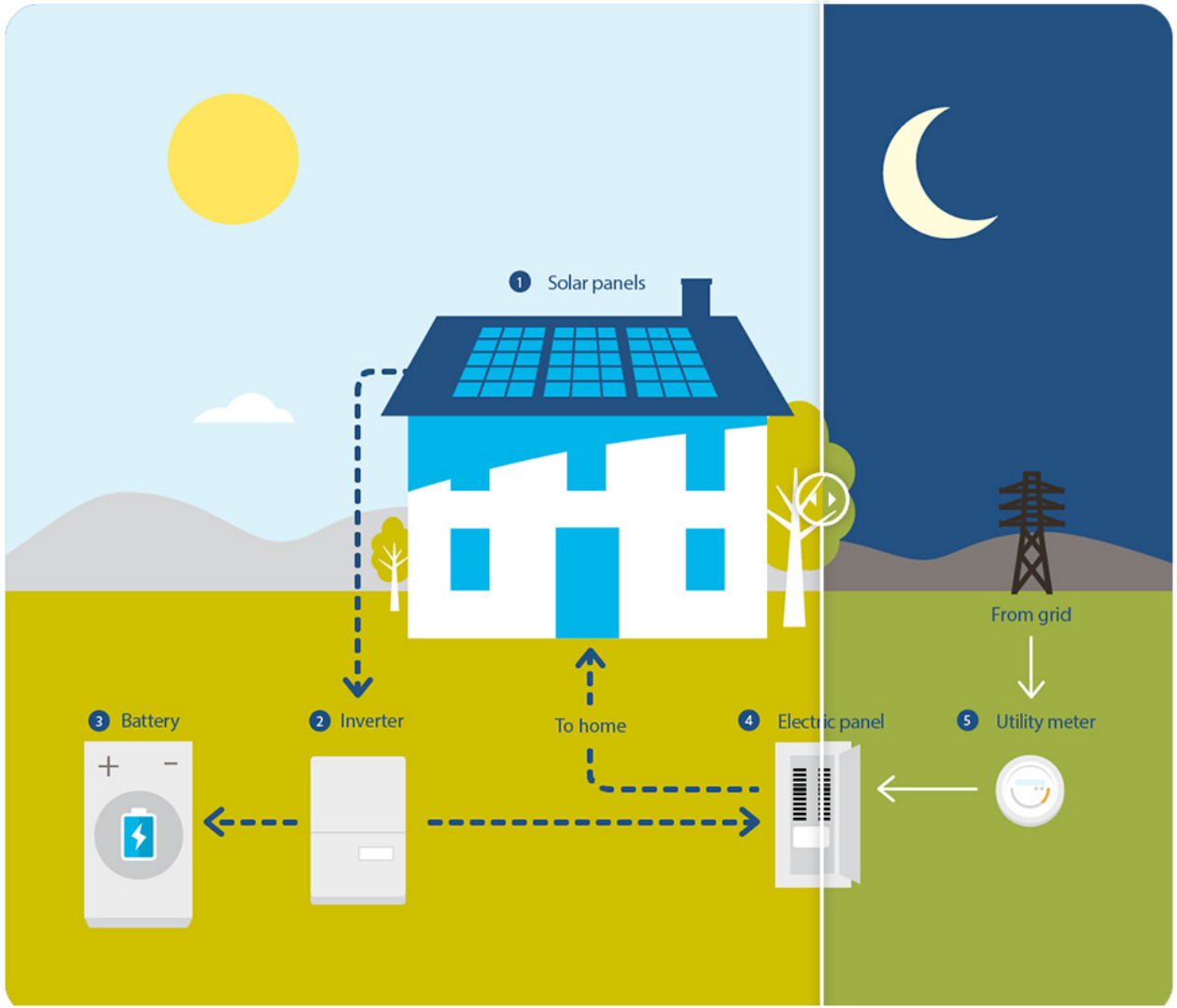

Figure 6: Residential Energy Storage (CleanTechnica, 2019)

1.2 Energy Supply & Demand

Introduction

Defining when energy is generated and when it should be available to the household, is essential when designing a storage system. Not only is the system required to have electric power available to the user, a storage system is only efficient when it is able to store solar energy whenever an excess is generated. Therefore, multiple scenarios of use are created. The graphs in this chapter are the two main scenarios that were plotted in Matlab and used later in this study for further design of the storage system.

1.2.1. Supply data

Solar power is a valuable, but unpredictable source of renewable energy. Bad weather conditions and on the other hand sunny days deliver an irregular day-to-day supply. In the requirements (Appendix B) was stated that a system should be capable of storing energy and supplying the household purely by solar power during a period of 24 hours. In Figure 7, the power (in kW) that is supplied by a set of solar panels during 24 hours of an average summer day in the Netherlands is displayed by the yellow line. The source data that was used was obtained from the Royal Netherlands Meteorological Institute (KNMI), and was given as solar power in Watts per square meter (W/m^2)[20]. Using the conversion factor

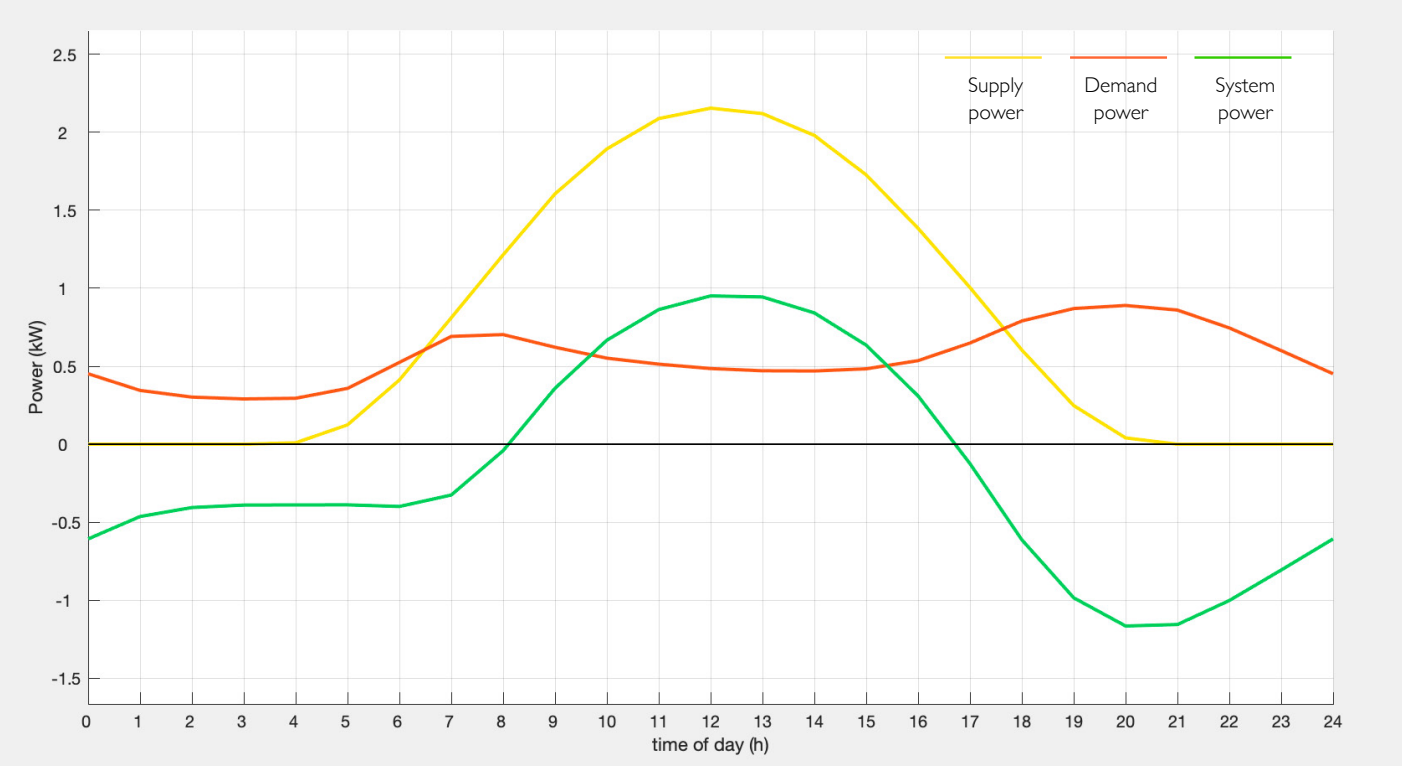

Figure 7: Supply, Demand and System power, during an average day of summer in the Netherlands.

for a commonly used type of solar panel, the JAM6 60-250 (JA Solar, 2019)[21] and a commonly used setup of 14 panels, the supply data was used for further calculations.

1.2.2. Demand data

The prospected daily household use for 2025 was estimated by Dobber (2018) at 13.5 kWh. This was spread over 24 hours using a demand profile that did not seem very trustworthy, since peaks seemed to occur at illogical times during the day. Therefore, demand data was obtained from an average household in the United States of America, in New York City (U.S. Department of Energy, 2013)[22] . The openly available measurement data shows a clear increase of the demand in the morning, when the average person wakes up and gets ready for the day. Since the majority of people works away from home, the demand drops and stays near constant for a few hours. At the time when people start coming home from work, demand increases and reaches a new peak in the beginning of the evening.
The values of this demand data were scaled to meet the estimated total of 13.5 kWh per 24 hours, and plotted as the red line in Figure 7.

1.2.3. System power

Subtracting the household's demand from the available solar power results in the power that can be seen as the storage/regeneration power of the system.

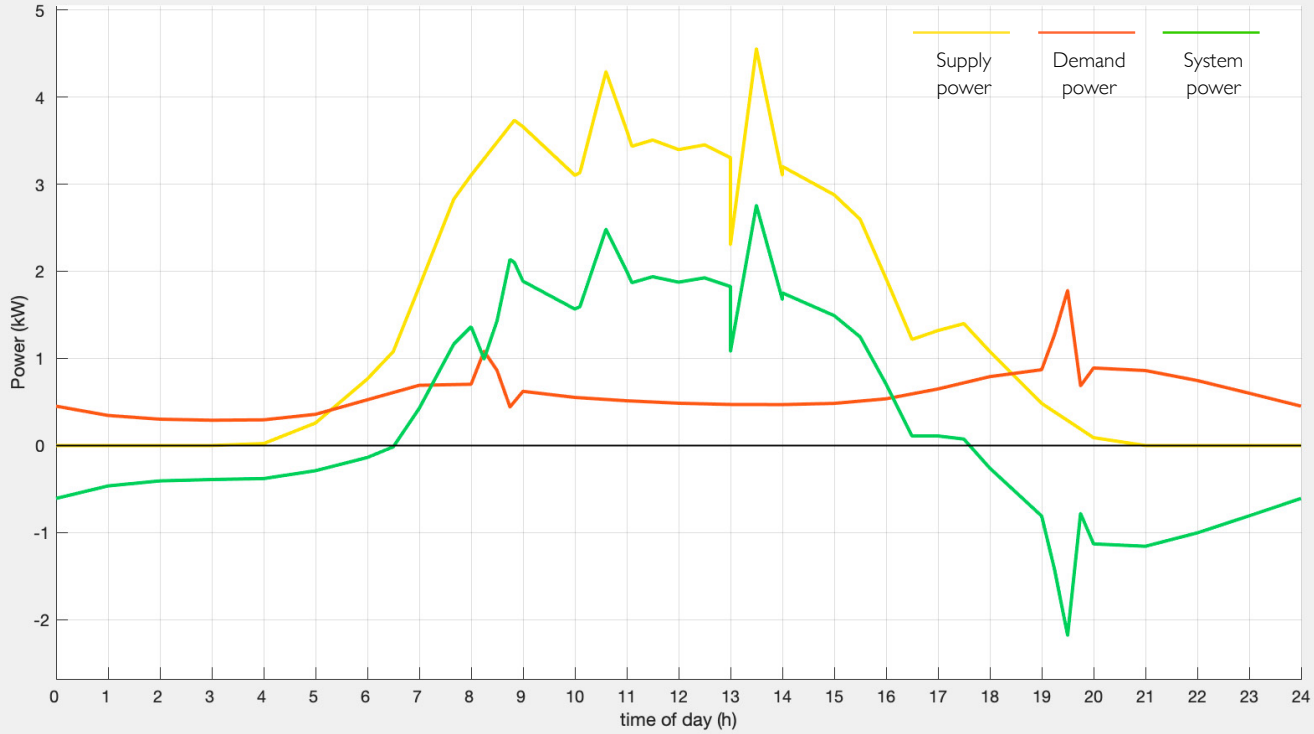

Figure 8: Supply, Demand and System power, during a nice day of summer in the Netherlands including peak power.

In Figure 7, the green line shows that the maximum power the system should be capable of storing lies close to 1 kW (between 12:00h and 13:00h), whereas the maximum regeneration power lies around 1.2 kW (between 20:00h and 21:00h). The latter is shown as negative, since the storage system is delivering power.

Supply & demand peaks

Simulations that are representative for real world use should not only contain average data. The system should be designed in a way that works for the average scenario, but it should not fail when the workload becomes somewhat more extreme. According to user data from the application "Solar portal" by SMA Solar Technology (2019)[23], occasional peaks were generated in the solar power supply curve. These highs and lows represent fluctuations caused by clouds that can block the sunlight, but also move away and cause direct exposure.
Peaks in energy demand were simulated according to a more extreme user scenario, where for instance kitchen appliances are switched on at some points during the day.
In case the system needs to work with the described peaks in supply and demand, the storage/regeneration profile is visualized as the green line in Figure 8.

Conclusion

Different supply & demand profiles result in different storage needs. The various storage methods that are available are capable of fulfilling different needs. This can be used to analyze potential methods for energy storage. The applicability of each of the methods to the described scenario needs to be explored and eventually compared.

1.3 Methods for Energy Storage

Introduction

In this chapter, a general overview of available methods for energy storage is given. This early phase serves as a guideline to be able to make a well motivated choice for the method to use in further product development.

1.3.1. Methods overview

To provide a general overview, the performance of different methods for energy storage were classified in terms of round-trip efficiency and energy density. For this project, storage at domestic scale is considered, limiting the system size to a standard sized garage/ storage room and smaller is preferable. A comparison between the total system sizes was added, since not all systems only consist of the medium where energy is effectively stored but require complicated mechanisms to be able to store and regenerate electricity.
Since a number of the methods concerned are depending on high pressures within the system, which brings into play suitability issues like domestic safety and high costs due to complicated machinery.

A distinction can be made in terms of the storage medium, this causes interesting differences when looking at applicability to this project.
The categories in which the overview is divided are the following: Electrical, chemical, thermal and mechanical. For illustrative purposes, the energy that can be "stored" in fossil fuels is added to the overview.

Figure 9 gives a schematic overview of the energy storage methods that were considered.
The full overview is given in Appendix A, to improve the readability of this thesis.

1.3.2. Rating by multiple aspects

Performance of an energy storage system (ESS) can be rated by many aspects. Storage capacity, energy density, environmental impact, round-trip efficiency and price are all considered in extensive comparison.
Environmental impact, round-trip efficiency and energy density both classify as important parameters for design. For this project, round-trip efficiency strongly influences the usefulness of the product. A system with a low efficiency is unlikely to provide the user with enough value for money.
Energy density determines the amount of energy that can be stored in a specified volume. Generally speaking, the method with the highest energy density is therefore the most interesting.
Since the core of the assignment is to develop an energy storage system that is sustainable, environmental impact will be addressed and taken into account when determining the method best applicable.

Conclusion

After reading about the storage methods, it will be clear that not all potential methods for storing energy have been described. This has been done deliberately, to improve the clarity of the general overview.
The first comparison that was done considered a number of different characteristics of energy storage systems. Of this, energy density and the storage period have proven to be interesting factors.

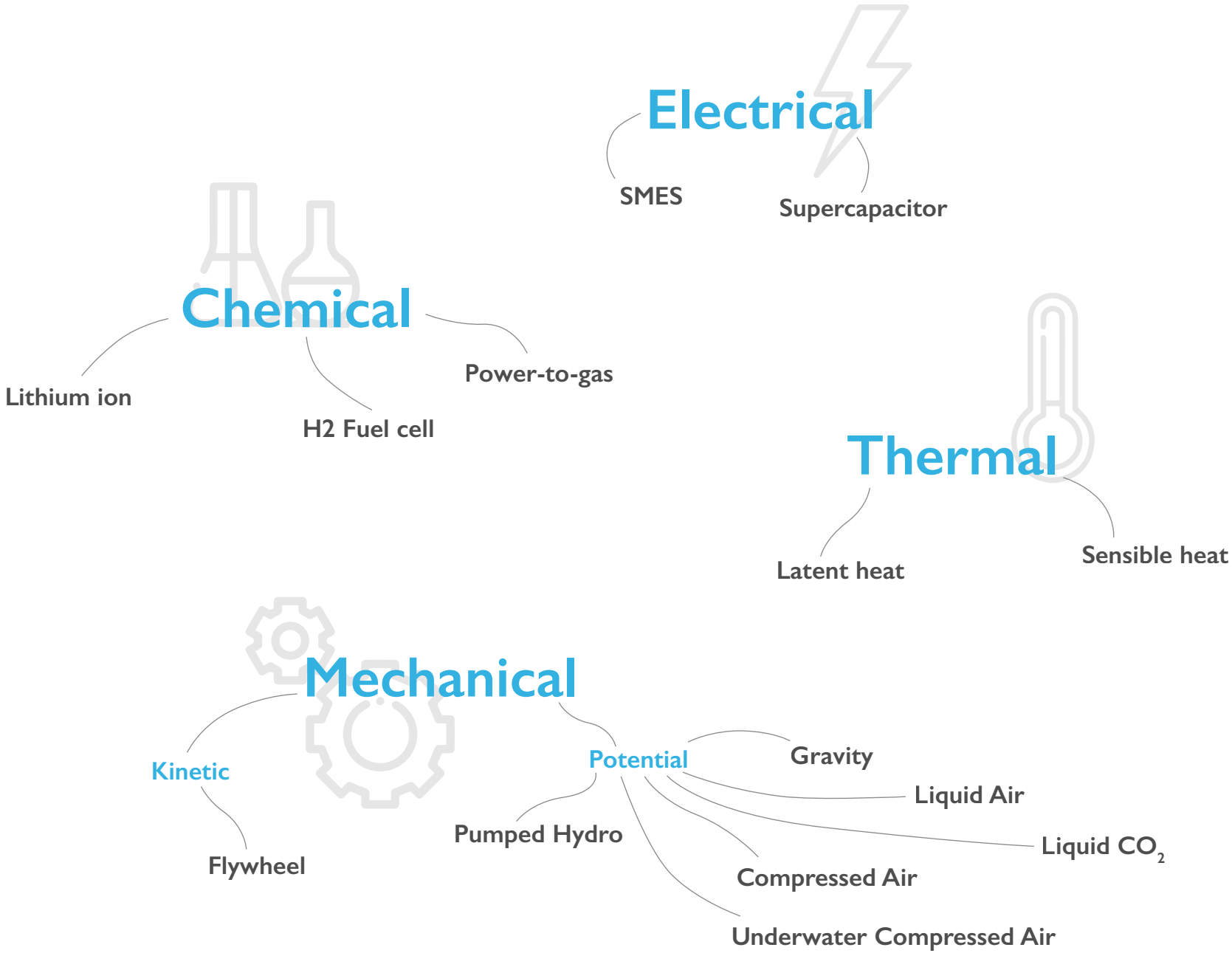

Figure 9: Schematic overview of energy storage methods

1.4 Choice of Storage Method

Introduction

After narrowing down the options to two storage methods in the previous paragraph, these methods are evaluated into further detail and the storage method for this project was chosen.

1.4.1. Rough comparison

On the right hand page, in Figure 10, a comparison chart is drawn. In this graph, a selection of storage methods has been ordered by size. For easy understanding, the size indication blocks have been drawn according to the size of a complete system. The amount of energy stored has been equalized for all systems and is set to the desired 13.5 kWh.

System size is dependent on energy density of the storage method. On the other hand, components necessary for storing and regenerating electricity could cause a significantly larger system. A system which is relatively large compared to the energy density of storage itself is isothermal compressed air energy storage (I-CAES). The grayed-out rectangle for I-CAES depicts the size of a vessel that is capable of storing 13.5 kWh, whereas the larger includes heat storage, two step compression and turbines for regeneration of electricity. A lithium ion battery pack, in this chart, has been drawn according to the dimensions of the Tesla Powerwall, and is an interesting point of reference.

In the figure, the energy density of the storage medium itself is displayed as grayed-out text since it is not directly applicable to the visualization. Including all components of the storage system will cause big changes to these numbers, creating an unfair comparison.

Pressure in bar is included in the comparison, since some of the methods require high pressure to achieve interesting energy densities. For three of the technologies, this value limits or challenges the applicability to this project.

Environmental impact has been rated according to production, use and end-of-life phases of the storage methods. A diesel generator scores very low since fossil fuel is used (use phase) and the lithium ion battery pack mainly causes problems when lithium is produced and lacks recyclability.

Round-trip efficiency of the storage methods has been included, but is mainly used to illustrate the big difference between diesel as a fossil fuels method for electricity generation and the analyzed sustainable storage methods.

The last criterion that was used for comparison is suitability to Amstel Engineering BV, which is important for the project since the company aims for a solution which is mainly mechanical and suits the company's expertise.

1.4.2. Narrowed down selection

From this comparison, which is still at the basic level of understanding the storage methods, two of the methods seem interesting.

Flywheel Energy Storage Systems (FESS) and Isothermal Compressed Air Energy Storage (I-CAES) seem promising when looking at the comparison graph. The system size achievable with both methods seems to meet the requirement of fitting in a standard sized home garage. Both of these systems are rated positively when looking into environmental impact, since no fossil fuels are used and high-impact materials like lithium are not required. Both FESS and I-CAES are suitable to Amstel Engineering BV, since energy conversion takes places in a mechanical way.

The main drawback of FESS is the fact that energy is lost overtime. Regenerating electricity from a rotating flywheel can be efficient and systems with a round-trip efficiency of 83% (Mousavi et al., 2017)[60] have been built, but losses have not been fully eliminated and cause the limited maximum storage time.

I-CAES can store a sufficient amount of energy in a reasonably sized vessel (Dobber, 2018), but the complete system requires much more space. Additionally, high pressures should be achieved to reach the desired energy density.

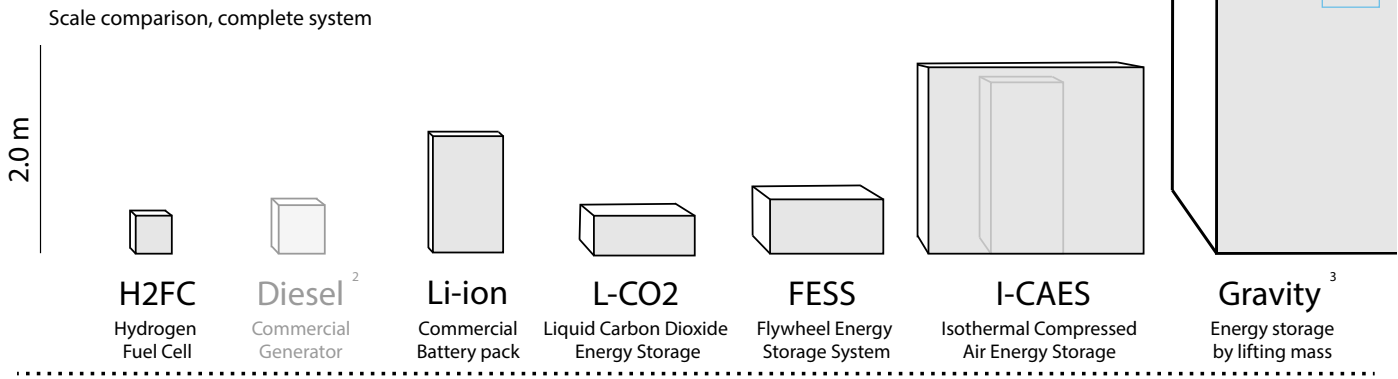

	H2FC Hydrogen Fuel Cell	Diesel [2] Commercial Generator	Li-ion Commercial Battery pack	L-CO2 Liquid Carbon Dioxide Energy Storage	FESS Flywheel Energy Storage System	I-CAES Isothermal Compressed Air Energy Storage	Gravity [3] Energy storage by lifting mass
kWh	13.5	13.5	13.5	13.5	13.5	13.5	13.5
m³	0.13 [1]	0.17	0.11	0.15 [1]	1.0 [1]	3.2 [1]	198.5
Wh/L	55	10,722	123	250	2	19	0.07
bar	300	N/A	N/A	70	N/A	200	N/A
Loss.	negl.	negl.	-5%/y	negl.	-45%/d	negl.	negl.
Env.	+	---	--	+	++	+	+-
Eff. %	60%	35%	95%	63%	80%	70%	80%
AE BV	-	--	-	--	++	+	+

= Limiting factor = Challenging factor 1 = Estimated value 2 = No storage of renewable energy, added for illustrative purposes 3 = Low density means off-the-charts scale

Figure 10: Comparison chart with considerable types of energy storage

1.4.3. Harris Profile

Both are theoretically capable of storing energy at a residential scale, but also have their limitations and challenges. This is why these two methods will be held along a list of wishes, to which both systems are scored using the Harris Profile (van Boeijen et al., 2014)[61] . The list of requirements (formulated as wishes) has been set up and used for comparison. Next to FESS and I-CAES, Li-ion storage has been added as a reference, since this is the main method that is used for residential energy storage nowadays (Tesla Powerwall). Since this method will not be a solution for this project, it is displayed in a grayed-out state.
The requirements are ranked according to their importance to the project, starting with the prospected size of the total system.

Different scores for all of the wishes are given, and the conclusion that can be drawn from setting up the Harris Profile is that I-CAES and FESS have different advantages and drawbacks. Both methods could theoretically suitable to creating a storage system but show important differences in suitability to this project.

Size and complexity

According to Dobber (2018), an I-CAES system can be built using a pressure vessel of 10 m^3 at a low pressure of 11.5 bar. Increasing the pressure to 200 bar, which is used in previous calculations, this storage vessel can be reduced in size and will fit within the boundary size of a household garage. However, to store the heat that is generated when compressing air, another vessel is needed. An important part of the system that is not fully developed by Dobber, is the regeneration phase. This requires a complicated system to reuse the heat directly when starting the expansion of the air. This was developed by LightSail Energy[62] , but discontinued.
Although the storage principle of FESS is relatively simple, optimization requires advanced technologies like active magnetic bearings for low-friction levitation. Technological developments rapidly follow each other and have delivered promising results, for example superconducting bearings that will allow a compact motor/generator (Kohari et al., 2011)[63]. Considering developments like this, the design of a compact household solution for energy storage will be challenging but seems feasible.

Suitability and Feasibility

Since this project was initiated by Amstel Engineering BV, their expertise should be taken into account when finding the method that is most suitable. Being experienced in the field of machine engineering, a more mechanical method means better suitability to the company. I-CAES requires specific knowledge of complex thermodynamics, which is available only up to a certain limit. FESS on the other hand, suits the expertise and is more likely to result in a fully developed product.
Within the scope of this graduation project, which is the design of a mechanical energy storage system at household scale, there is a difference between the two methods as well. It is more likely that a FESS system can be developed into a consumer product within the set duration of the project. In addition, my personal skillset allows for a more advanced development of a FESS, since knowledge and understanding of mechanical systems is at a higher level than that of thermodynamics.

Storage and regeneration

One of the main drawbacks of FESS is its passive energy loss. Storing energy and keeping it for multiple hours has been a challenge that has been taken on by researchers, who are attempting to characterize and diminish discharge losses (Skinner, 2017)[64]. Although currently a FESS for household application is not available on the market yet, potential storage and regeneration durations are increasing and approaching the long-time storage area (Schulz et al., 2015)[65]. Regeneration of electricity can be done relatively efficient, when choosing an optimized motor/generator design. However, the losses during passive spin-down are still present during regeneration.
Storage duration for I-CAES depends mainly on heat losses overtime. Even when using a well-insulated heat storage vessel, these losses should not be neglected. A long duration of continuous energy supply can theoretically be achieved, but lower pressure differences cause lower efficiency of a turbine.[66] This results in a lower efficiency after the system reaches a low storage level.

Costs

Prospected costs of the two systems have not been estimated into detail, but can be assumed to be mostly dependent on system complexity. The fact that Maia et al. (2016) have tested a micro-CAES system consisting of commercially available parts is promising, but higher efficiency and larger scale will most likely drive up the costs of this system. Since an active magnetic bearing system for a FESS can be combined either with an integrated motor/generator or with a commercially available brushless motor (Park, 2010)[67], the costs of this system type are estimated to be lower.

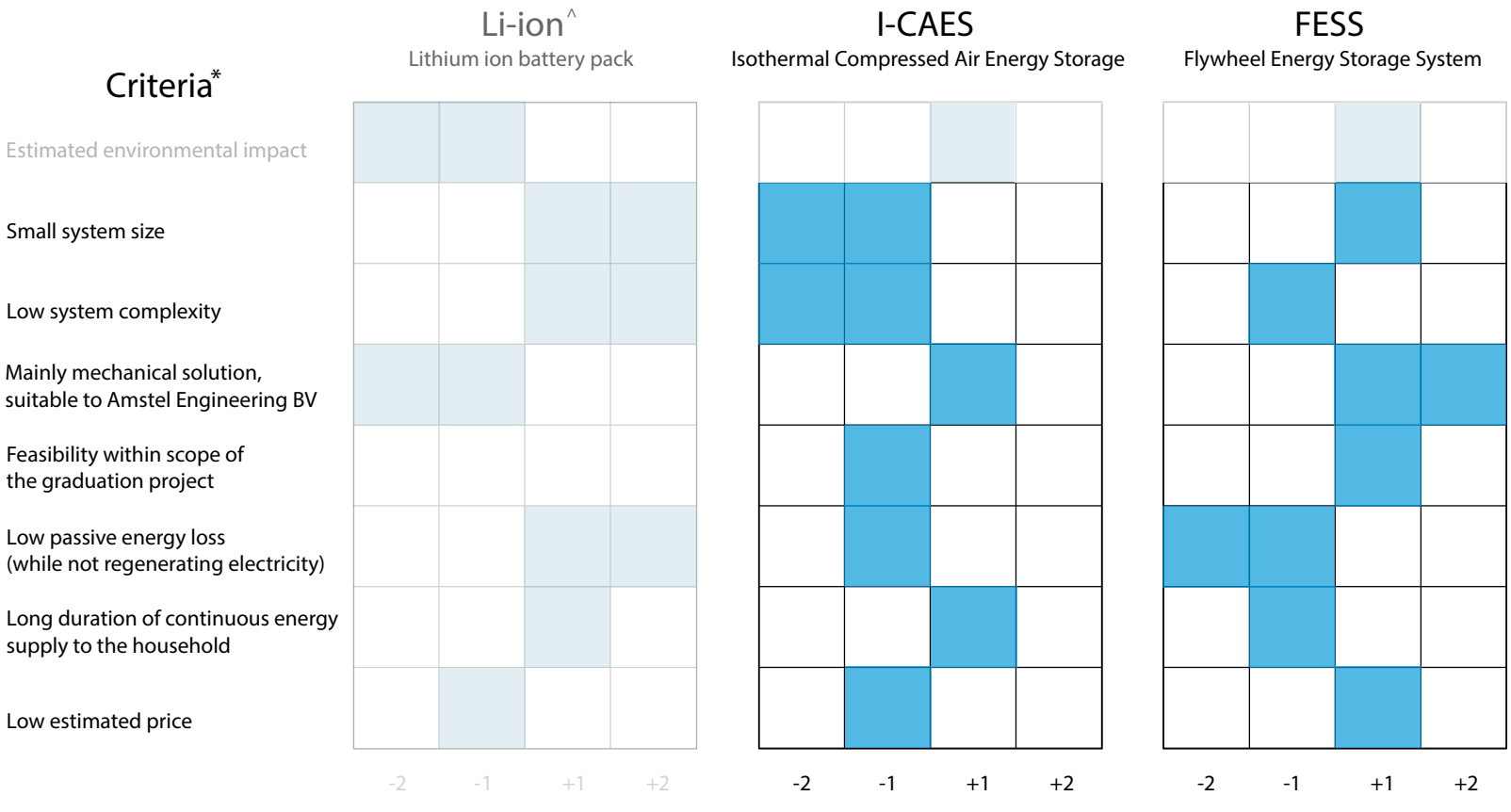

^For illustration purposes only, not fully justified data

*Clarification of criteria in additional text

Conclusion

A Flywheel Energy Storage System has been chosen as the energy storage method for this project, with suitability to the company and the system's size and complexity as main drivers. The energy loss in idle state is the most important challenge to overcome. Interesting studies have been conducted considering minimization of rotor losses and further optimization of flywheels, this has caused faith in the successful applicability of this storage method in this project.

System size is an important factor that lowers the applicability of I-CAES, since storage at residential scale requires a system that would fill the major part of a conventional garage. Keeping in mind that the goal of this project is a consumer product, this lowers the method's chances of success.

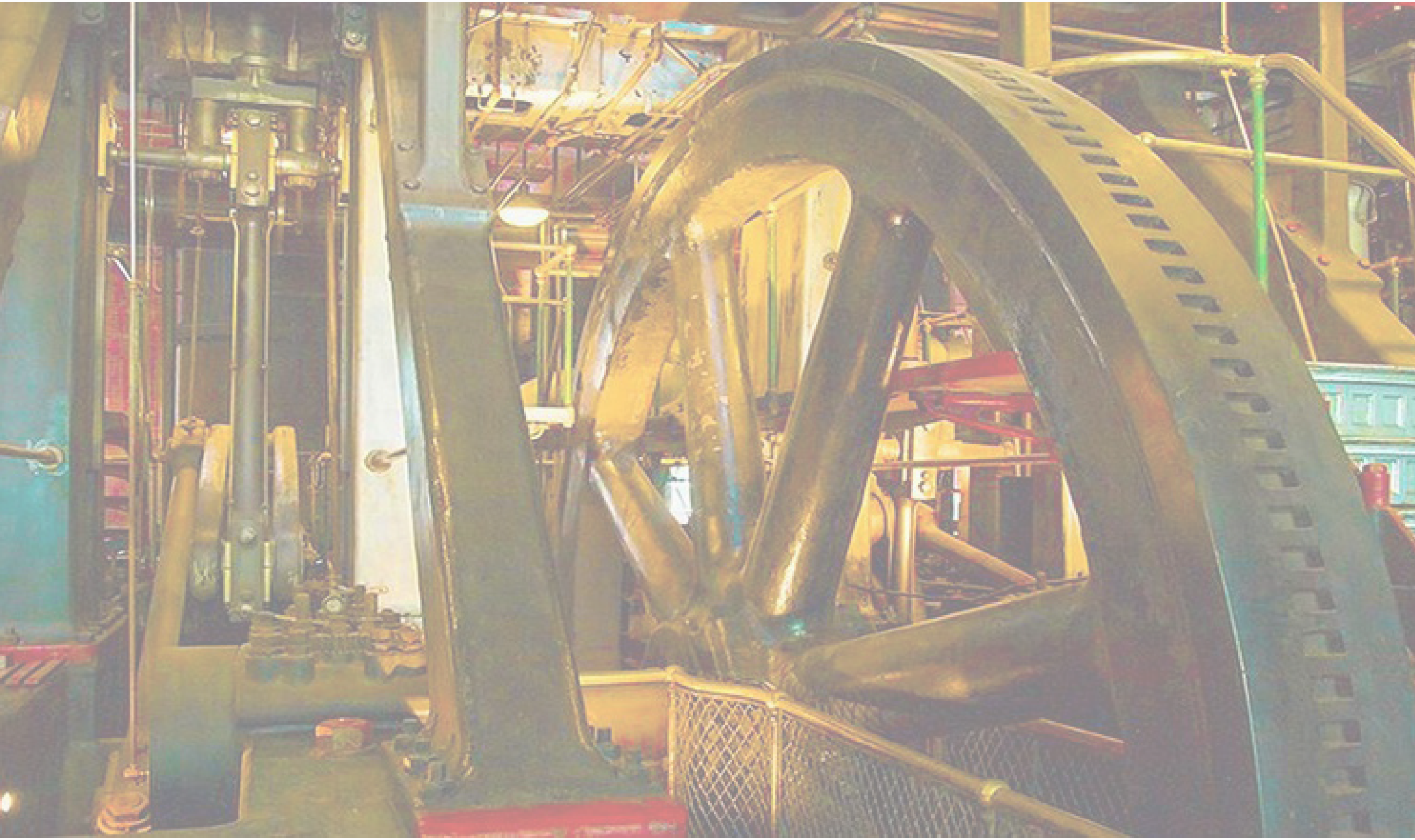

Figure 11: A flywheel in a well known form of use: helping continuous large movements by storing kinetic energy and providing it to the system when needed. (Watt-Logic, 2017)[68]

2. Technology Driven Design

Before diving further into the embodiment phase, various possibilities for the system's technical specifications were explored. To get a clear overview of the parts to be taken into account, the system is split up into subsystems, which are then separately analyzed.

2.1 Technical System Design

Introduction

Storing electricity in the form of kinetic energy by using a flywheel is not a novel technology by itself. It is however novel to use it within a household. Since the requirements to the system are different for this application than for existing solutions, all aspects of the technical system need to be thoroughly evaluated.

This chapter starts with a description of proven applications of flywheel energy storage systems and continues by splitting up the system in subsystems and exploring their existing solutions.

2.1.1. FESS characteristics

Flywheel energy storage systems (FESS) are listed in comparative research as short-term energy storage. Systems that are currently available achieve a storage time of several seconds to minutes (Chen et al., 2009), an hour of storage or longer is uncommon. Therefore, this type of energy storage system is mainly used as a solution for Uninterrupted Power Supply, as can be read in the following paragraph. Long-term storage systems have been attempted (Velkess, 2019)[69] , but have not been commercialized successfully.

Uninterrupted Power Supply (UPS)

In some locations, for instance in data centers, a continuous supply of electricity is essential. Power supply is in that case "mission critical" and an uninterrupted power supply is required. Vycon Energy[70] , Beacon Power[71] and Active Power[72] are companies that sell UPS systems where flywheels are used. For these systems, the most essential property of the storage system is quick response and high storage density. Storage time is less important, since application allows for continuous charging. The system is designed for regeneration of electricity during a power cut, when electricity is needed for a short period of time, until the backup generator (usually a diesel generator) has started up.

One of the systems made by Active Power, CleanSource HD675 UPS[73] is designed for a power output of 675 kW during 15 seconds. This system is displayed in Figure 12. The maximum regeneration time listed in the available fact sheet is 59 seconds, confirming the system is capable of short-time electricity regeneration only.

The systems offered by the aforementioned companies do not list any storage time, making it difficult to understand passive losses of the systems. Since no losses or run-down times are mentioned, they are most likely too low to be used in household energy storage.

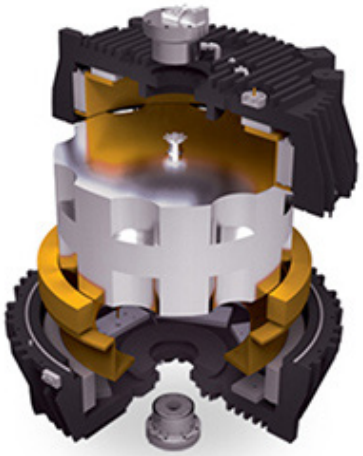

Figure 12: CleanSource HD675 UPS, by Active Power.

Long-term storage

Although comparative studies like that of Chen et al., (2009) and Molina (2009)[74] mainly mention FESS as a short-term option (visualized in Figure 13), suitability for longer storage times is being studied by TU Wien and Laval University in Canada. At TU Wien a system was developed with the aim to apply it to residential storage and therefore reaching storage time of 12 hours (Schulz et al., 2015). Results show a 5kWh FESS with a passive spin down to 78% of its speed taking 7 hours. With this result they have not reached their goal, but proved that longer storage time has potential. Researchers at Laval University claimed a passive spin-down time from 9000 to 4500 rpm of 17.5 hours (Bakay et al., 2010)[75].

Amber Kinetics is a company from the United States (Amber Kinetics, 2019) that has developed a flywheel storage system optimized for maximum duration of electricity regeneration. This U.S. startup currently sells a type of flywheel energy storage system that is able to store 32 kWh and deliver 4 hours of constant electric power at 8 kW with a round-trip efficiency over 86% (Amber Kinetics, 2019). The maximum time of storage has not been listed.

An interesting report was presented by Sandia Laboratories back in 1979 (Brobeck & Associates., 1979)[76], in which a complete flywheel energy storage system is discussed in-depth. Albeit conceptual, the design sounds promising, making it difficult to find where it "went wrong" and why this system is not on the market.

At the end of their report, it was recommended that a prototype model is produced for demonstration purposes. However, no literature is available concerning building and testing a prototype.

The information found is therefore considered as an interesting step in the right direction, but since no development is to be found in literature, there has probably been at least one critical aspect that has resulted in a failed design.

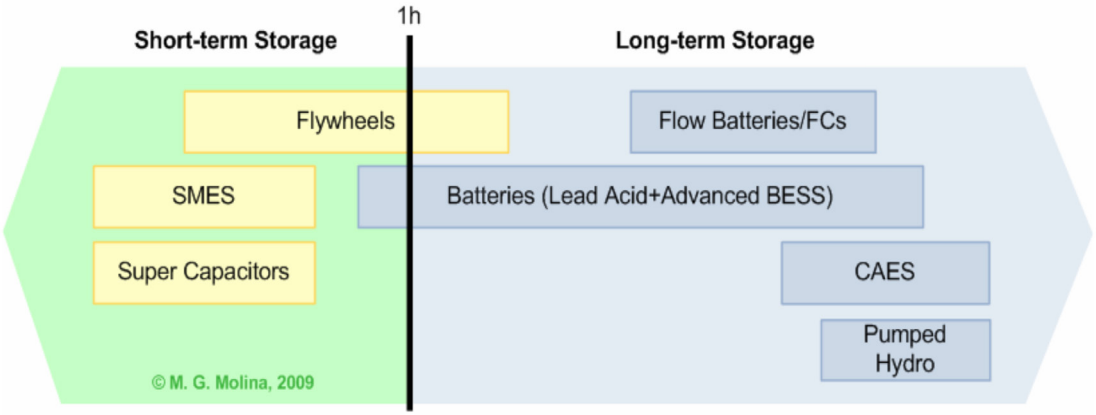

Figure 13: Short-term and long-term energy storage systems, Molina (2009)

2.1.2. Subsystems approach

Storing energy in a flywheel is a rather simple concept, since it is based on only one principle. Energy (E) is stored according to the following equation:

$$E = \frac{1}{2} I \omega^2 \qquad \text{(eq. 2.1)}$$

With I the moment of inertia in mm^4 of the rotor and ω (omega) the rotational speed in rad/s. The moment of inertia is determined by:

$$I = \frac{\pi \rho h}{2} (r_{out}^4 - r_{in}^4) \qquad \text{(eq. 2.2)}$$

Where ρ is the density of the material, h the height of the rotor and r_{out} the outer, and r_{in} the inner radius. Combining these expressions, one can understand that a larger diameter at the same speed will store more energy. To help in understanding differences in flywheel dimensions, one might think of a figure skater turning pirouettes, which is assumed to have a certain amount of kinetic energy in its movement. The moment of inertia of the skater is larger when the arms are spread, compared to when the arms are folded closely to the body. Neglecting frictional losses, the energy in the "system" should remain constant, and therefore pulling in the arms result in a higher rotational speed.

Conclusion

Flywheel energy storage is currently successfully being applied as an uninterruptile power supply. Long-term storage with this technology is being studied but has not resulted in products on the market.

Analyzing the system by subsystems will make it possible to develop a long-term storage system step-by-step and to see where limitations occur.

2.2 Subsystem Solutions

Introduction

Optimizing a flywheel to build a system with acceptable performance requires looking into more than just the basic principle that was described on the previous page. To be able to build a system suitable to residential energy storage, a FESS should be realized that is optimized to having the lowest possible "passive discharge" and therefore the highest "charge holding capabilities". FESS was split up into four subsystems: Suspension, Rotor, Electrical Machine and Housing. The division into subsystems has been displayed in Figure 14.

2.2.1. Subsystems overview

The medium for storing energy, the flywheel rotor, should be optimized in terms of maximum storage and is crucial for determining the amount of energy that can be stored. Since the applicability of a rotor is fully dependent on the fact that it should be supported by a suspension system, the subsystem suspension is considered just as important. The shape and dimensioning of the rotor will be determined together with the type of suspension used.

With respect to energy conversion, the system should be able to convert electricity into a rotational movement and reverse this process in the most efficient way possible. The subsystem that realizes this is often called the motor/generator (M/G). Choosing the type is strongly driven by the rotor and suspension types that will be used. Many of the studied FESSs make use of a M/G that combines suspension and electric drive/electricity generation in the form of an active magnetic bearing (AMB) (Takemoto et al., 2004)[77]. When studying the subsystems, alternative solutions will be examined.

The fourth subsystem that is considered is the housing, the enclosure in which the actual system is mounted. Most importantly, the housing should be capable of safely containing the flywheel, which is rotating at significant speed.

Feasibility of this storage method is mainly dependent on losses in the flywheel due to drag and aerodynamic losses. Current development in different types of bearings determines which technology would be applicable to the suspension of the flywheel rotor of a storage system at household scale.

Every subsystem is considered in its separate paragraph, potential solutions have been chosen and eventually combined into multiple versions of complete systems that will then be tested to determine whether all requirements have been met.

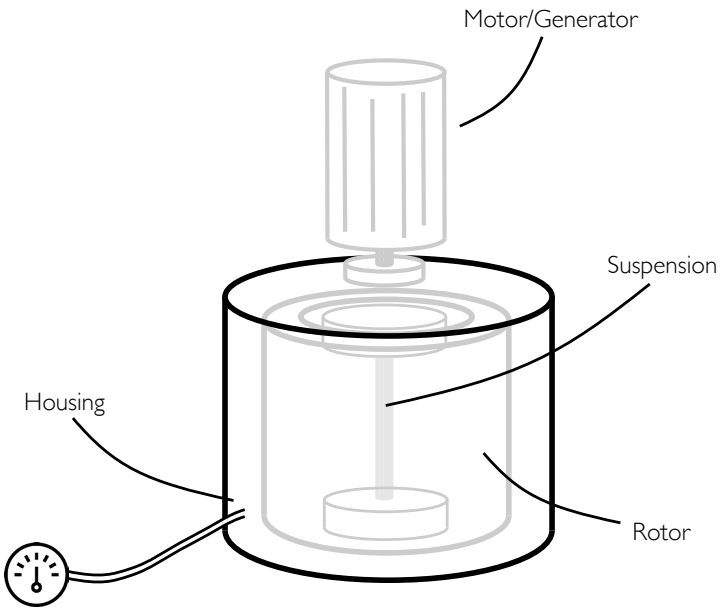

Figure 14: Subsystems approach of FESS

2.2.2. Subsystem 1: Rotor

Shaping and dimensioning a flywheel rotor should be done according to a number of limiting factors. High stresses occur at the central area of the rotor, where tension on the material reaches its maximum due to centrifugal force (Riccardella & Bamford, 1974, cited in Jiang et al., 2017)[78]. The material property that determines a material's resistance to these stresses is the yield point, which is the amount of stress at which the elastic behavior of the material ends and it starts to deform plastically.

As seen in Equations 2.1 and 2.2 given before, the kinetic energy stored in a flywheel strongly depends on its radius and rotational speed. In addition, it can be seen from the expression that a higher density will cause a higher value for its moment of inertia. With this in mind, studies were conducted to find the optimal shape for a flywheel rotor. Among others, Kress (2000)[79] and Jiang et al. (2017) found comparable shapes, which all seem consistent with the explanation above. As seen in Figure 15, a significant portion of the rotor's mass is located far from the rotation axis (visible on the left of the image) to maximize the energy that is stored. On the other hand, thickness is added around this axis, since the highest tension is present in this area.

Tension peaks also occur in the material at the inner surface, when a bore or ring-shaped rotor is introduced. This is the reason why Sanders et al. (U.S. Patent No. 10167925B2, 2019)[80] filed a patent for a rotor design containing extra material near the rotational center, meant for better stress distribution when connecting the shaft that supports the rotor.

Figure 15: Rotor optimization by Kress (2000)

Considering a ring-shaped rotor has its advantages over the optimized shape described before, since an integrated system for support can be designed and a more compact system can be designed (Toh & Chen, 2016)[81]. This design type allows for energy storage in a ring in which other components of the system are located and coupled through a (lightweight) hub (Yulong et al., 2017)[82]. The fact that a compact design can be achieved, without advanced shape optimization and high manufacturing costs, makes a ring shaped rotor an interesting solution for a household FESS.

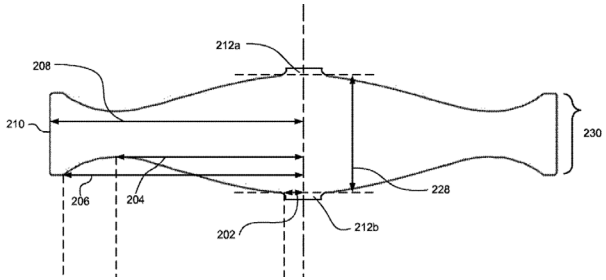

Figure 16: Flywheel rotor patent by Sanders et al. (2019)

Shape and dimensions of the flywheel determine the stresses that will be caused at certain rotational speeds, to be able to withstand these stresses, the optimal material should be chosen. Since the project is focused on designing a storage solution for households, it makes sense to assume no high performance composites will be used since material costs will be too high to keep the market price low. For comparison purposes these materials will be included in some of the calculations.

Dimensioning

Analysis of different dimensions was done by writing the Matlab-script FlywheelCalc, which is included alongside an in-depth description in Appendix C.

The main function of this script is to determine whether a certain combination of dimensions, material and rotational speed can result in meeting the set requirements. Figure 17 shows a plot of the results for energy storage for increasing rotational speeds. The hatched part displays the rotational speeds for which the maximum tensile stress will be exceeded. Calculations that are done consist of the basic energy storage expressions (equation 2.1 and 2.2) and include maximum tensile stress analysis according to Ryder (1969)[83] in the following equation:

$$\sigma = \frac{1}{16}\left(\frac{3\nu}{8}\right)\omega^2 r_{out}^2 \rho \qquad \text{(eq. 2.3)}$$

Here, it can be seen that the tensile stress will increase when increasing either the rotational speed ω, the outer radius r_{out}, or changing to a material with a larger Poisson's ratio ν or density ρ.

If a solution is found while increasing the rotational speed to the set maximum, this is plotted and its data is entered in a table. However, according to Merrit et al. (1994)[84] and considered by Bakay et al. (2010)[75], electricity can only be generated at 100% to 50% of FESS initial rotational speed. With this in mind, the script will find the first solution for which the usable energy meets the storage requirement. Thus, subtracting the energy left in the system at 50% of the initial speed. At the rotational speed of this solution, another point is plotted and maximum stresses are compared to the yield strength of the material.

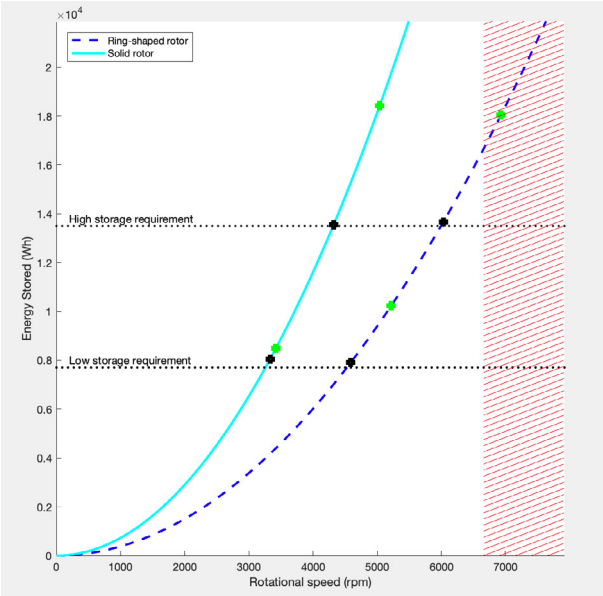

Figure 17: Energy vs rpm plot from Matlab-script FlywheelCalc

In addition to the calculation of the stored energy, aerodynamic losses are taken into account to determine the duration of a passive spin-down. Since storing the energy for a long period of time is crucial for application of the FESS to household energy storage, this gives interesting results. Air resistance dependent on Reynolds number by Bayley & Owen (1969), cited by Miles (2011)[85].

Bearing losses were estimated using the expression by Gurumurthy et al. (2013)[86]. In this study, the relation between rotational speed and losses in a standard ball bearing was determined by doing a small-scale test.

All of the expressions for loss calculation can be read in paragraph 3.1.4. The script in Appendix C contains explanation of the necessary lines of code.

Multi-rotor flywheel

A flywheel system can be optimized for roughly two situations. It can be designed to have the longest possible passive storage time, which will mainly be done by minimizing passive losses. Or it can be designed to have the most quickest charge and discharge response, this logically results in minimizing inertia.

The different optimizations will result in different systems, which is illustrated by the fact that UPS systems like the one by Active Power, described on page 30, generally have a larger height to radius ratio and higher rotational speed than experimental long-term storage systems like the one studied at Laval University, mentioned on page 31.

The first is more suitable for peak shaving and the second functions better as long-term storage option by its larger inertia, but therefore less quick to respond to changes. Two different height to radius ratios are displayed in Figure 18, with on the left side a low-inertia quick response flywheel and on the right side a high-inertia long-storage flywheel.

Applying two or more differently optimized systems to a household could mean that at any time of day, the best suitable system is put to use and overall losses are minimized. Short-term, quick response storage is suitable during daytime and right after sunset, while long-term storage is needed to supply the household during the night and the morning before sunrise. Simulations with prospected data for supply and demand will be done to validate the hypothetical advantage of a multi-rotor system.

According to Gurumurthy et al. (2013), the main portion of passive losses in a flywheel system is caused by aerodynamic drag. As seen in Figure 19, drag increases significantly with increasing rotational speed, making a long-term storage option more feasible when operated at lower rotational speed. Storing the same amount of energy in a lower-speed system requires the

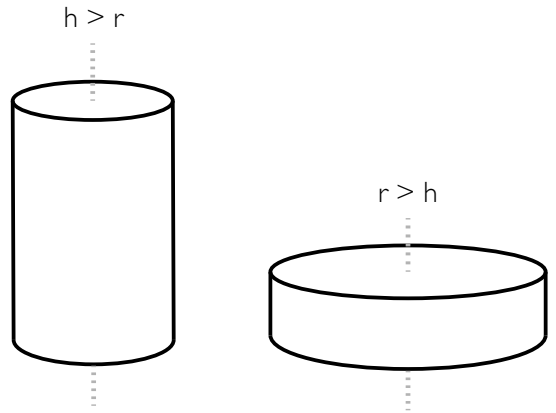

Figure 18: Flywheels with a different height to radius ratio.

height to radius ratio to be less than one, as can be seen in calculations later in this thesis.

Another reason why a multiple-rotor system can be chosen is to minimize the required motor performance. For example the cascaded system by Ghaemi and Mirsalim (2017)[87], displayed in Figure 20, which uses multiple electrical machines to increase the maximum achievable rotational speed without additional power supplies. Each motor that is added to the first stator functions as a rotor and adds to the stored energy in the system.

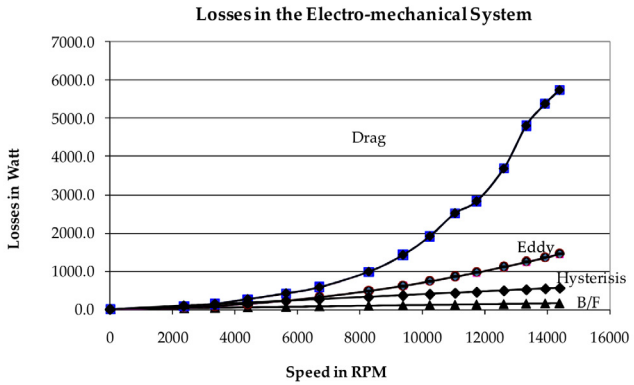

Figure 19: Losses in a flywheel system, by Gurumurthy et al. (2013)

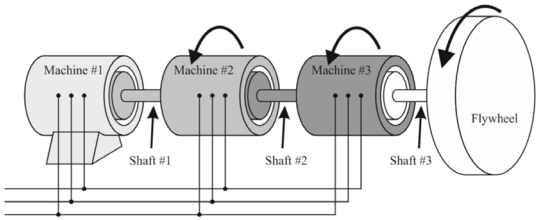

Figure 20: Cascaded flywheel system, by Ghaemi and Mirsalim (2017)

A different multi-rotor system is introduced by Dugas in the patent application for a flywheel (U.S. Patent No. 10103600B2, 2018)[88], where a ratchet-type mechanism is used that achieves connection through centrifugal force. The connection type allows for a flywheel system that has a variable inertia by rotating either a single or multiple rotors. The system is claimed to have a reduced charge-up time compared to single-rotor systems, since the increase of the motor load is increased less steeply.
A large rotor in the system should be supported by relatively large bearings, which generally experience higher losses (Schweitzer & Maslen, 2009)[89], which is an important drawback of larger size systems.
Higher mass might require mechanical bearings rather than low friction magnetic bearings and might change the graph of Figure 19 to one where the bearing friction (displayed as triangles and B/F) is larger than aerodynamic losses (displayed as squares and named Drag).
On the other hand, more mass is required for a higher amount of energy stored. A flywheel rotor can be optimized to regenerate the largest amount of electricity immediately after the energy supply has stopped, or differently directed optimization can be done to increase storage duration by minimizing losses.

The Matlab-script that was written for testing different dimensions, has been extended to be used for a feasibility check for a multi-rotor flywheel system. Please refer to Appendix C for the complete script.
This script allows two or three dimension sets to be entered and calls the previously described script to obtain system specifications. It determines the feasibility of the multi-rotor design using the maximum duration of energy storage and the maximum duration of electricity regeneration. Specifying the power and efficiency of the used motor/generator is required to determine the latter, and is obtained from motor manufacturer Nord (Nord Drivesystems, 2019)[90].

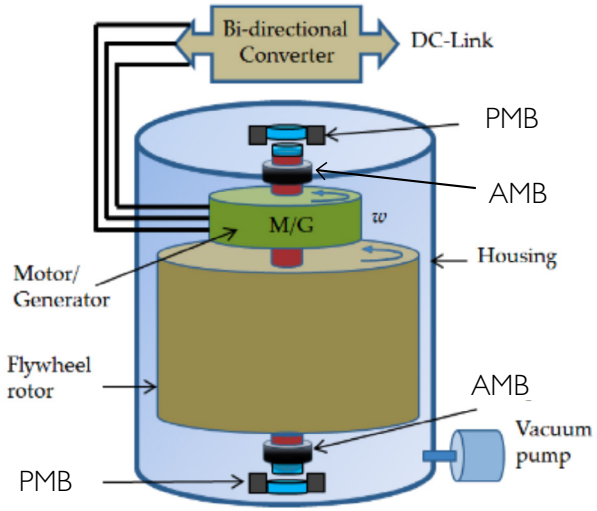

Figure 21: Example of using a thrust bearing for axial force, by Amiryar & Pullen (2017)

2.2.3. Subsystem 2: Suspension

Since ball bearings inevitably cause friction, they will also degrade overtime, hence introducing the need for maintenance (Schweitzer & Maslen, 2009). Beacon Power has filed multiple patents in which their solution for loss reductions and optimization are protected. Interesting information can however be found when reading for example the patent that describes an axially free flywheel system (U.S. Patent no. 6710489B1)[91]. The phenomenon of a deforming rotor and its axis at high rotational speeds is called the Poisson Effect[92], this means that the axis shortens and the radius increases due to centrifugal forces. This effect is made acceptable by avoiding restriction of the axial axis. The company claims that this allows for high-speed operation with use of mechanical bearings, since axial loads on these are significantly reduced.

To reduce bearing losses even further, choosing magnetic bearings as a suspension system seems to be a logical decision. Bearings with mechanical contact like ball bearings usually result in losses too high to be considered an efficient system since heat is introduced by friction and therefore accounts for energy losses.
The first thing to consider when attempting to magnetically levitate an object is Earnshaw's Theorem[93], this practically results in the fact that there is no possible static configuration that can stably levitate an object against gravity. This means that there will always be the need for some kind of control system. In common flywheel systems where the rotor is magnetically levitated, stability is commonly ensured by a control system in an active magnetic bearing (AMB) like in a design by Smolinski et al. (2017)[94].
Suspending a vertical axis flywheel rotor by combining permanent magnet bearings (PMB) for axial thrust with a radial active magnetic bearing (AMB) is a widely-used solution. An example is given in Figure 21, which displays the system by Amiryar & Pullen (2017)[95] .

A Halbach-array (Merrit et al., 1994) is a commonly used way of organizing magnets in a way that makes it possible to concentrate the magnetic flux on one side and minimize it on the other side. Such an array, as seen in Figure 22, is capable of supplying the major part of the axial force needed to carry the rotor.
Losses that are most significant to slowing down of the rotor are Eddy current losses in the winding and in the magnet. Santiago et al. (2008)[96] have determined that the dominant loss mechanism for coreless flywheels that are using active magnetic bearings is eddy current losses induced over drag losses and bearing losses.

AMB

Active Magnetic Bearings (AMBs) can support the flywheel's rotor by a constantly changing magnetic flux, an example is displayed in Figure 23. A control system is always needed in order to stabilize the system. AMBs can be divided into two groups: homopolar and heteropolar bearings. The main advantage that is caused by lowering the number of pole pairs to a single one (homopolar) is the lowered losses and less coupling between the control axes (Smirnov et al., 2017)[97]. Coupling in this context means the influence of this bearing on the rest of the system, which can have a negative effect on other control systems (Combrinck, 2010)[98]. However, heteropolar AMBs can be produced at lower costs because of easier manufacturing, and can therefore offer an interesting solution. The control system that will be responsible for stabilization requires complicated dynamics control. Designing the control system lies outside the scope of this project, but will be considered during the next development phase by Amstel Engineering BV.

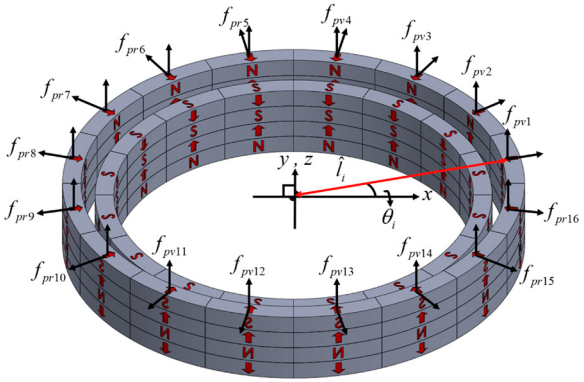

Figure 22: Halbach Array for passive axial support, by Toh et al. (2016)

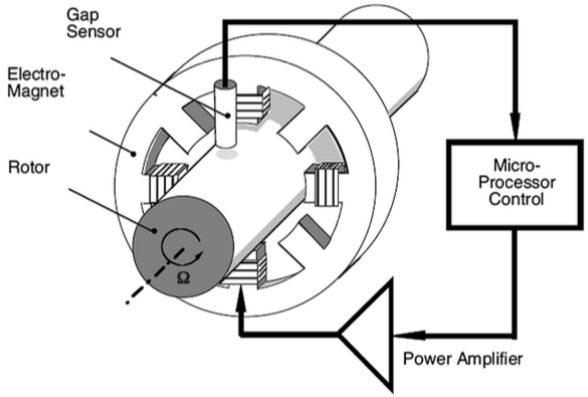

Figure 23: Active Magnetic Bearing, by Schweitzer & Maslen (2009)

Nano magnets

Denmark's government is funding the development of a high performance flywheel energy storage system named MagFly (flywheel.dk, 2019)[99], which is being studied at Aarhus University (scitech.au.dk, 2019)[100]. Particularly interesting is that in this study nano magnets are being considered. This type of magnets will significantly improve the properties of the magnetic levitation system and potentially allow for long-term energy storage for up to 24 hours.

2.2.4. Subsystem 3: Electrical Machine (Motor/Generator)

As mentioned before, the electrical machine is the subsystem that will combine the two directions of energy conversion. The storage step involves conversion of electricity into kinetic energy in the form of rotation of the flywheel rotor. The regeneration step on the other hand, involves using the M/G as an electrical generator that regenerates usable electricity for the household. One main distinction between types can be made concerning speed of the flywheel's electrical machine. A motor classifies as high speed when the peripheral speed reaches 100 m/s, and has its advantages over a lower speed version. According to Smirnov et al., (2017), high-speed electrical machines have an improved system efficiency and can be constructed in a smaller form factor.

Self-bearing motor/BSRM (Driven AMB)

An active magnetic bearing can effectively combine radial stability with storage and regeneration. Rotor stabilization and drive/regeneration can be synthesized into one electrical machine, which thus controls radial force and torque. Figure 24 displays the working principle of a combined system as developed by Yuan et al. (2015)[101] . When the rotor is not positioned perfectly

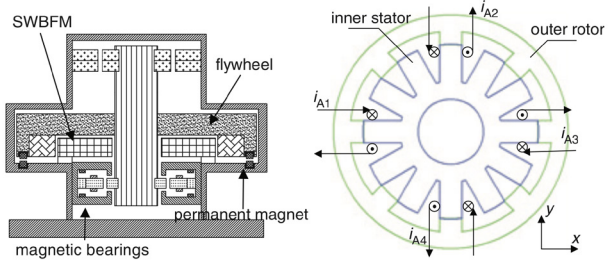

Figure 24: Self-bearing motor, by Yuan et al. (2015)

centered within the stator, a difference in magnetic flux density occurs. Therefore, a radial force can be generated that centers the rotor within the stator. (Sun et al., 2018)[102]. When one of the poles of the rotor is not perfectly aligned with its opposite pole at the stator, a difference in magnetic flux density also occurs. Similar to an electric current, magnetic reluctance strives to its minimum value, which occurs when the pole has rotated to the corresponding location at the stator. In the case of a rotational misalignment, the torque current that occurs causes rotational movement. After perfect alignment, rotation theoretically stops. The system can now be considered aligned. However, to cause a continuous rotation, the rotational unbalance should be kept in place. This is done by constantly switching the reluctance. Hence the name of a system as described: a Bearingless Switched Reluctance Motor (BSRM).

Decoupling motor/generator

Allowing the rotor to spin freely, without any resistance of the motor/generator (M/G), requires total separation of the flywheel and motor/generator. One system that uses an external motor has been patented by Chakratech (U.S. Patent No. 9667117B2, 2017)[103], and consists of a rotor that is supported within a vacuum, without any motor/generator parts. The EM is positioned outside the vacuum and coupled using a magnetic clutch system, as seen in Figure 25.

A commercially available type of motor/generator can be applied, preventing costly design of integrated and system specific M/G's. Higher rotational speeds might be necessary to achieve a sufficient amount of stored energy in a relatively small system. Since the sizing of the M/G is not crucial when it is located outside of the flywheel's enclosure, a transmission can be used to allow for application of a low-cost commercially available motor/generator and high-rpm flywheels can be powered in a cost-efficient way.

Decoupling the motor/generator from the flywheel enables the motor to stop while passive storage takes place, reducing the losses that would normally be caused. As mentioned before, these Eddy Current losses are responsible for a significant percentage of the total losses. Another advantage of decoupling is the possibility of multiple flywheel rotors that are driven by only one or two M/G's, which could reduce costs of a multi-rotor-type FESS which was discussed before. David et al., (2017) also describe, in the same patent application, a system where the M/G is movable along an array of flywheels. This creates the possibility of designing a system with multiple rotors that are optimized for different situations (e.g. amount of energy stored and storage duration).

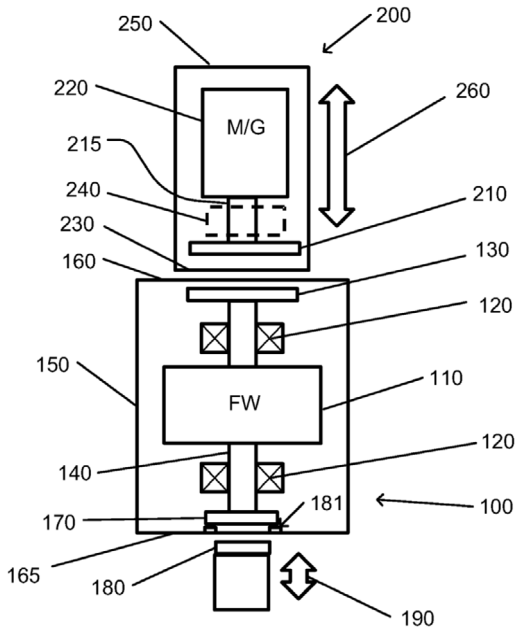

Figure 25: Decoupled motor/generator, by Chakratech (2017)

2.2.5. Subsystem 4: Housing

Performance of a mechanically levitated flywheel at high rotational speeds depends strongly on air resistance (Skinner, 2017)[104]. Lowering pressure and causing a (near) vacuum significantly reduces resistance and is therefore desired. Santiago et al. (2008) have determined that aerodynamic losses are significantly lower at 100 Pa than at atmospheric pressure (10^5 Pa). Therefore, a low pressure enclosure is likely to be part of the FESS design.

Including a pump in the system to reduce pressure requires valuable space and would increase electricity usage. Therefore depressurizing the housing ideally happens during assembly of the system. Possibilities for a (semi-)permanent vacuum will be analyzed.

Conclusion

Since the described subsystems are dependent of each other, influences in all directions can be appointed. The influences that are important to consider during the design process are visualized in Figure 31.

This will be used as a guide to develop a number of potential technical solutions.

To determine the effect of certain design choices, different simulations are done with the aforementioned Matlab-script. The results of this are addressed in the next chapter.

2.3 Potential Systems

Introduction

With the potential advantages of a multi-rotor flywheel system in mind, three technological systems were sketched. For these potential systems, the various methods for each of the subsystems were taken into account. First, the solutions for each subsystem are sketched in a morphological overview, which can be viewed in Appendix D. The subsystem solutions are displayed above the system sketches. Each of these potential systems uses a different combination of solutions for each subsystem and therefore has its specific pros and cons.

Stacked multi-flywheel, multi-EM

A compact form factor of the flywheel energy storage system can be achieved by stacking multiple rotors while kept within their own enclosure, this is displayed in Figure 26. By separating the rotors, they will not influence each other in their movement and therefore this type of loss is prevented.
Driving the rotors and regenerating energy is done by a hybrid double stator bearingless switched reluctance motor (HDSBSRM), as studied by Sun et al. (2018). Each of the flywheel systems have their dedicated EM, which can be optimized according to its specific rotor dimensions.
Since many configurations of differently optimized flywheels are possible, the system can be tailored to a specific use case. A user's electricity generation and demand can be analyzed and the system can be designed accordingly. Since the systems are completely independent, they can be changed after installation.

Important questions to be answered when developing this system are:

What are the losses in the HDSBSRM? Is this a viable solution?
Is it necessary to separate the vacuums?

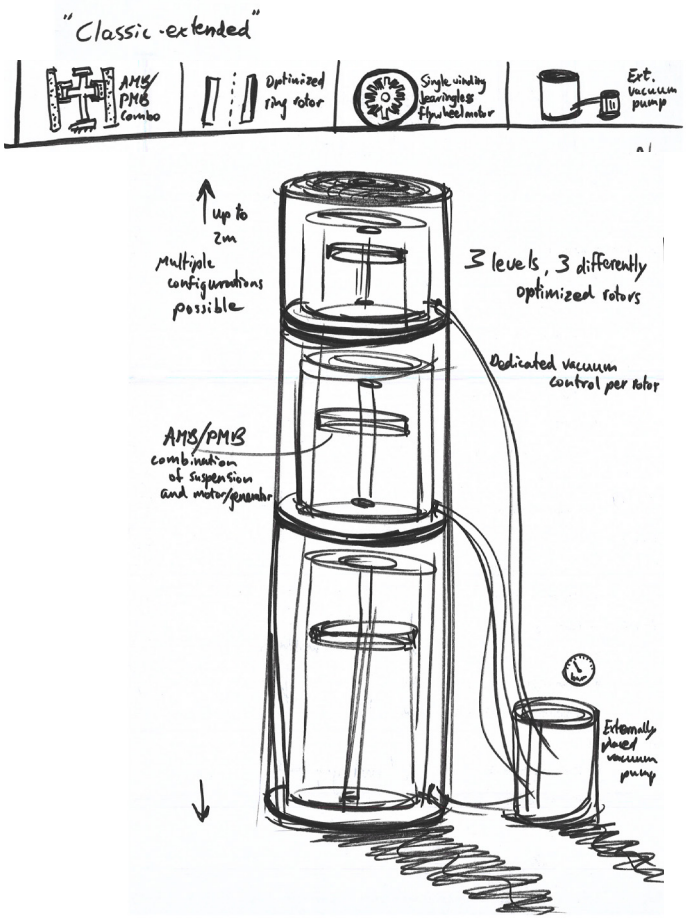

Figure 26: Stacked multi-flywheel system.

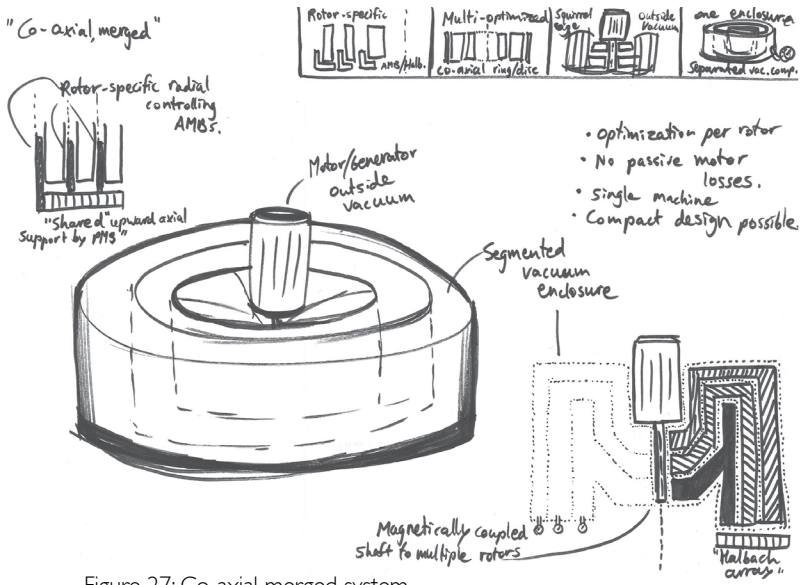

Figure 27: Co-axial merged system.

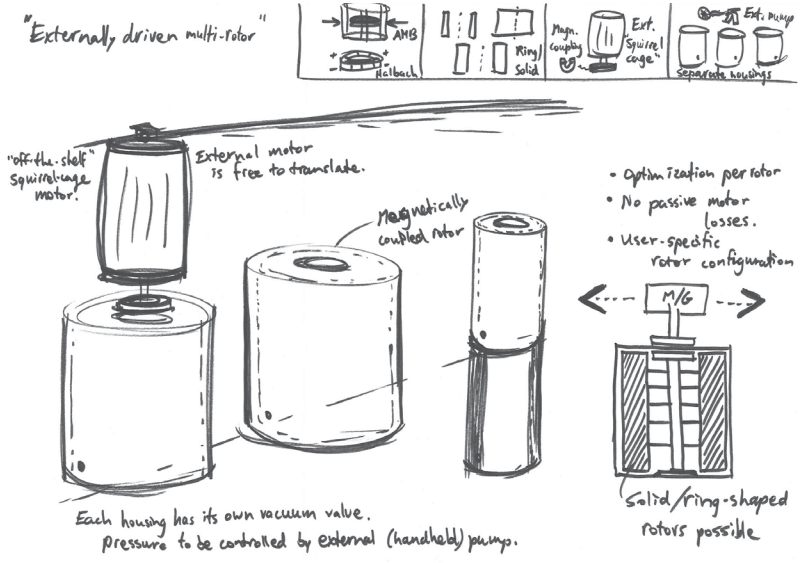

Figure 28: Multy-flywheel array with movable EM.

Co-axial merged, single fixed EM

This concept, shown in Figure 27, consists of three rotors that are enclosed in a single vacuum housing. The electrical machine is connected via a long shaft and is excluded from the vacuum, making is possible to decouple it from the rotors. Motor losses during passive storage are eliminated since continuous rotation is not required. Another advantage of placing the motor outside of the vacuum is the passive cooling can take place. Off-the-shelf squirrel cage motors, as the type that is produced by Nord Drivesystems[105], depend on air cooling which would not function in a vacuum.

The main part of the added mass of all rotors will be supported by a large Halbach-Array of permanent magnets and is therefore passive. Controlling the magnetic suspension will be done by an active magnetic bearing system, which is located on the outside of each rotor.

Coupling and decoupling the motor will be done by a radial magnetic coupling system. This part will have to be defined further in a later stage.

Important questions to be answered when developing this system are:

Is it necessary to separate the enclosure into dedicated space per rotor?
Does movement of one rotor influence the others, even when a (near) vacuum is achieved?
How to achieve the variable magnetic coupling?
How to achieve radial stabilization through AMB?

Multi-flywheel array, movable single EM

Similar to the patent application by David et al. (2017), this system uses an array of separate flywheels that are located in their individual enclosure. Above the array, the EM is suspended to a system that allows it to translate along multiple systems. A similar motor to the type described in the "co-axial merged" concept can be used, combined with a magnetic coupling plate.

An important question to be answered when developing this system is:

Can the use of multiple coupling plates and a transmission between the motor and the rotors allow a fixed position of the motor?

Conclusion

To be able to provide a fair comparison between the presented systems and prove their applicability, it has shown to be valuable to analyze the behavioral differences of various shapes of rotors. Therefore, after exploring the potential systems as done in this paragraph, further research was done into the effects of rotor shapes in a single rotor system.

Figure 29: Embodiment in progress; a prototype flywheel rotor is being lathed.

3. Embodiment

This phase of the project was split up, since there are parallel processes that have been done to get to a final result. The first step was to create a technical concept.

Simulation

In the first place, the most desirable technical product details were chosen by using the subsystems knowlegde and implementing this in a set of calculations; a Matlab-script. Therafter, relevant scenarios are analyzed to test applicability of the system in various contexts.

Prototyping

Validation of the calculated flywheel behavior was done using a functional model; a prototype which is suitable for testing key functional features of the Matlab-script.

3.1 Technical Concept

Introduction

The first phase of embodiment design is defining the inner workings of the system, in other words, the technical concept. This starts with determining the solution's requirements and continues with various options for the rotor subsystem of a flywheel energy storage system. This chapter focuses on the first subsystem, the rotor, since its design is expected to be responsible for all other design aspects.

3.1.1. Requirements

Setting up the list of requirements, which is included in Appendix B, was done with the wishes from paragraph 1.4 in mind. The most important functionality requirements were formulated as follows:

*The system is capable of **mechanically storing** an **excess** of electrical energy produced by a **renewable source** that is generated during an average summer day in the Netherlands.*

*The system is capable of **supplying** the stored energy to the household with energy when renewable energy is **not being generated**.*

3.1.2. Cross-influence of subsystems

As can be seen in Figure 31, the subsystems into which a FESS has been split up, can all influence and be influenced by another subsystem. This is indicated by the dashed gray lines in between.

To illustrate this cross-influencing, Amber Kinetics provides an interesting example:
A system where the optimized rotor is supported by separate parts in the form of stub shafts has been patented by Amber Kinetics in 2019 (U.S. Patent No. 10167925B2, 2019)[106]. The shafts of this type of rotor are supported by a bearing system on the upper and lower end, and driven by a homopolar motor (U.S. Patent No. 20180006539A1, 2018)[107]. This confirms the fact that choosing the rotor shape directly influences the type of motor that should be used. On the other hand, this type of motor/generator limits the possibilities for support bearing solutions.
When combining solutions for different subsystems into concepts, their influence on other subsystems is taken into account.

3.1.3. Multi-rotor advantage

Before generating multiple concepts, the Matlab-script FlywheelCalc (Appendix C) was used to determine the potential advantage of a multi-rotor flywheel system. This was done at this point in the process, since it represents an important design decision. It can also be used to validate the fact that it is possible to design a system that meets the household requirements by combining short-term and long-term storage.
However, further paragraphs will show that the focus shifted to analyzing a one rotor system rather than validating the multi-rotor advantage. This appeared to be necessary, since little was known about the workings of this specific type of FESS and its applicability at residential scale.

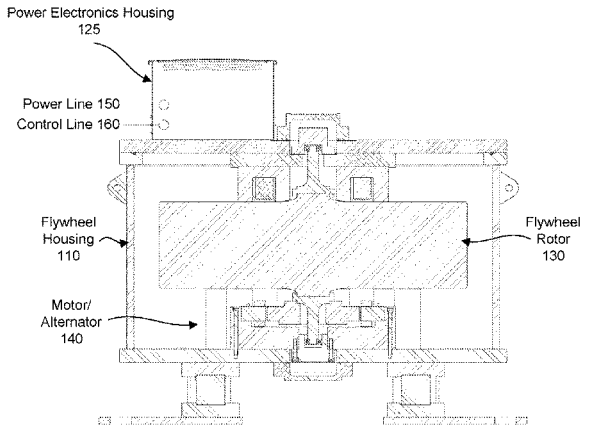

Figure 30: Cross-influence of subsystems,
from U.S. Patent No. 2018006539A1, (2018)

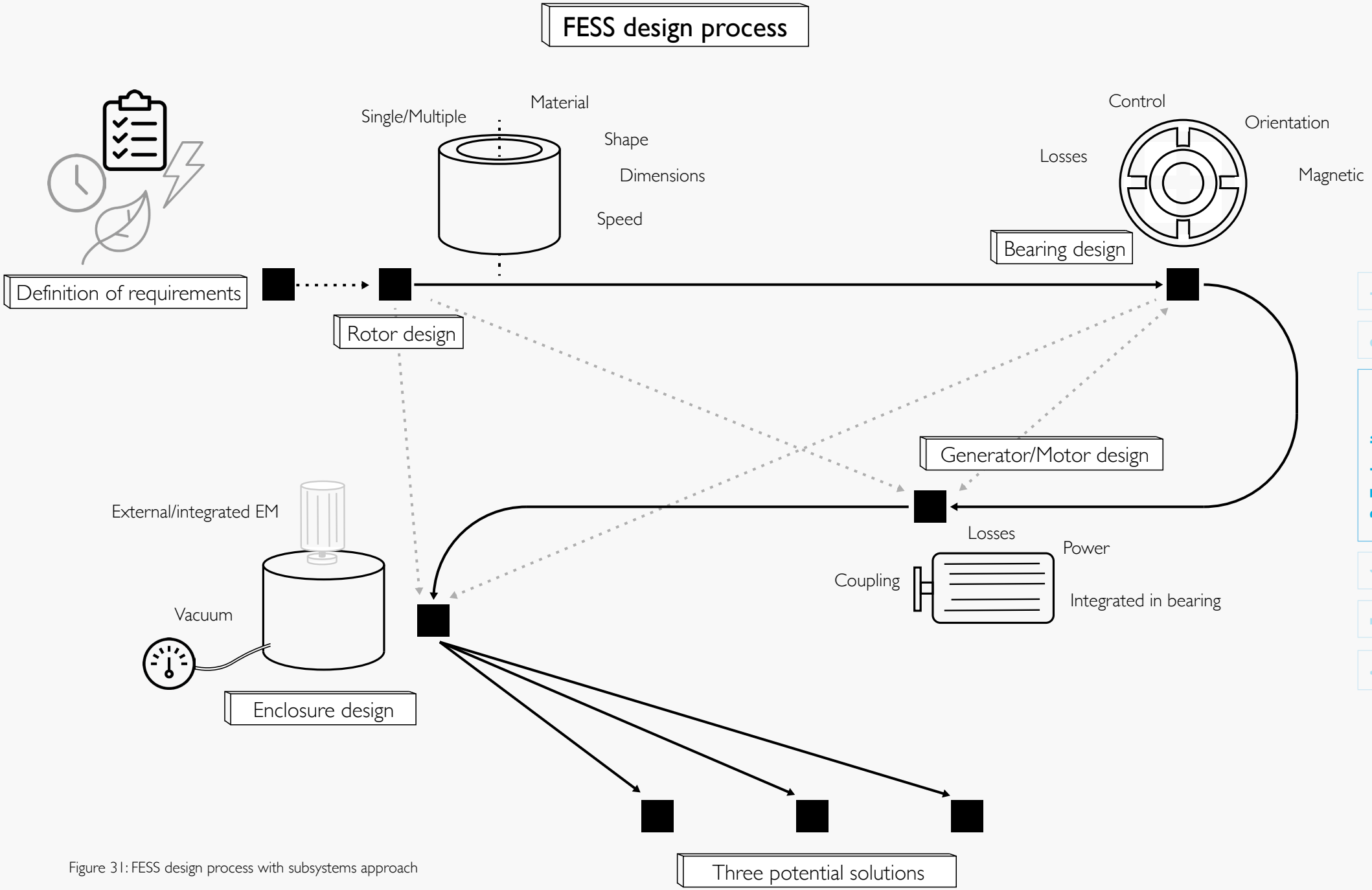

Figure 31: FESS design process with subsystems approach

3.1.4. Rotor dimensions

FlywheelCalc allows the user to define rotor specific dimensions, desired storage capacity and maximum rotational speed. As expected by interpretation of the expressions for energy storage, air resistance and maximum stress, a larger diameter/height ratio results in higher storage capacity at lower speeds.

A short description of the differences between the two main rotor types was given in chapter 2.1, and is further analyzed here.

In general, the following hypotheses are stated:

1. *Lower aerodynamic losses cause longer spin-down times for a larger radius to height ratio of the flywheel rotor.*
   (from initial speed to half speed)

&

2. *Smaller radius*
   =
   Better peak storage

The first of these follows from eq. 2.1 and 2.2 on page 31, since the radius is included as power 4. Increasing this naturally increases the energy that is stored in the flywheel.
The second hypothesis is stated considering inertial effects. A smaller radius results in smaller inertia, which theoretically requires less motor torque to be accelerated. This effect is analyzed in section 3.1.6 on page 46.

The first hypothesis is supported by the first spin-down simulations done with the Matlab-script. As can be read from Figure 32, different spin-down times occur when equal amounts of energy are stored. When looking once more at the first formula for energy storage (eq. 2.1), it can be seen that the rotational speed should be higher when inertia is lower. With one of the main sources of energy losses being aerodynamics, it makes sense to analyze the parameters that influence this.
In the script, aerodynamic effects are simulated using an approach that was developed by Broecker (1959) and used by Skinner (2017)[58]. The following equations show how the resistance is mainly determined.

$$P_{aero} = (M_{top} + M_{bottom} + M_{side})\omega \quad \text{(eq. 3.1)}$$

with:

$$M_{bottom} = M_{top} = \frac{1}{2} c_m \rho_{air} r_{out}^{24/5} \omega^2 \quad \text{(eq. 3.2)}$$

and:

$$M_{side} = 2\pi r_{out}^2 h\tau \quad \text{(eq. 3.3)}$$

$$\tau = \frac{M_{top}}{2\pi\, {}^{5}/_{23}\, r_{out}^3} \quad \text{(eq. 3.4)}$$

Equations 3.5 (Miles, 2011)[82] and 3.6 show how the Reynolds number influences the aerodynamic effects. More on this can be read in paragraph 3.3.
Without going into the meaning of the equations, it can be seen that the influence of the side surface is directly proportional to the height of the rotor. This means that for a larger height-to-radius ratio, the aerodynamic resistance relative to the total surface is larger.

$$c_m = 0.131 * Re^{-0.186} \quad \text{(eq. 3.5)}$$

$$Re = \frac{\rho v r^2}{\mu} \quad \text{(eq. 3.6)}$$

Example of rotor dimensions

Results are a lot easier to grasp than pure formulas, therefore the following example is given. Two rotors are put into the script, with the following characteristics:

Flywheel 1.	**Flywheel 2.**
r = 0.225 m h = 0.7 m	r = 0.7 m h = 0.3 m
max. 15,260 rpm	max. 2400 rpm
8 kWh stored (= 6 kWh usable)	8 kWh stored (= 6 kWh usable)
9.2 h to half speed	**55.3 h** to half speed

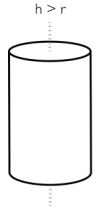

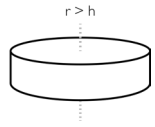

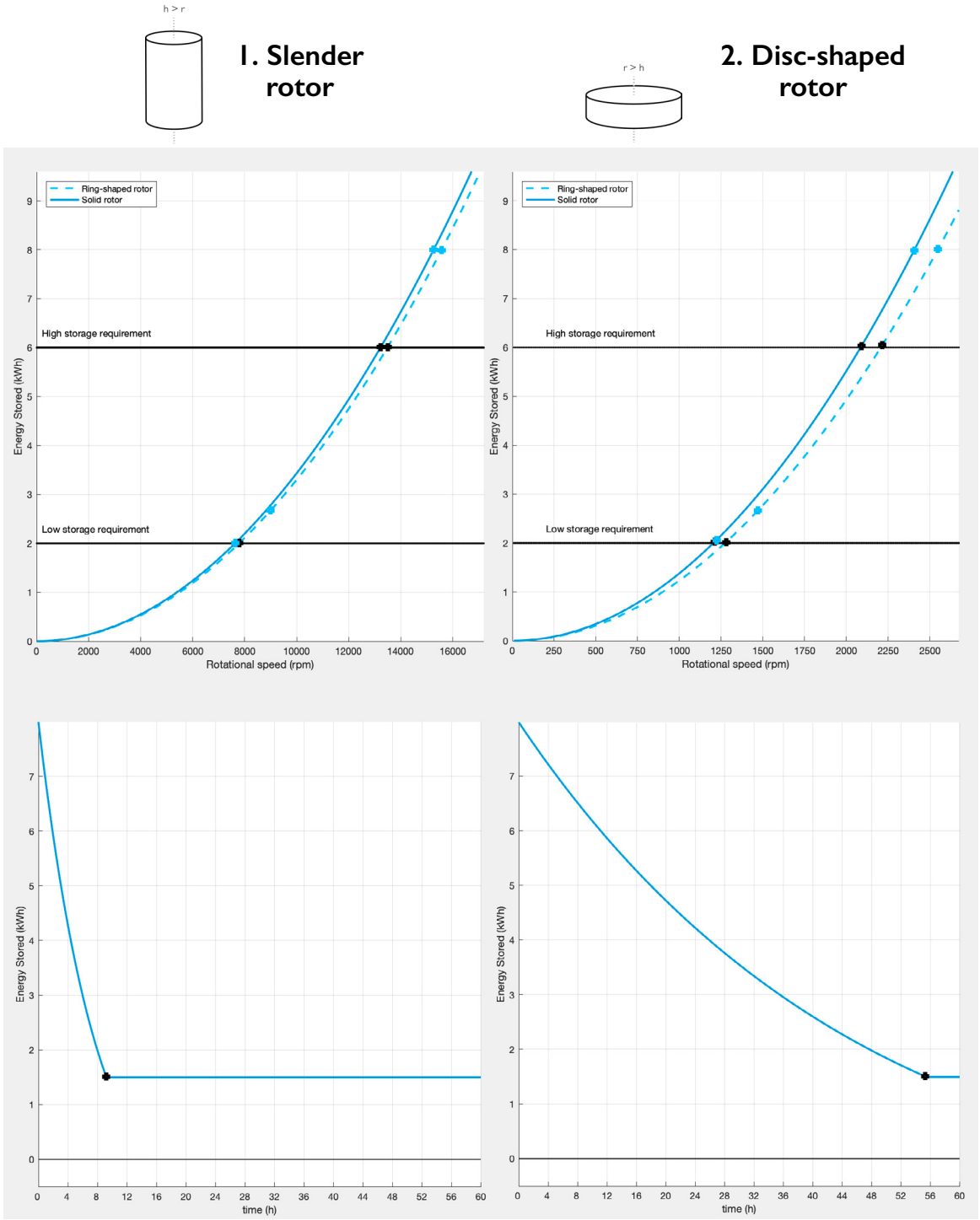

Figure 32: Energy storage and spin-down of differently shaped rotors.

From these results, it immediately becomes clear how the effects of passive losses influence the time that is needed for a spin-down to half of the initial speed. As described in paragraph 2.1, this is the period when electricity can be regenerated.
At an equal amount of energy stored, the slender rotor rotates a higher speed than the disc-shaped one. Since bearing resistance is related to the rotational speed as well, this is also influential. However, it is of much less importance since bearing losses are significantly lower. Especially at the start of the spin-down, meaning at higher speeds, the aerodynamic losses at the slender rotor are responsible for over 85% of the total passive losses. This is therefore the main reason why a slender rotor will be less suitable for long-term storage.

This initial analysis of rotor shapes was done at a pressure of 100 Pa, which classifies as a medium vacuum and is achievable with technology that is currently available. It also results in aerodynamic losses that are low enough to achieve storage for multiple hours.

3.1.5. Validation of calculations

Since the script only approximates aerodynamic resistance using the aforementioned formulas, it is useful to check whether this approximation can be considered a realistic one.
To do so, a functional model, described as number 19 by Loughborough University in their iD Cards (Evans & Pei, 2010)[108], was built. This prototyping and the tests that were done are described in the next chapter.

3.1.6. Peak storage capabilities

As mentioned in the previous paragraph, the hypothetical effect of inertia to energy storage is that lowering the inertia is beneficial for the system's peak storage capabilities.

Since storing energy in a flywheel is basically done by accelerating a mass, the maximum acceleration determines how much energy can be stored within a period of time. The flywheel is accelerated by a motor, which has a maximum torque. For example the motor made by Nord Drivesystems, displayed in Figure 33, which has a maximum torque of 6.75 Nm. According to equation 3.7, dividing this torque by the total inertia gives the maximum acceleration that can be realized in the system.

$$\alpha_{max} = \frac{T_{max}}{J} \qquad \text{(eq. 3.7)}$$

To determine the acceleration that is required to be able to store all available energy, the supply/demand/system power profiles from chapter 1.2 were used.

In certain scenarios, sudden peaks in solar power require a large amount of extra energy to be stored in a short period of time. The increase of charge power is high at these moments, requiring a higher acceleration of the flywheel.

To help in understanding what is calculated, Figure 37 was drawn. In this figure, two methods of calculating the charge rate of the system are compared.

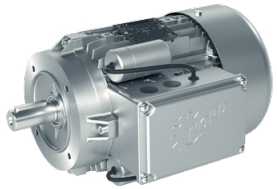

Figure 33: Nord Drivesystems single phase 2.2 kW electric motor. (Nord Drivesystems, 2019)[92]

Method P_charge

The most simple way of calculating the amount of energy that will be stored in the flywheel is to calculate the power transfered from the solar panels to the motor, keeping into account both panel and motor efficiency. This directly results in the amount of energy that is stored. To compare to the maximum acceleration, which is limited by motor torque, this difference in energy is converted into the required acceleration for storing this amount of energy. This is done by calculating the rotational speed that belongs to the system's energy stored at a certain point in time, and determining the difference with the speed one second later.

Method I_charge

The calculation method where inertia can be included makes use of the current that is generated by the solar panels at a certain irradiance (W/m^2). The data source for this is the same as the other method, the only difference is that the data is handled differently.

The current can be translated into the torque delivered by the motor, via the motor constant that is supplied by the manufacturer. The last step is to divide this value by the inertia of the flywheel. Motor inertia is neglected, since it is much smaller than this of the flywheel.

Inertial effects

This calculation method has shown that the fraction of energy that can be stored is limited by certain combinations of motor and rotor.

For a supply-scenario where steep peaks occur (Figure 34), combined with a high-inertia flywheel, high torque is required from the motor. Figure 35 shows the theoretically available charge power during 24 hours (in kW) as the light line and the transfered power to the system due to inertial effects as the dark thick line. The area enclosed by the two lines can be understood as the power that is "lost" by lack of acceleration.

Lowering the inertia by adjusting the flywheel's dimensions prevents these losses, as shown in Figure 36. The settings for this simulation are identical, except for a reduced rotor radius, which reduced the inertia. It is easily seen that the area below the peaks has become smaller and therefore less energy is prevented from being stored because of inertial effects. Another solution for loss prevention is choosing a motor that has a higher maximum torque.

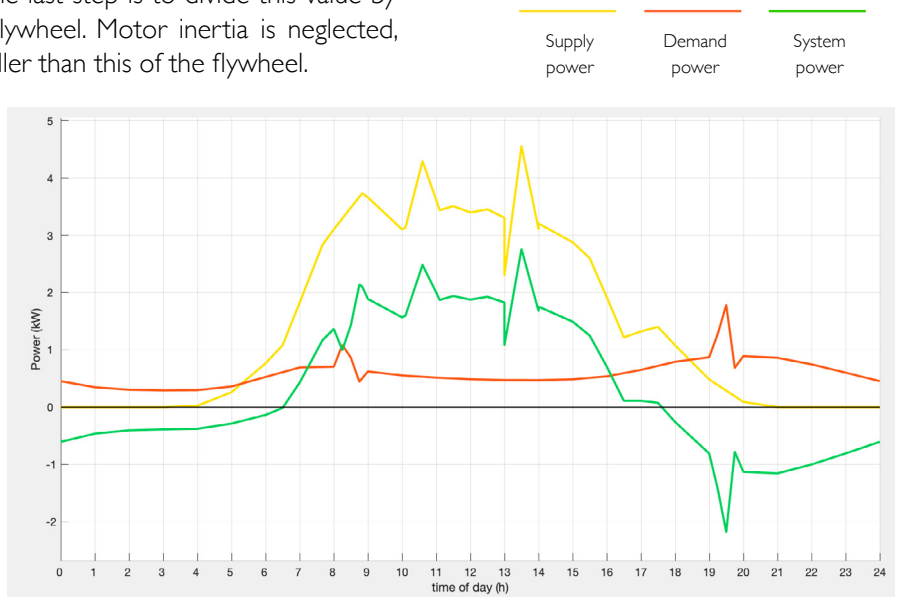

Figure 34: Supply & Demand profile with solar power peaks.

Initial moment of inertia

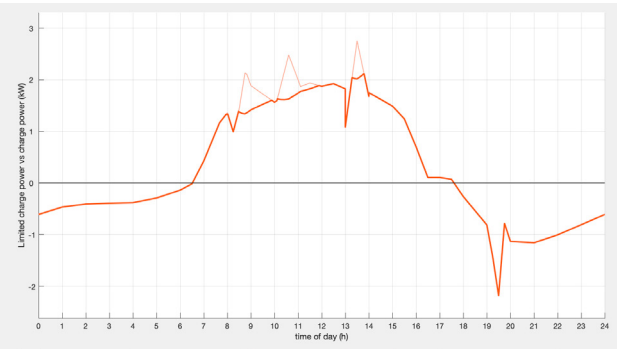

Reduced moment of inertia

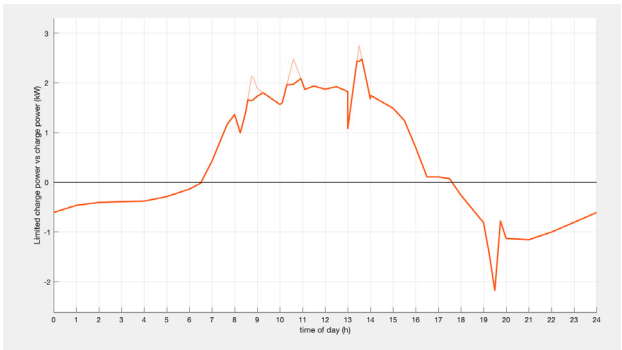

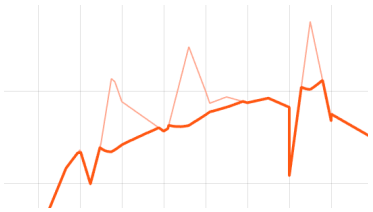

Peak charge power

Transfered power

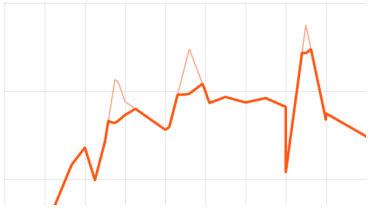

Figure 35: Limitation of charge power by intertial effects.

Figure 36: Reduced limitation of charge power by intertial effects.

Smaller radius
=
Better peak storage

Conclusion

Torque losses occur when a large amount of energy needs to be stored within a short period of time. These losses can be minimized by optimizing the inertia to motor torque. The hypothesis that is displayed above is therefore confirmed, since a smaller radius does result in a smaller moment of inertia. It is however not complete, since there are more influencing aspects. Especially motor torque, which has proven to be an important factor.
Expanding the script's capabilities to be able to do this, is therefore done during the product detailing phase. The inertial effects were kept in mind during dimensioning of systems, but optimization is left for a potential next phase.

The analysis in this paragraph has proven the importance of rotor design to the development of a flywheel energy storage system. On one hand, its shape and dimensions determine how much and for how long energy can be stored. On the other hand, its moment of inertia combined with the applied motor/generator determines whether energy will be lost due to inertial effects during the conversion from electricity to kinetic energy.

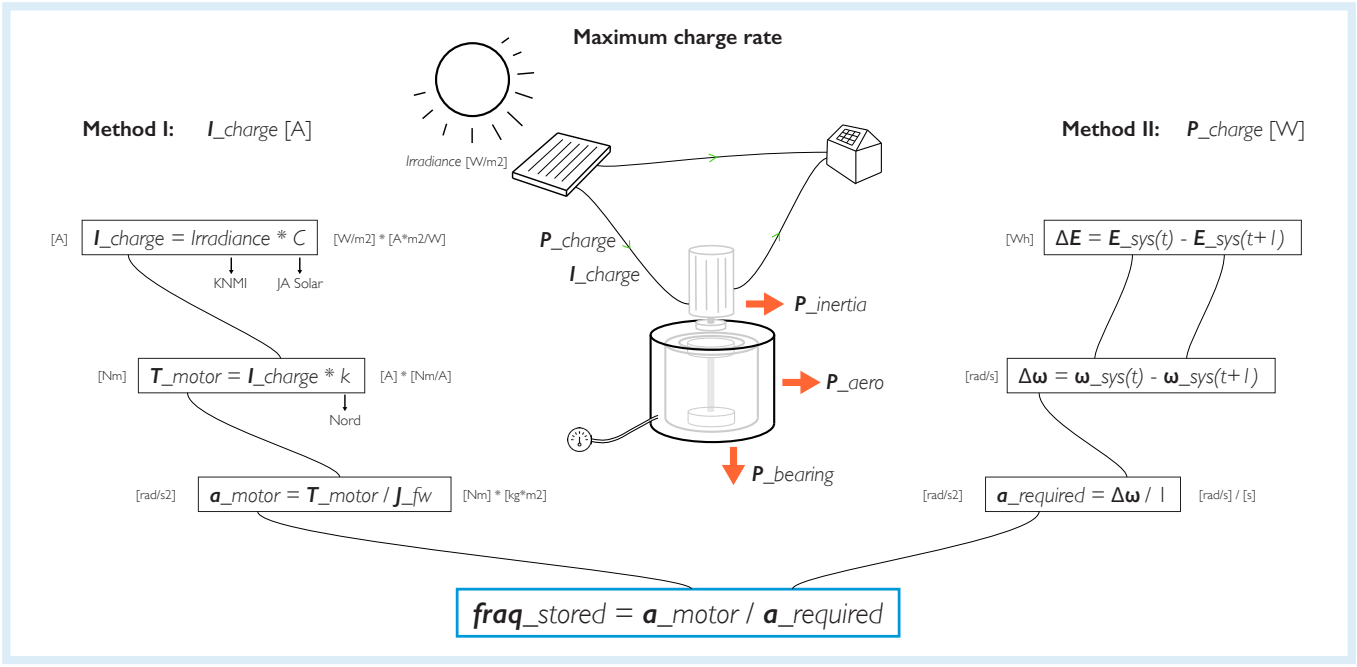

Figure 37: Calculation steps for determining inertial charge losses.

3.2 Scenario simulation; Embodiment phase I

Introduction

The script FlywheelCalc helped picturing the effects of applying different dimensions to various scenarios and allowed further specification of the design.
As described in section 3.1, the script was already used to understand the effects of changing the flywheel's dimensions. Using the results and virtually "testing" the systems for various scenarios has provided insight in the link between the dimensioning of a flywheel and the scenario in which it is applied as method for energy storage.
FlywheelCalc allows manual input of the flywheel's characteristics and offers a choice of scenario data. As displayed in Figure 38, visual feedback is given by displaying a small drawing of the flywheel's size (in meters).

3.2.1. Average daily energy profile

In Chapter 1.2, two different scenarios for supply & demand were drafted. These are the main comparative sources for checking the applicability of a FESS.

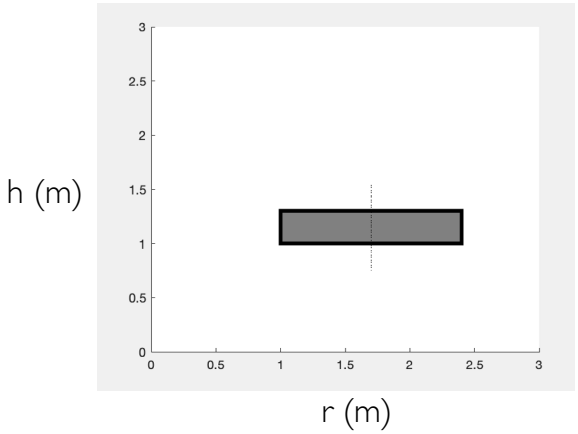

Figure 38: Visual feedback of the set flywheel's dimensions

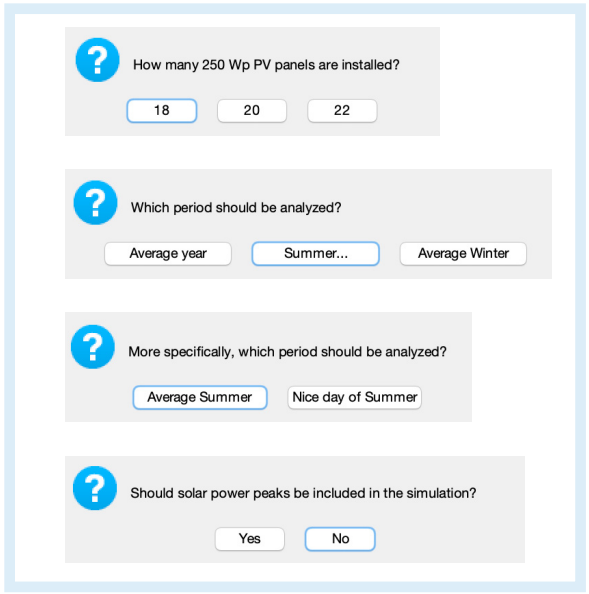

Figure 39: Data selection pop-up selection of FlywheelCalc

A series of pop-ups lets the user select which scenario should be applied for the simulation. The main reason for this is ease of use, even though I am currently the only user. This is done as a step in the direction of a user-friendly application that can be used in the design process of a FESS.

When selecting 18 panels with a peak power of 250 Wp (Watt-peak) and choosing such that the average summer day without occasional peaks is considered, the supply & demand data as displayed in Figure 40 is given. Consistently with the scenario that was described in Chapter 1.2, this is the scenario for which the system is designed. The FESS should be able to store a sufficient amount of energy and mitigate the need for grid power. FlywheelCalc takes this data and combines it with the manually entered flywheel characteristics and uses this to determine the applicablility of this system.

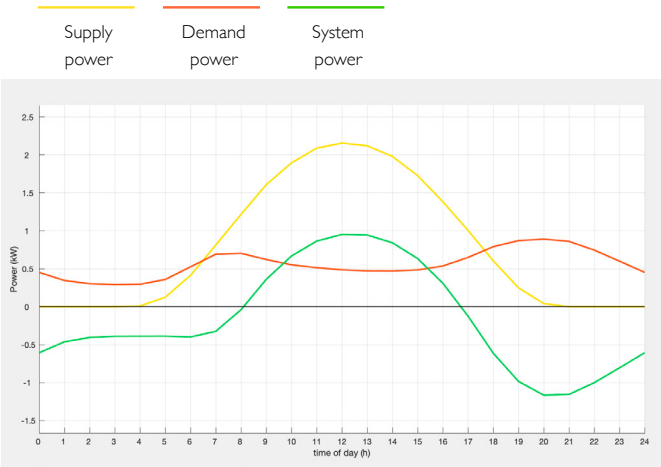

Figure 40: Suppy & demand plot for an average summer day.

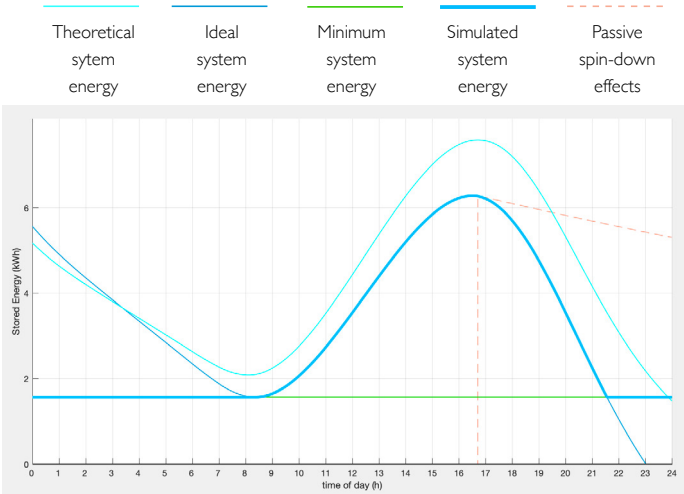

Figure 41: System energy during an average summer day.

3.2.2. Required vs available energy

To determine whether the household can be provided with electricity from the flywheel during the moments without available solar power, the energy that is stored in the FESS at that point in time should be known. As seen in the green line in Figure 40, this is required from around 16:30h until 08:00h on the next day.

Not only does this require a passive spin-down time of at least 16 hours, the energy in the system should add up to around 10 kWh of electricity. However for this scenario, the excess of solar energy is only 5.51 kWh during the 24h that were simulated. This means that during an average summer day with 18 panels of 250 Wp, insufficient solar power is generated for off-the-grid living.

Two scenarios

As mentioned in section 2.1, the energy stored in a flywheel can be regenerated until it has slowed down to 50% of its initial rotational speed. Keeping in mind the equation for flywheel energy storage (Eq 2.1), this means that 25% of the energy stored should be accepted as leftover in the system. Therefore, designing a system that is capable of storing all of the excess solar energy, requires it to be capable of storing at least 25% of additional energy. Storing this amount of energy was analyzed for two scenarios.

Partially off-grid day

Since the energy demand between 16:30h and 08:00h exceeds the available excess energy, it was accepted that grid power is needed. The amount of energy that can be stored is sufficient for household use until 21:30h in the evening. Meaning around 5 hours of electricity is regenerated from the flywheel's rotation in this scenario (see Figure 41).

After the minimum rotational speed has been reached, it is proposed to keep the flywheel spinning by using grid power. This prevents the system to come to a full stop, which would induce unwanted control problems (Ahrens, 1996)[109] and require extra energy input for acceleration. During the time where the rotor is kept at this speed, the only power that is needed is the added power of all types of losses. Bearing resistance and aerodynamic losses at this speed (~1200 rpm) are respectively 59.5 W and 11.1 W, adding up to 70.6 W of power required to retain this speed. During the hours when no solar power is available, until 05:00h the next morning, this energy is drawn from the grid. This adds up to 7.5 hours, which equals 1.9 kWh.

Although this number is high, it is lower than the average household's energy use between 16:30h and 21:30h, which lies around 4 kWh. This means that close to 80% of the excess of solar energy was made usable on a later moment, by means of the FESS.

Lowering the losses would mean that retaining minimum rotor speed requires less energy would increase efficiency of the system, but is not considered in this study. The possibility of letting the rotor come to a full stop and then accelerating it is also not analyzed. However, these effects might be less critical than estimated before.

A full day "off-the-grid"

When analyzing the supply & demand-profile that was displayed in Figure 34 of the previous chapter, different results are obtained. This profile is shaped according to a nice summer day (July 8th 2018) and includes occasional peaks in both supply and demand.

When 18 solar panels with 250 Wp are used, 15.37 kWh of excess energy is generated. Storing all of this requires a higher rotational speed, increasing the passive losses. However, analyzing this scenario showed that the household does not require any grid power during all 24 hours of this day. Since this simulation is done for only one day and energy is only stored starting around 06:30h, one should keep in mind that multiple consecutive days have to occur for the system to work as simulated.

Figure 43 shows the energy in the system when the nice-day-scenario is simulated. What is most important to note here, is that the energy in the system (for the ideal case) will not dip below the minimum-energy line, meaning that the system does not require grid power to keep spinning.

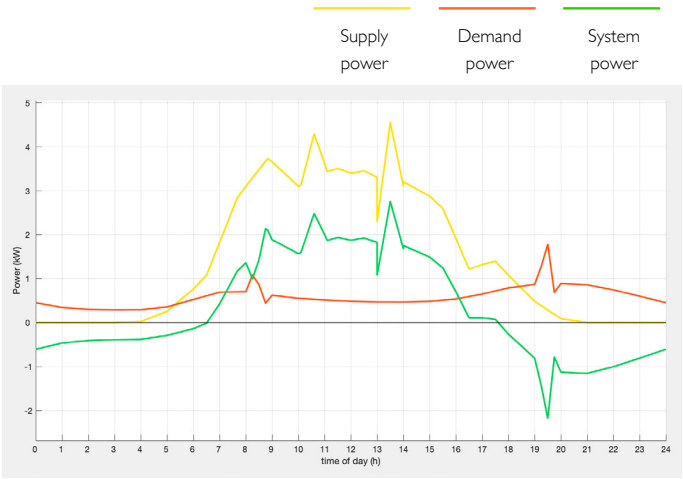

Figure 42: Suppy & demand plot for a sunny summer day.

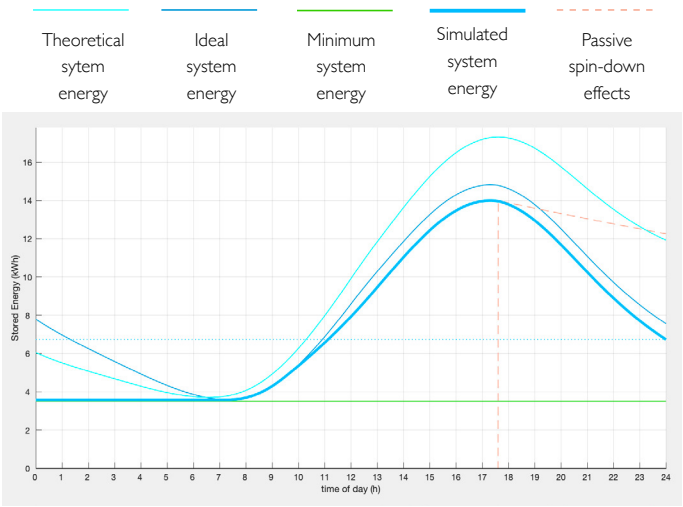

Figure 43: System energy during a sunny summer day.

However, including the inertial effects that were described in paragraph 3.1 shows that in this case not all of the available energy will be stored, causing the storage peak around 17:30h to be lower. This means a full off-grid day cannot be achieved with the setup as simulated. An even sunnier day, or a day with different peaks can result in such a day even for the system as defined for this simulation.

3.2.3. Scenario specific optimization

Another solution would be to install a larger number of solar panels, which would increase the available power. Without changing any other aspects, the inertial losses will be higher, which introduces the need for another motor or lowered inertia.

Conclusion

From this, one can conclude that each scenario requires a different setup to store and regenerate as much of the excess solar energy as possible. Because of the many cross-influencing design aspects of a FESS (see Figure 31 on page 43), creating an all-round system is complicated. In order to apply to as many different users as possible, the final product will be made household-specific according to a supply & demand analysis. More about market implementation can be read in chapter 4.2.

3.2.4. Types of households

As mentioned before, the final product will be made household specific. It is important to set the boundaries within the product will be customizable, this is done by two user profiles, described as households.

Two-person household, work from home

In a home where only a few people live (Figure 44), the energy consumption typically has lower peaks. Less electronic devices are used simultaneously and for example smaller kitchen appliances are present. However during office hours, the house is still used actively and electricity is needed for lighting, heating and a computer. All in all, the energy demand profile is flattened and allows for a relatively small set of solar panels. Combining this with higher mid-day energy use means there will be little excess of solar power.
This persona fits with the previously described scenario of a "partially off-grid day". This means that the suggested storage system will be one that is designed for short-term storage.

Six-person household

A household with six people (two parents and four children, Figure 45) typically has a high energy consumption. A set of solar panels will be calculated according to the utilization of large kitchen equipment and for instance a higher frequency of wash cycles. In a family where, during weekdays, both parents are working away from home, the house will be in a low-usage state between 08:00 am and 17:00 pm. The relatively large set of solar panels generates enough energy during higher demand phases but leaves more excess at mid-day. The storage system for this family will therefore require to store more energy for a longer period of time.
This persona fits with the "full day off-the-grid" scenario. A flywheel energy storage system designed for this family will look very different from the short-term version described above.

Figure 44: Two-person household. (Top image)

Figure 45: Six-person household. (Bottom image)

3.3 Prototyping & validation; Embodiment phase II

Introduction

As mentioned in chapter 2.1, different rotor dimensions have different characteristics. Especially concerning aerodynamic resistance, it is necessary to test whether the FlywheelCalc script is calculating this aspect in the correct way. Therefore, a functional model was built, that is suitable for testing two types of rotors; a flat disc-shaped rotor and a tall slender one. The model will be scaled down by a factor of 10 compared to the calculations that were done, making the prototype feasible to build within a limited time and keeping costs to a minimum. Another advantage of scaling down is caused by the characteristics of aerodynamics. On page 53, scaling effects are explained. In Figure 46, the main measurements of both rotors are displayed. The test speed, energy stored and spin-down times below the figure have been determined by FlywheelCalc.

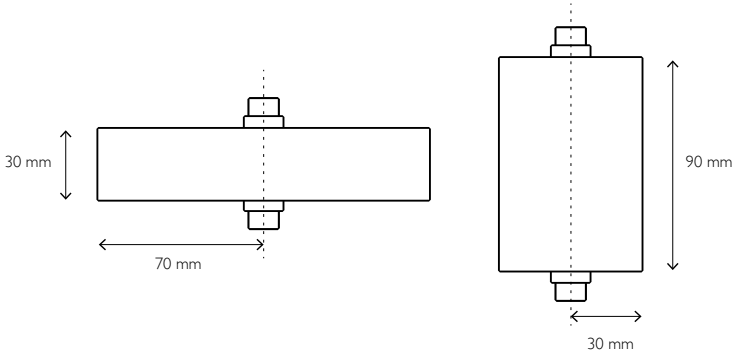

Speed:	**1404**	**rpm**	**4412**	**rpm**
Energy stored:	**96**	**J**	**96**	**J**
Spin-down:	**278**	**s**	**67**	**s**

Figure 46: Disc and slender test rotors and calculated data.

3.3.1. Goal of the prototype

Validation of the calculations will be done by a spin-down test. One rotor at a time will be placed in the prototype's housing and rotated up to its initial speed. From that moment, it will experience bearing resistance and aerodynamic losses. These losses will cause the rotor to slow down, up to the moment when half the initial speed has been reached. The half-speed spin-down is an important characteristic for flywheel energy storage, since energy can only be efficiently regenerated during this time (see paragraph 2.1).
Spin-down tests were executed with both rotors, under various levels of vacuum. Since aerodynamic losses are influenced heavily by air pressure, this will confirm or deny whether differences in spin-down times are occurring because of this phenomenon or if they have a different cause. From the hypotheses stated in paragraph 3.1, the following is expected from the test:

> *Lower aerodynamic losses cause longer spin-down times for a larger radius to height ratio of the flywheel rotor.*
>
> *(from initial speed to half speed)*

Fair comparison

Making sure the test is only considering the differences in aerodynamic losses was done by keeping as many of the influential parameters constant for both rotors. Only the type of rotor, rotational speed and air pressure were varied. As can be seen in Figure 46, both rotors, even though spinning at different speeds, store the same amount of energy.

3.3.2. Bearings

The prototype uses standard ball bearings, a decision that has two main reasons. The first one being complexity of the system, and the second being the good availability of ball bearing's characteristics. One of the world's leading bearing manufacturers SKF provides the online tool "SKF Bearing Select"[110] which outputs

bearing friction for a defined load and rotational speed. The original version of FlywheelCalc makes use of magnetic bearings, and was adjusted to calculate the model's spin-down effects as realistically as possible by entering the bearing friction from SKF's data.
To be able to compare the test results with the full scale flywheel, bearing data was also obtained for the corresponding rotor mass and the effects were calculated.

3.3.3. Magnetic drive

Positioning the motor outside the vacuum offered a simple solution for keeping the low pressure chamber as small as possible, but introduced the challenge of connecting the driving end to the rotor axis.
Decoupling the motor from the rotor during the spin-down test eliminates unspecified motor losses and ensures bearing and aerodynamic losses are the only significant losses at play. However, decoupling a rigid connection at high speeds is challenging.
A magnetic coupler solved both of these challenges by allowing the vacuum to be fully closed and the rotor to be driven by two circular magnetic plates at a few millimeters distance from each other. Figure 48 shows how the plates are positioned. The drive system consists of two 3D printed discs with both 16 neodymium magnets, each having a magnetic force of around 9 N. The actual connection force will however be lower, since the magnets are positioned with an air gap in between. Figure 49 shows the circular pattern in which the 16 magnets are placed. The poles of the magnets are positioned in an alternating way, this way the attracting force establishes a connection and the repelling force to the next magnet prevents "hopping" to a neighboring magnet. Lowering the chances of skipping.

A basic test was done by 3D-printing a standing axis, two magnet-containing discs and a few spacers with

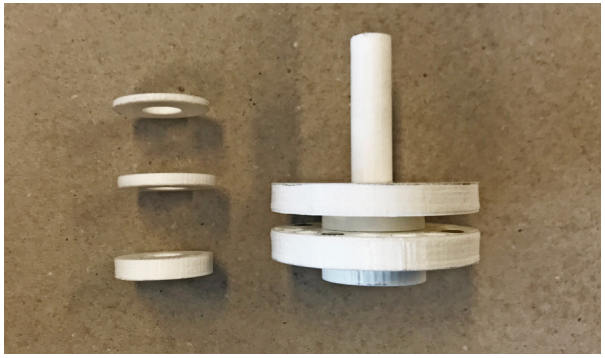

Figure 47: Magnetic drive test model

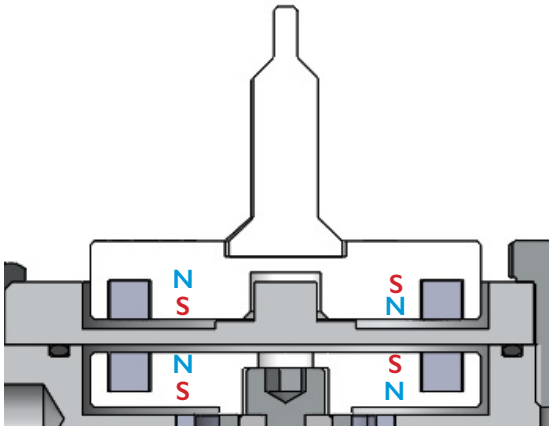

Figure 48: Magnetic drive positioning, with magnet poles

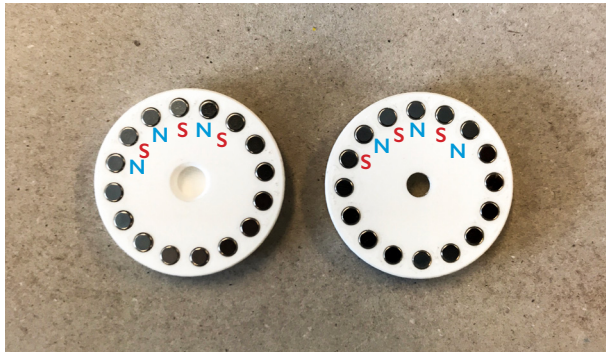

Figure 49: Magnetic drive discs, with pole indication

varying thickness, to determine the maximum distance between magnets for which the drive torque reaches an acceptable level. The results of this tests were purely to get an indication of torque, and since the rotational inertia of the test rotors is relatively low, a simple hand-powered test was considered sufficient to determine the acceptable torque level. The magnetic drive model is displayed in Figure 47, where the chosen distance between the magnetic discs is 4 mm.

3.3.4. Vacuum: Scaling effects

Aerodynamic drag is calculated by using equations 3.1 to 3.4, as discussed in paragraph 3.1. An important factor that is found in all components of the drag calculation is the reduced moment coefficient c_m, which depends on the dimensionless Reynolds number *Re* according to equation 3.5 on page 34. The expression for the Reynolds number when rotation is considered was stated in equation 3.6, and shows the influence of the radius.

$$Re = \frac{\rho v r^2}{\mu} \qquad \text{(eq. 3.6)}$$

To obtain representative aerodynamic effects with the scaled-down model, the Reynolds number should be equal to that of the full-scale calculation. Since this equation includes the radius squared, scaling down with a factor 10 means that the Reynolds number can be kept equal by multiplying the density by 100. This can be achieved by decreasing the level of vacuum, which comes down to a smaller pressure difference to realize. Therefore, a full scale simulation at 4 Pa means that a 1:10 scale model needs to operate at 400 Pa.
Fortunately, this only decreased the difficulty of building a scaled model, since forces on the model are relatively low and a conventional vacuum pump was sufficient.

3.3.5. Structure of the model

A functional model captures the key functional features and underlying operating principles. It has limited or no association with the product's final appearance. Number 19. (Evans & Pei, 2010)[105] The design of the prototype that was built is consistent with the definition in Loughborough University's iD cards. It allows the previously described testing of two different rotors and is built in a cost-efficient way.

Two aluminum main plates that were CNC milled, combined with threaded rods allow mounting the rotors without changing costly components. Figure 51 shows how the model was made capable of swapping the rotors, and how other parts are used to allow for easy testing of the two rotors.

Figure 50: Partially-assembled prototype.

In the cutaway render, the slender rotor is mounted, with its narrow plexiglass tube to retain the vacuum.

The top and bottom plate contain grooves in which O-rings are mounted. These rings are compressed by fastening the nuts on the threaded rods and ensure sealing of the vacuum. Figure 52 shows how the O-ring seal is configured at both the top and bottom edges of the plexiglass tube. A two-stage groove allows a maximum O-ring compression of 25%, protecting the ring from breaking and ensures the chamber to be sealed sufficiently

An O-ring is also placed below the top plate that seals the vacuum enclosure near the magnet coupler.

The top plate contains two air channels that help realizing the low pressure. The one that is visible in the cutaway makes connecting the vacuum pump possible. A similar channel is positioned at the other edge of the top plate and connects a manometer to the model.

The air gap around the rotor is kept constant for both rotors, adding to the equal aerodynamic comparison.

Mounting the magnetic coupling plate to the rotor has been done through a simple screw that is flattened on both sides and glued inside the 3D printed part. The top of the coupler that is positioned outside of the vacuum connects to an electric drill or high speed rotary tool and is positioned by hand on the top plate. This makes it possible to remove the electric drive after the initial rotor speed has been reached.

Technical drawings of the three CNC milled plates, as well as the ones used for lathing the rotors, can be found in Appendix D.

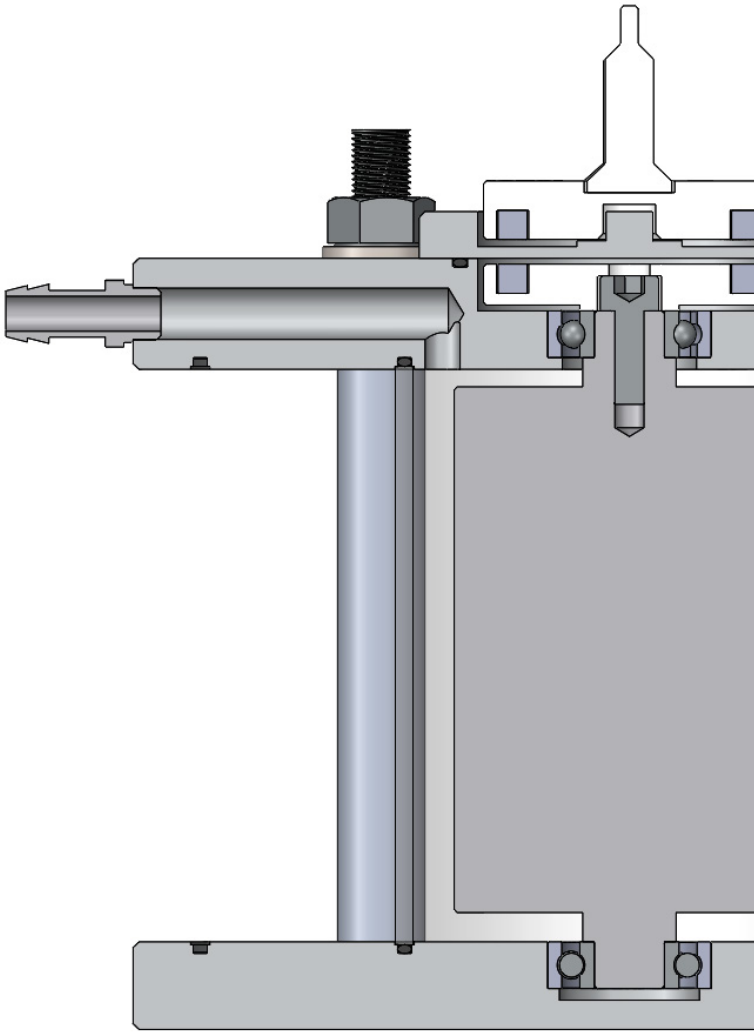

Figure 51: Cutaway of the 3D prototype model, with the slender rotor

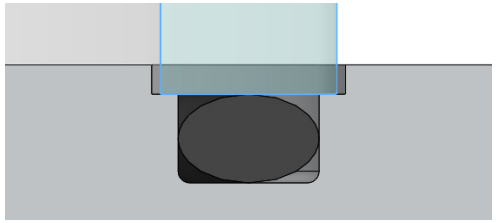

Figure 52: Cutaway of the O-ring configuration

3.3.7. Unforeseen effects

A number of trials were conducted before starting actual validation of the script. During these trials, two factors were discovered that negatively influenced the testing.

Bearing resistance

After the first trials, the conclusion following conclusion was drawn:

When two of the standard type, open cage deep groove ball bearings (SKF 6001) are used, their resistance strongly influences the rotor's spin-down time. It should be minimized to be able to analyze aerodynamic losses.

Test conditions and potentially some design aspects of the prototype cause the friction losses to be higher than calculated with the SKF bearing select calculator.[112] Removing the top bearing resulted in reduced friction, but spin-down times were still far from the calculated duration.

Implications to validation

Varying air pressure did not noticeably influence spin-down times, when the standard type bearing is used. Therefore, more tests are conducted with an energy efficient type of bearing, the SKF E2.6001. This type was recommended by the bearing specialist at supplier Eriks during a phone conversation. (Tollig, F., 2019)[111]

Figure 53: The standard open type 6001 bearing and the energy efficient alternative; E2.6001. Both made by SKF.

Using the E2 bearings shows marginal improvements of the spin-down times. However, during assembly, another phenomenon was discovered.

Induced electromagnetic force

When the rotor was rotated without the magnetic coupling plate mounted to it, resistances seemed much lower than before. This motivated to conduct a full test without this coupler.

The resulting spin-down times were significantly longer than with the magnet coupler attached. An explanation for this difference can be found when looking into Lenz's law. (IsaacPhysics, 2019)[112] This law states that a current is induced when a conducting material (such as aluminum) moves relatively and perpendicular to a magnetic flux.

A counterclockwise rotating current is induced at the front edge of the magnet, and a clockwise current at the rear end (see Figure 54). These currents (displayed as ***i***) are called Eddy currents (Wikipedia, 2019)[113] and create magnetic fields in the aluminium seal plate. According to Lenz's law, the first is directed upwards and the second downwards (***B***). Both fields are interacting with the permanent magnets' fields and create forces (***F***) that are working against the motion of the disc, slowing it down and therefore reducing the spin-down times of this test.

Implications to validation

Unfortunately, driving the flywheel within the vacuum became impossible. Testing now required accelerating faster than the initial test speed, then mounting the seal plate and setting the air pressure before starting the measurement.

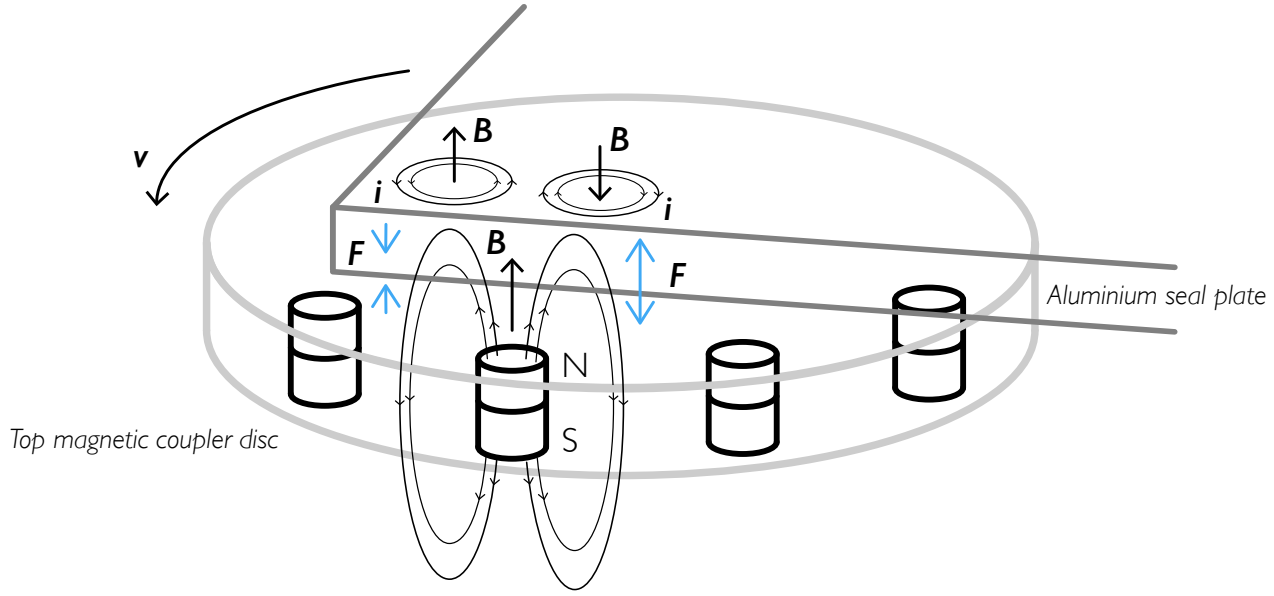

Figure 54: Visualization of induced currents, causing Eddy current braking (adapted from Wikipedia, 2019)

3.3.6. Validation

The original procedure for conducting spin-down tests was as follows:

1. The pressure is set to 1, 0.5 or 0.1 bar.

2. The magnetic drive plate, mounted to a variable speed electric drill is positioned on top of the seal plate.

3. Acceleration of the flywheel is done by slowly increasing the speed of the electric drill.

4. The tachometer is turned on and measures the rotational speed every second.

5. When the flywheel reaches its initial speed, the magnetic drive is disconnected and the spin-down starts.

6. At the moment of disconnection the timer is started, it is stopped when the rotor reaches half of its initial rotational speed.

However, because of the induced electromagnetic force, explained in the previous paragraph, step 1 to step 3 were switched and pressure was set after driving the rotor by directly connecting it to the electric drill.

To determine which type of resistance most significantly influences the spin-down time, not only air pressure is varied, but alternative setups of the suspension by ball bearings have been tested.

The rotor speed for the disc-shaped rotor that was mentioned in Figure 46 (1404 rpm) appeared to be relatively low and resulted in short spin-down times. This also meant that only small differences were measured when varying the pressure. Therefore, the initial speed was increased to 2000 rpm.

Script vs Prototype

To validate the calculation script, the test results should be consistent with the simulation results. As mentioned before, the prototype's ball bearings are simulated using SKF's calculator to allow for a fair comparison.
The lowest internal pressure that can be realized with the prototype is 0.1 bar. Validation pressures therefore lie between this and atmospheric pressure (1 bar). At these pressures, the script is executed and spin-down times are noted for both rotors.

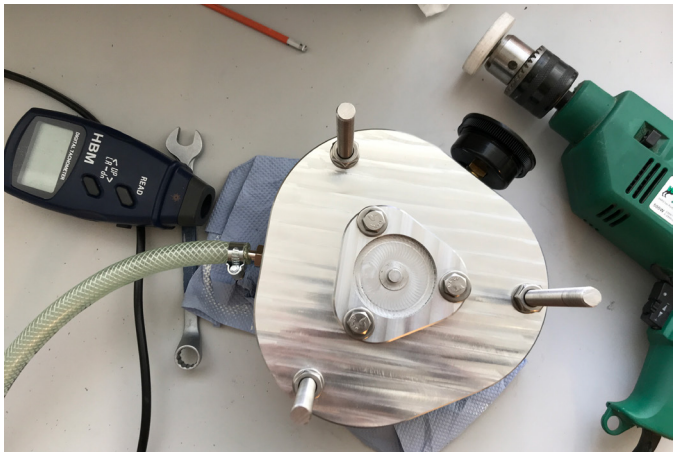

Figure 55: The setup for validation testing. The laser tachometer on the left, the electric drill on the right.

Spin-down comparison of the disc-shaped rotor resulted in:

Disc-shaped rotor (2000 - 1000 rpm)

Pressure	Script	Prototype	Δ	%
1 bar (atm)	168 s	302 s	134	44
0.5 bar	212 s	332 s	120	36
0.1 bar	285 s	355 s	70	20

Here, the script seems to be accurate for the lowest tested pressure of 0.1 bar.

The spin-down results of the slender rotor resulted in:

Slender rotor (2200 - 1100 rpm)

Pressure	Script	Prototype	Δ	%
1 bar (atm)	41.4 s	46.6 s	5.1	11
0.5 bar	43.6 s	47 s	3.4	7
0.1 bar	46.5 s	45.8 s	0.7	1.5

The most accurate results for the slender rotor also occur when simulating closer to atmospheric pressure.
Since spin-down times for the disc-shaped rotor are generally longer, this allows for larger spreads of the measurements. The calculated values for the slender spin-down all lie within a spread of a few seconds, making the accuracy of the measurements a problem. However, the results seem promising for the lowest pressure. Only a small difference with the simulation was shown.

Spin-down resistance

The graphs in Figure 56 and Figure 57 represent the measured and simulated data for the disc-shaped and the slender rotor respectively. The continuous lines illustrate the measurements obtained from testing the prototype, whereas the dotted lines are produced by simulation using the Matlab-script.
Both graphs are plotted with the spin-down time (s) on the x-axis and the rotational speed (rpm) on the y-axis.

What immediately stands out, is that the simulated lines are starting to flatten out at lower rotational speeds than the measured lines. Until the half-speed point has been reached, the slope of the lines varies.
For both rotors, decreasing the pressure from 1 bar down to 0.5 and 0.1 bar shows a decrease in the difference between simulation and validation.
Analogous to the data on page 56, the measured spin-down times for the disc-shaped rotor lie relatively far from the simulated values. When looking at lower speeds, for example at 1/4 of the initial speed (~500 rpm), the measured times approach the simulated.
Simulating the half-speed spin-down of the slender rotor seems to be more accurate, since the lines drawn according to the measurements show similar slopes to the calculated. The next paragraph will go into the potential reasons for these results.

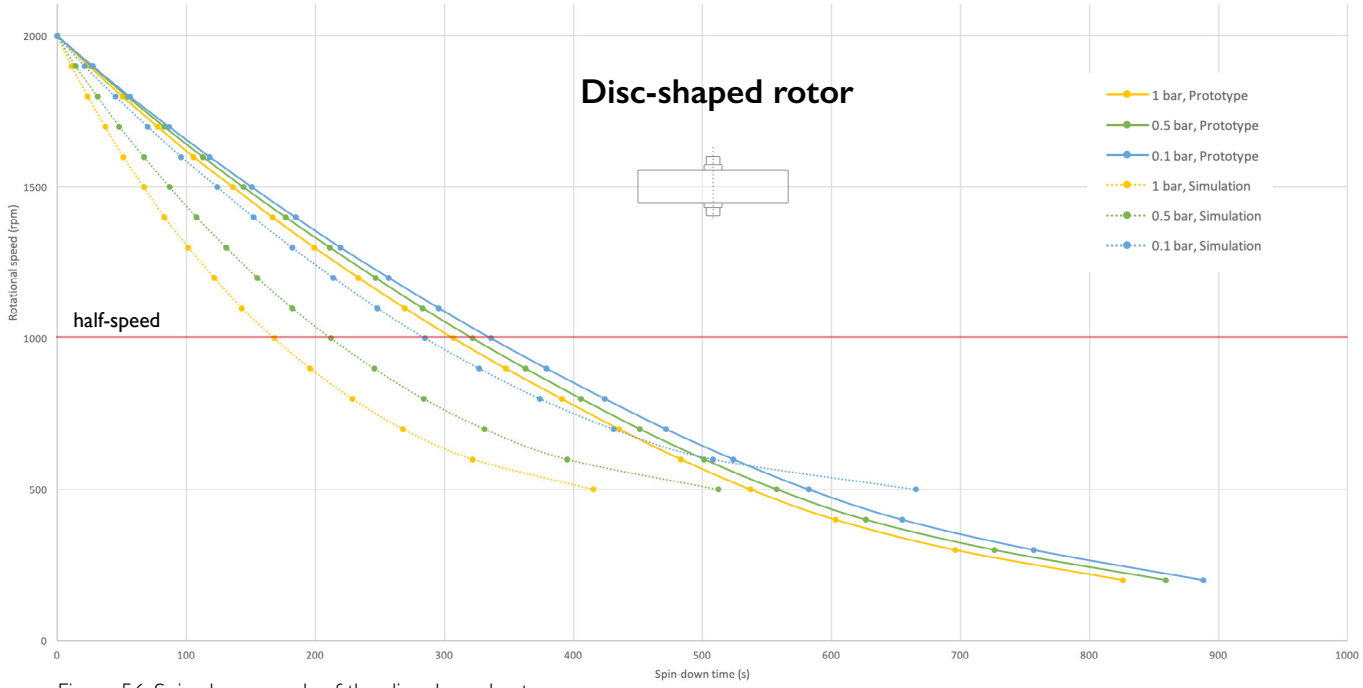

Figure 56: Spin-down graph of the disc-shaped rotor

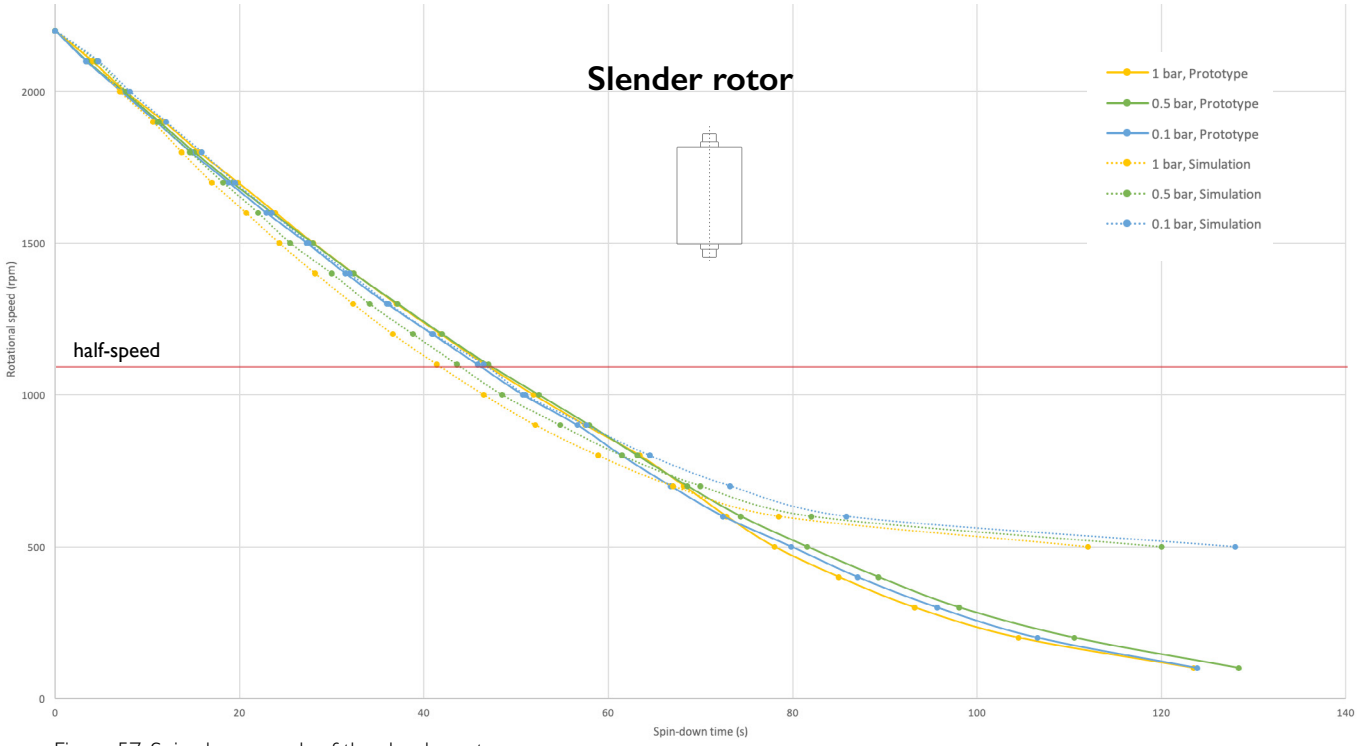

Figure 57: Spin-down graph of the slender rotor

Aerodynamic/bearing losses

The ratio of bearing losses to aerodynamic resistance could not be validated through the spin-down test. Whereas the script was written to separately produce a graph of both types of losses, measurement do not allow this characterization.

Plotted in Figure 58 are the losses that occur, calculated by the script. This plot, which is drawn for atmospheric pressure (1 bar), shows the significance of aerodynamic drag (indicated by the red line).

At a lower pressure of 0.1 bar, the resistance profile is influenced stronger by the bearings. This is made visible in Figure 59.

Looking at the spin-down graphs on page 57 with calculated and measured data shows that the calculated drag depends stronger on the aerodynamic drag than the script indicates. Every step the pressure was lowered, the spin-down time became longer. This effect is visible in the measured data, but smaller differences between the various pressures occur.

Figure 60 and Figure 61 show similar plots for the slender rotor. An interesting difference with the plots for the disc-shaped rotor is the very low portion of aerodynamic losses that shows at both atmospheric pressure and at 0.1 bar. The simple explanation for this is that the surface speed of the outer edge is lower for this rotor, since it has a smaller radius and is rotating at the same number of rotations per minute.

The rotational speeds at which measurements were done do not give accurate results for the comparison in energy storage, because at the tested speeds the slender rotor stored significantly less energy than the disc-shaped rotor. Driving the prototype up to a speed of 6200 rpm would result in similar energy storage. In addition, as indicated by the light red areas on the right of the graphs, higher rotational speeds should show stronger influence on total losses by aerodynamic drag. Unfortunately, this could not be achieved with the available equipment.

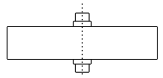

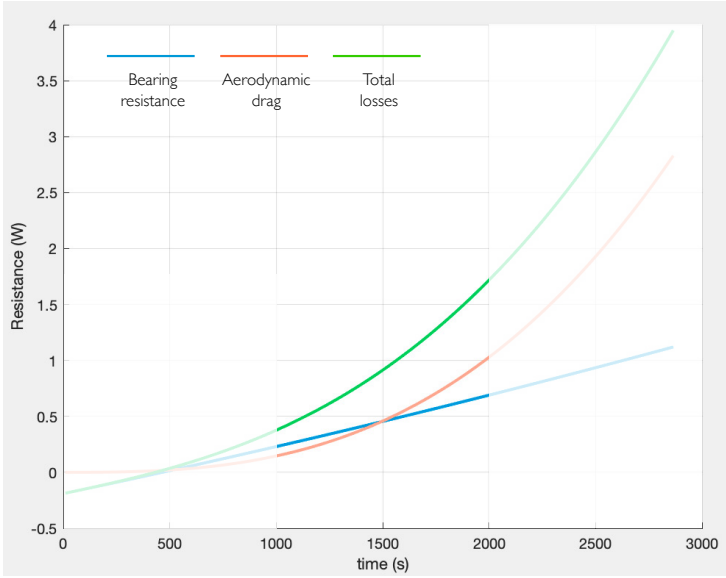

Figure 58: Ratio of disc-shaped rotor losses at atmospheric pressure

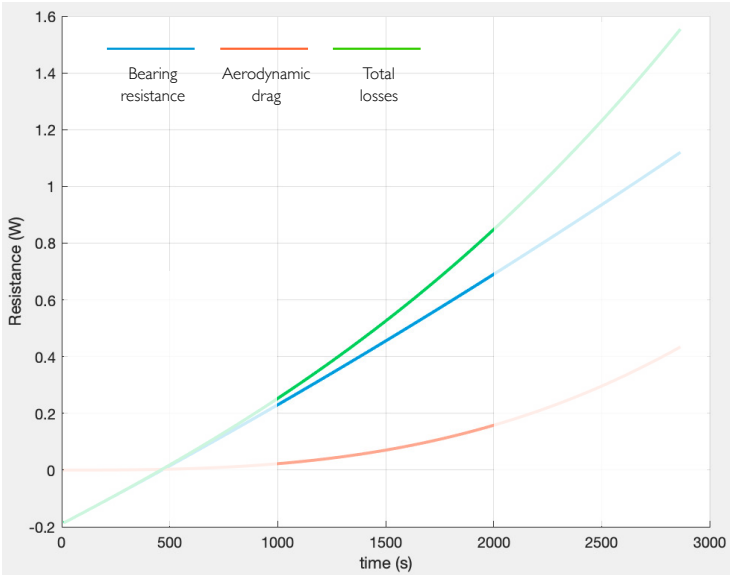

Figure 59: Ratio of disc-shaped rotor losses at 0.1 bar

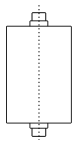

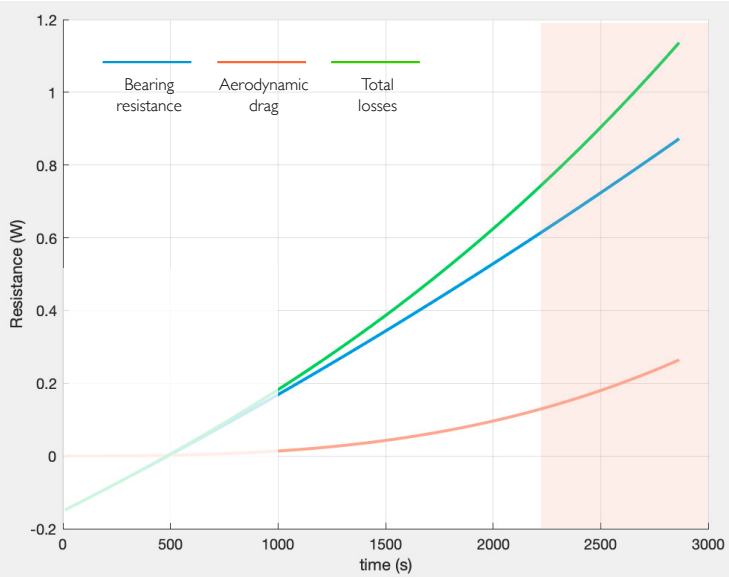

Figure 60: Ratio of slender rotor losses at 1 bar

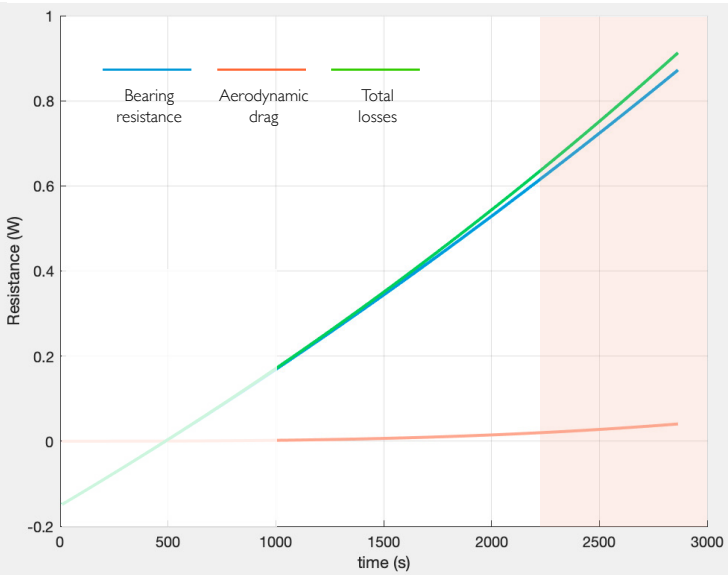

Figure 61: Ratio of slender rotor losses at 0.1 bar

3.3.8. Limitations by equipment

The test setup with most importantly the prototype, was designed for testing at 1400 rpm for the disc-shaped, and 4400 for the slender rotor. However, during the validation tests, these initial speeds were adjusted.
For the disc-shaped rotor, a higher initial speed was chosen after the differences measured when varying between pressures were insignificant. On the other hand, the initial speed of the slender rotor could not be reached with the available equipment for two reasons. In the first place, a standard electric drill cannot reach speeds higher than 2400 rpm. Secondly, a high speed rotary tool that can be connected to the magnet drive does not allow the slow acceleration that is necessary.
Therefore, the maximum rotational speed at which the slender rotor has been tested is 2200 rpm.
This resulted in the following numbers calculated by the script:

	Disc-shaped	*Slender*
Speed:	**2000 rpm**	**2200 rpm**
Energy stored:	**196 J**	**24 J**
Spin-down:	**339 s**	**52 s**

Unfair comparison

The numbers above indicate a significant difference in the energy that is stored in both of the flywheels. Because the main goal of the test was to validate the script, this has not resulted in direct problems. Interesting results have been obtained with the tests that were conducted. However, proving the differences in aerodynamic losses between disc and slender rotors could not be done.
Initially, the validation process was made as fair as possible. This was done by varying as little of the parameters as possible. However, limitations of the test setup added restrictions and determined a maximum rotational speed that was reached.

Figure 62: Accelerating the disc-shaped rotor using an electric drill

Hypothesis

Lower aerodynamic losses cause longer spin-down times for a larger radius to height ratio of the flywheel rotor.

(from initial speed to half speed)

Conclusion

The spin-down tests have concluded in the following:

- The aerodynamic effects are programmed more influential than reality has shown.

The spin-down tests are inconclusive when it comes to validating the Matlab-script.
Where some of the measured values of the validation tests were very similar to the simulated ones, others were up to 44% off. The aerodynamic effects calculated by the script appeared to be less significant while testing. Parameters that were used when calculating aerodynamic drag should be analyzed and their accuracy improved.

- The script is suitable for determining the magnitude of the flywheel rotor.

Validation tests have shown that the order of magnitude of the calculated spin-down times is right. The script can therefore be used to get an idea of the rotor measurements that would be applicable to a certain scenario. This means that the simulated flywheel in paragraph 3.2 is likely to be capable of storing the excessively generated electricity.

The hypothesis that was stated (displayed again to the left), can not be confirmed nor denied with the obtained testing data.
Further testing is needed to fully understand the effects that are showing, and to confirm or deny the hypothesis.
The script FlywheelCalc is however sufficiently accurate to use for roughly determining rotor dimensions.

LEFt

Leftover Energy Flywheel technology
by Amstel Engineering

Figure 63: The LEFt-family, introduced in this chapter.

4. Final Design

Combining all knowlegde into a finished product that can be placed within the context. It is provided with visualizations of the product and context and a description of the product's configuration.

User-specific market positioning

Energy supply and demand that varies significantly among households, this is why the design of the final product was aimed to be user-specific. This part is concluded with the design of a system configurator.

Cost- and sustainability analysis

Determining the feasibility of the concept requires a cost analysis, which resulted in a consumer price and market plan. In addition, to check whether the goal has been achieved, the sustainability of the concept was analyzed.

4.1 Final Design

LEFt

Leftover Energy Flywheel technology was developed according to the conclusions from previous chapters. The inner structure is based on the functional model and was expanded with components that make the system applicable to households. These components were chosen based on the subsystem approach from chapter 3.1.

4.1.1. Household applicability

LEFt was designed in such a way that its configuration can be chosen according to the type of household. Depending on the supply & demand data of the residence, suitable flywheel dimensions are chosen and a parametric design allows for various system setups. As shown in Figure 63, LEFt is presented as a product family of three main versions; the Flat, Slender and Extra Slender configurations. In Figure 69 on page 67, the Slender and Extra Slender versions are shown at two neighboring houses.

The Flat version, which is suitable to scenarios where longer term storage is needed, can be placed in the crawl space of a house or dug underground in a garden or driveway.

Choosing one of the three versions does not mean that there is that it is only applicable to one scenario. There is room for some variations in rotor dimensions. The exact measurements of the rotor depend on the choice of main version and is then chosen according to the supply & demand scenario.

Figure 65 shows the Slender configuration of LEFt, which is capable of storing enough energy to supply a household with electricity until the end of the evening. The rotor inside has a diameter of 60 cm and is 90 cm high, requiring it to spin at 4400 rpm to store the available amount of energy on an average summer day.

4.1.2. Communication to the user

LEFt continuously measures the rotor speed and can calculate the equivalent electric energy that will be available to the user. A circular display (5 inch diagonal) displays the charge level in a visual way, every time someone walks past (Figure 64).

In addition, tapping the display once shows the equivalent regeneration capacity, when the stored power would be used directly for one of the displayed applications. Since every households gets their LEFt made to fit, this menu will show only the data that is relevant to the household. The middle screen in Figure 66 shows an example of the equivalent regeneration capacity for a household where a dishwasher and an electric vehicle are used. The bottom screen that is displayed in the same figure shows the supply & demand curve for the current day. The current charge level is displayed, as well as the charging rate in Watts. The continuation of the curve is estimated by using the data of the last known day with comparable weather up to the current time of day.

On all of the screens, a little icon in the top center communicates that LEFt is storing solar power and charging.

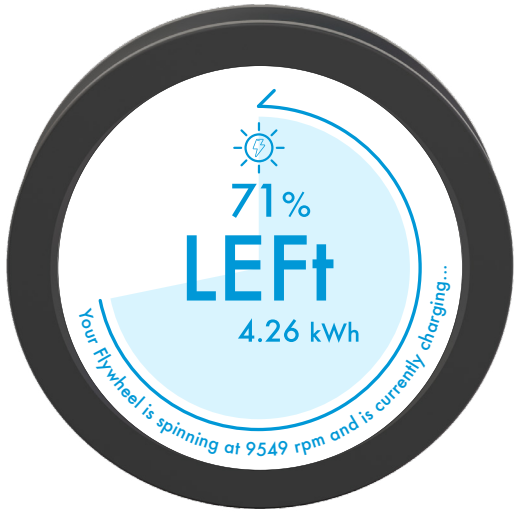

Figure 64: The circular display, communicating charge level

Figure 65: The Slender version of LEFt placed in a garage, with inverter box and solar panels

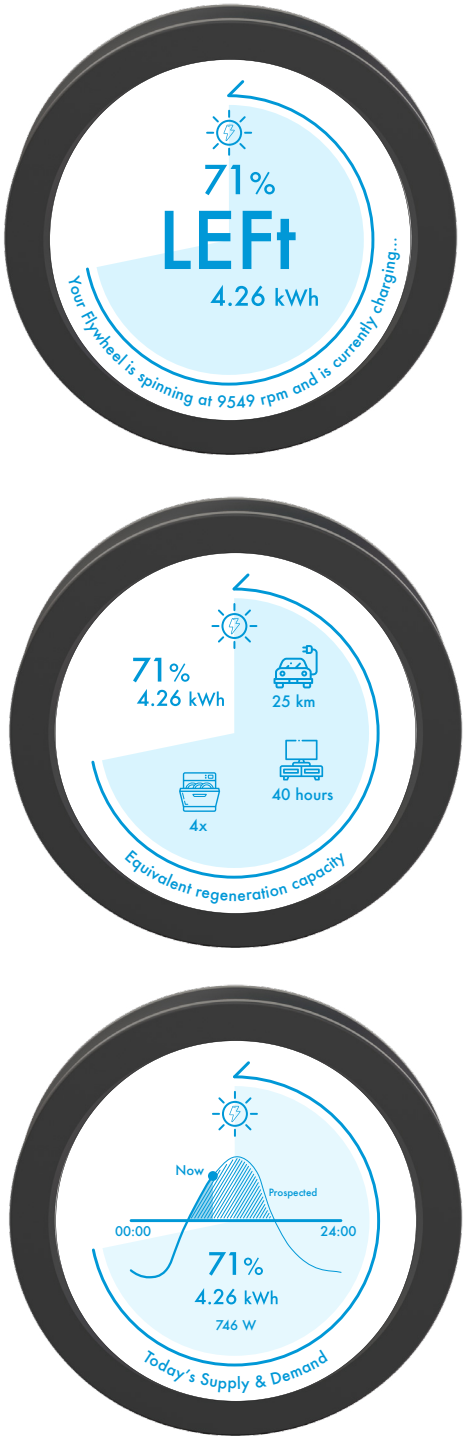

Figure 66: User interface of LEFt.

4.1.3. Components

Many of the components in the final design are similar to the ones that were used in the prototype. However, scaling up the model requires a few important adjustments. The main components, described from top to bottom, are as follows:

A 2.2 kW motor will accelerate the flywheel and with that stores the excess solar energy. The simulation that was done for designing this configuration showed that the supply and demand for the flywheel system are rarely exceeding the power of 2 kW. In order to keep the system as compact as possible, the closest available power up from 2 kW was chosen.

The display is mounted above the rotor and therefore prominently visible, for this version it is placed at approximately 130 cm height.

While the maximum rotational speed of the rotor lies about a factor three above the motor's capability, a 1:3 transmission is needed. The transmission is combined with a magnetic coupler, similar to the one that was used in the prototype (Chapter 3.3). These combined components have currently not been designed into detail.

In case of any unbalance, the Active Magnetic Bearing will force the rotor in its neutral position by giving axial pulses. The workings of this type of bearing are explained in paragraph 2.1.

For this version of the design, a steel rotor was chosen. A relative high specific mass and a high maximum tensile stress give the possibility of storing a sufficient amount of energy at an acceptable rotational speed.

Enclosing the entire rotational system is a steel vacuum tube. Since the working pressure is very low at 4 Pa, the enclosure should be able to withstand high forces. It consists of 2 mm thick steel tube, closed off at top and bottom with 10 mm plates that are welded on.

To make LEFt blend into the household environment, the functional parts are enclosed by an elegantly shaped cover. The shape of this has been inspired by the two-plate design from the prototype, and made more elegant by introducing smooth shapes. From the top, LEFt is in between circular and triangular, which on one hand communicates the rotational movement that takes place inside, and on the other hand tells something about the structure of the functional parts. A number of design sketches for the enclosing cover can be found in Appendix F.
As the material for the cover, recycled HDPE is used. This enhances the "green" character of the product.

The second part of the magnetic suspension system is the Halbach Array, which is positioned below the rotor. This part, as described in paragraph 2.1, ensures the thrust force that is needed to levitate the rotor. Dimensioning this part to ensure the rotor's mass will be supported continuously will need further studying of the Halbach Array.

Lastly, the entire product is supported by six stabilization feet. The continuous movement inside the system can cause some instability, which is prevented from being transfered to the house's foundation by these feet. From the other side, in the case of an earthquake, the stabilization feet will prevent the rotational movement to be interfered too much.

LEFt
Leftover Energy Flywheel technology
by Amstel Engineering

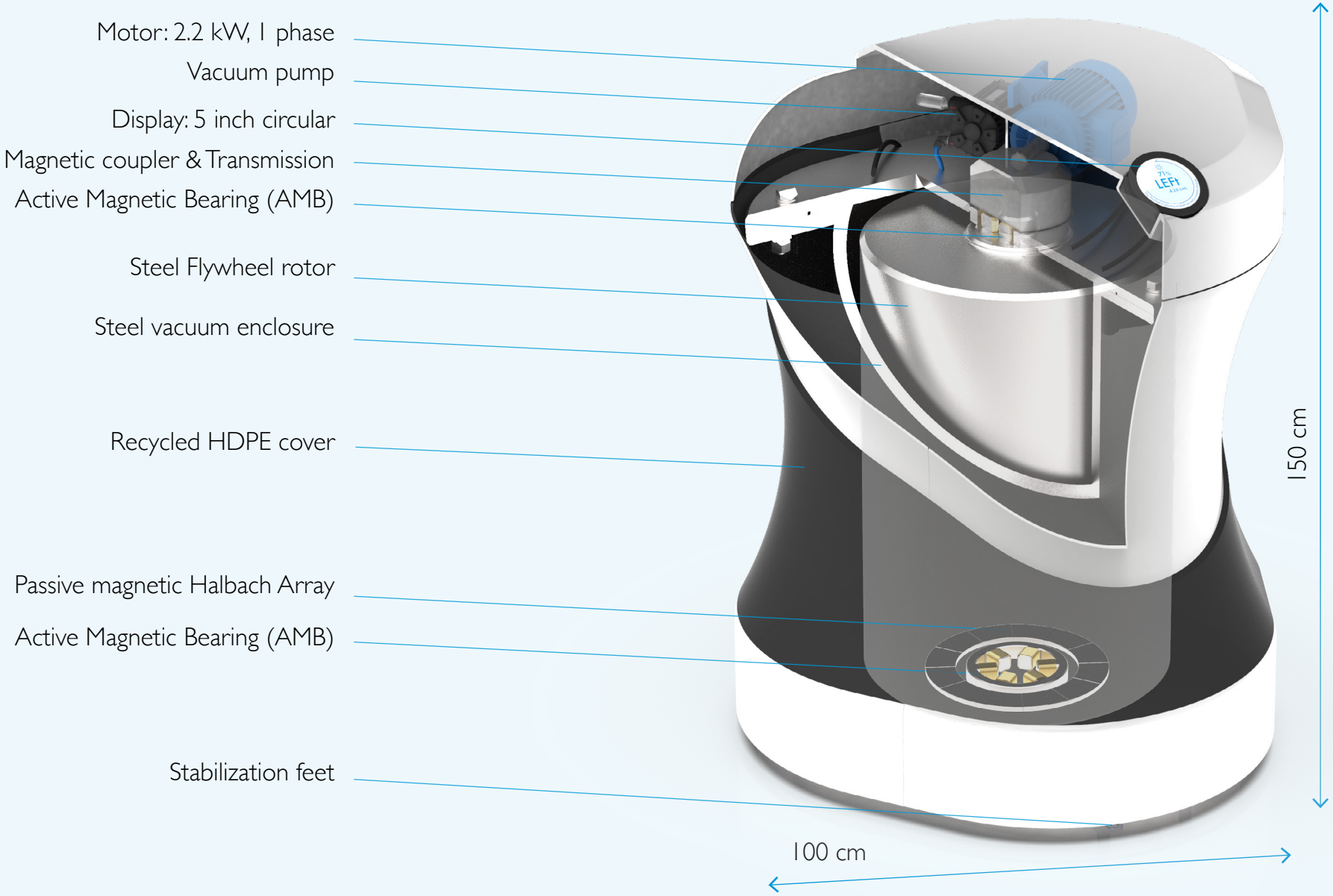

Figure 67: The Slender version of LEFt, cutaway rendering

4.1.4. Technology readiness levels

A method for determining the level of maturity of a certain technology that was developed in the 1970 by NASA is the use of Technology Readiness Levels (TRLs). (Thuy Mai, 2012)[114] The levels reach from a basic principle that was observed (TRL 1) to a "flight proven" system (TRL 9). These levels were used to check the readiness level of some of the essential technologies that were used in LEFt, as can be seen in Figure 68. Defined by the subsystems, their levels can be determined as follows.

Subsystem 1: Rotor

TRL 4; Component validation in laboratory environment.

Storing electricity in the form of kinetic energy by spinning a flywheel in a vacuum is a proven concept. This can be concluded from the number of studies that have been done and the availability of FESS on the market. By conducting experiments to validate the calculations that were done, the concept of a flywheel energy storage system at residential scale was proven. Scenarios of residential supply and demand were used in storage calculations and have shown promising results.

Matlab-script Flywheelcalc

TRL 3; Analytical and experimental critical function and characteristic proof-of-concept.

The script that calculates the magnitude and the rotational speed that is needed for energy storage in a certain scenario, is in the stage of a proof-of-concept. More experiments with different environmental conditions and at significantly higher speeds are needed to determine the actual influence of aerodynamic drag and the value of adding a vacuum housing.

Subsystem 2: Suspension

TRL 3.

Both essential components of the suspension system of LEFt have been used in practice. Albeit in different configurations and at different scale. It has been proven by researches that a nearly frictionless suspension system can be created with combining a Halbach Array of permanent magnets and a set of active magnetic bearings (AMBs).

Subsystem 3: Motor/Generator

TRL 4.

Using a standard single phase squirrel cage type motor for this application has been proposed to allow cost-efficient design. However, proven flywheel energy storage systems all use integrated custom motor/generator devices. Application of a standard single phase motor requires the development of a transmission/coupler, since this type has to be positioned outside the vacuum.

Magnetic coupler

TRL 3.

Driving the rotor from outside the vacuum using two magnetic discs has been proven during the validation tests with the prototype. However, this only included manual operation of the motor (the electric drill). The final version of the coupler requires a control system for automatic coupling and decoupling, and should be designed in a way that no unwanted electromagnetic currents occur.

Subsystem 4: Housing

TRL 6; Subsystem model in a relevant environment.

Allowing a flywheel to rotate within a vacuum chamber is currently applied in various products on the market. The dimensions of the housing for a system at residential scale, with the necessary safety regulations for indoor use have to be analyzed into detail and tested before being used in the final product.

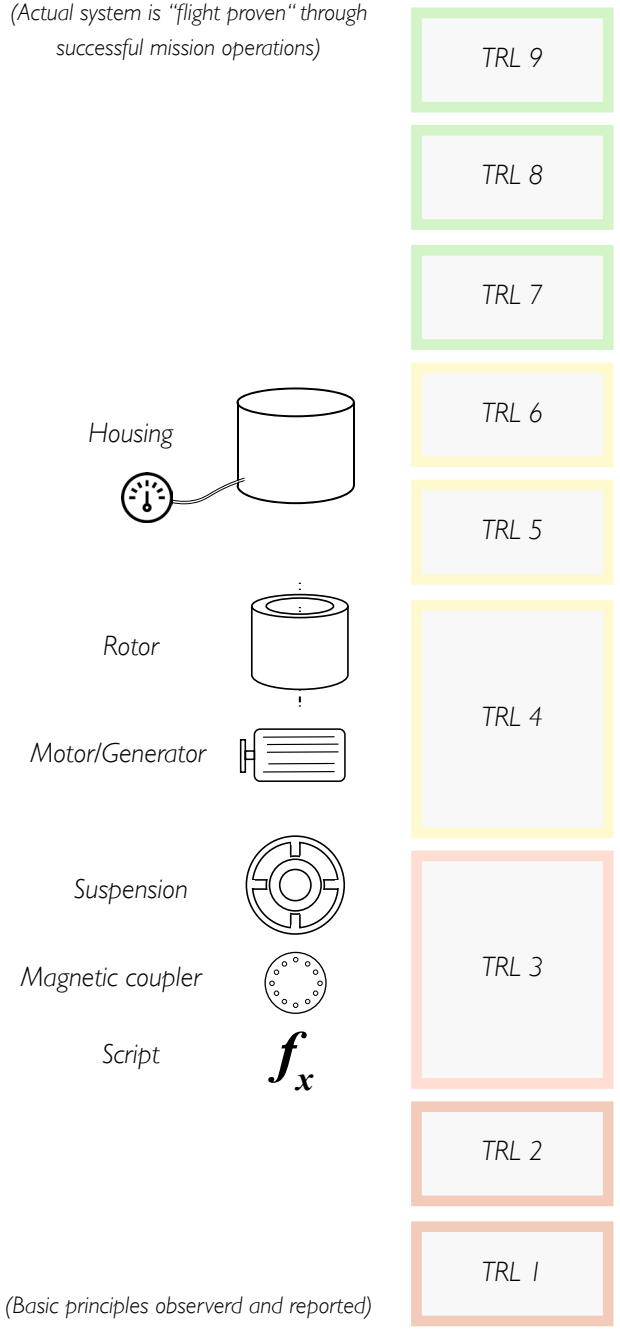

Figure 68: Technology Readiness Levels for LEFT. Adapted from Thuy Mai (2012)

Figure 69: LEFt in two different form factors, both suited to similar but different households.

4.1.5. Number of rotors

In paragraph 3.1, the potential advantages of a multi-rotor FESS were discussed. Although prototyping and testing has confirmed the effect of differently shaped rotors, the advantage of a multi-rotor system for household use has not been confirmed. Keeping in mind the high costs involved with added or integrated suspension systems, the final design was determined to have a single rotor in its basic configuration. Since various design parameters are determined by the user's household characteristics, the customer is able to configure multiple separate FESSs.

Conclusion

LEFt is the first residential scale flywheel energy storage system. It was designed in three versions to suit various types of households, according to analysis of their supply & demand scenario.
The low technology readiness levels of the components in the system show that there is still a significant amount of development needed before the product is ready for production.

4.2 Market Strategy

Introduction

Every household is different on many aspects, in this case the various energy demands are most interesting. As discussed in chapter 1.2, LEFt was calculated for a full day of energy storage in the case of an average summer day. However, different households can have very different wishes to the system. It might, for example, be normal for a family to be away from home the entire day, resulting in a peak in electricity use only in the late afternoon and the evening. This family would require a different type of rotor than a household where two people work from home. This was explained into detail in paragraph 3.2.4.

4.2.1. LEFt configurator

In Figure 70, the LEFt configurator webpage is displayed. This allows a potential customer to get an idea of how their LEFt will be dimensioned and how much of their excess solar energy can be stored. Since not everyone is familiar with the effect of one kWh, the money saved when using this system for a year is estimated. In addition, the kilograms of CO_2 equivalent that were prevented from being emitted by fossil power plants is calculated. For this visualization of the webpage, currently dummy data has been used. To calculate the actual savings in both price and CO_2 equivalent, more information is needed.
The settings of the configurator are as follows:

The number of people living in the household, which is important for the estimation of demand data.
The house type and its energy label influence the electricity use, mostly when electric heating is installed.

The current amount of solar panels installed can be set. When the calculations show insufficient power is being generated for storage to be interesting, it can suggest installing extra panels.

The location in the world is important for an accurate estimation of the solar data for the calculation. The customer can either point their location on the map or supply their country and postal code.

The demand of the system depends strongly on the type of life that someone is living. Therefore, selection boxes allow to specify what is done during a typical day. For example, working from home means that more electricity is used in the middle of the day and therefore less excess is available to be stored in LEFt.

On the bottom right of the page, a graph is drawn that visualizes the estimated supply & demand curve for the household setup. The green area corresponds with the daily amount that is stored.

In the middle of the page, a render of the recommended version of LEFt is displayed. This render resizes according to the settings and gives the user an idea of the size of the product compared to the amount of energy that can be stored.

Below the render, a big button is located. Clicking the button allows the customer to transfer the setup to Amstel Engineering BV, where the model is made ready for production.

The indication for annual savings on electricity costs is based on the current electricity price in the Netherlands (Essent, 2019)[115]. The prevented CO_2 emissions are determined according to the emissions caused by production of electricity in the Netherlands (CBS, 2018)[116]. For these indications, a number of 200 sunny days per year is considered.

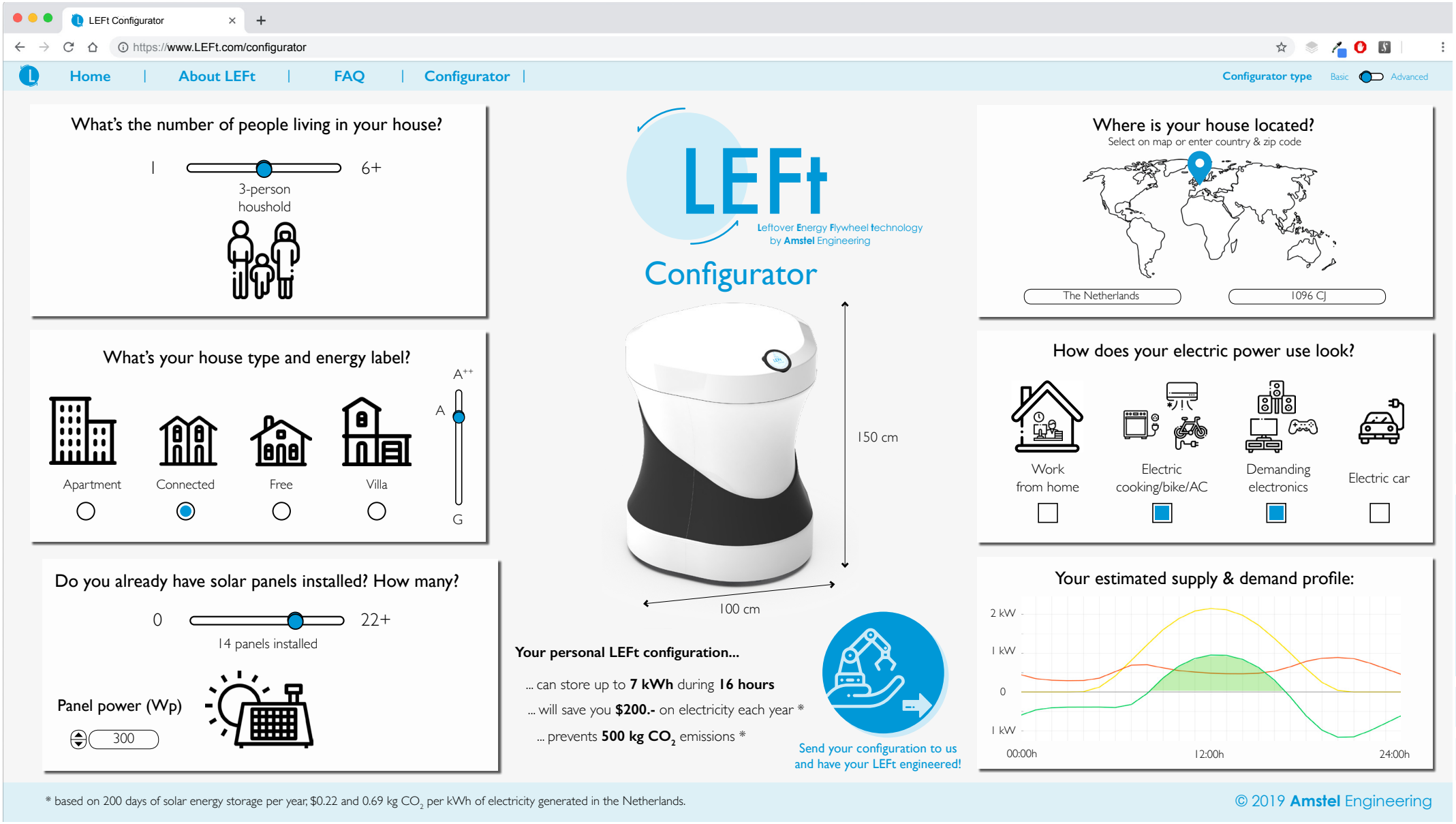

Figure 70: LEFt configurator webpage

Figure 71: Rooftop with several solar panels installed

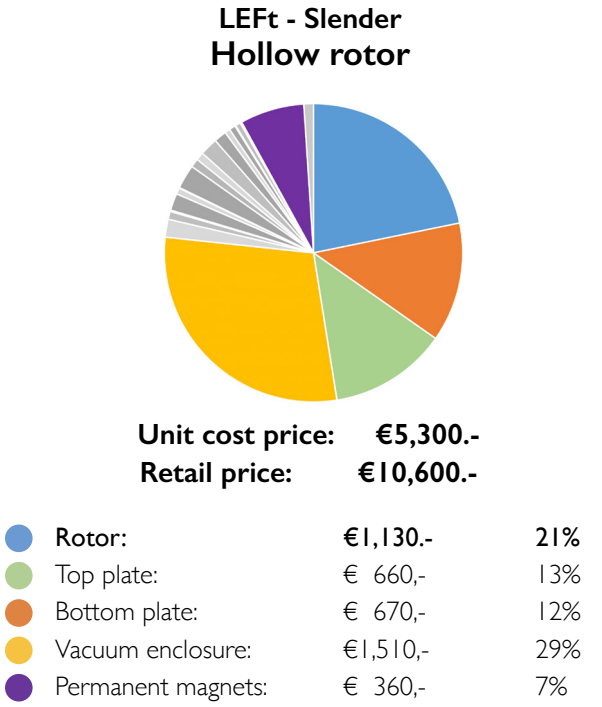

Figure 72: Cost price estimation of LEFt with a hollow rotor

4.2.2. Cost & retail price

The price of the slender type LEFt was calculated using estimation methods by Kals et al. (2007)[117]. A detailed Bill of Materials was set up and for each of the parts a price was calculated. After a proposed cost reduction by choosing a hollow flywheel rotor instead of a solid, the cost price is €5.300 which results in a retail price of €10.600. The full calculation and foundation can be found in Appendix G.

Comparison to Tesla Powerwall

The most interesting direct competitor on the market, the Powerwall by Tesla, costs around €8.200 and has an warranty of 10 years. With a longer warranty period of 20 years which results from the lack of wear, the annual costs of LEFt will be around €530 compared to €820 for the Powerwall. Although this seems lower, one should keep in mind that the functionality of LEFt is slightly different, since it does not store electricity for multiple days.

Leasing LEFt

Since an initial investment of over ten thousand euros is high for the average household, it is recommended to set up a lease construction that allows the customer to pay LEFt via a monthly or yearly payment plan.
Energy companies in the Netherlands, for instance Essent, already uses lease plans for buying solar panels (Essent, 2019)[118]. This method might also work for selling LEFt. More on this in the next paragraph.

4.2.3. Collaboration

Selling LEFt directly from Amstel Engineering BV does not seem interesting, since no experience is present in direct product sales and therefore the company is not known as a manufacturer. As mentioned in the previous paragraph, the full retail price might also be too high to spend at once.

Potential customers, like the households that were envisioned on page 50, will be familiar with instances that have sold them their solar panels (i.e. Essent). Therefore, it is recommended to bring LEFt to the market by Amstel Engineering, in collaboration with one or more companies like these. By advertising to buy a storage system in addition to new or already installed solar panels, a broad audience can be reached.

Customer approach

Two types of customers are envisioned; households that have solar panels installed and households that do not.

Of the first group, it is interesting to know whether the installed amount of panels is sufficient and will be suitable for adding a storage system. Data can be supplied by the user or obtained from measurements done by one of the companies. After analyzing the results, an offer can be made. The same analysis can be done for newly installed solar panel setups.

Combination lease

Households that do not have solar panels installed can be motivated to lease a LEFt storage system in addition to a set of panels, when they are offered a combination deal. Storing the excess energy is added value to solar panels, since their practical efficiency increases since more of the generated electricity is utilized. Naturally, the panels' efficiency does not literally increase, but losses that occur when not using the power are reduced.

LEFt

Collaboration with solar panel suppliers

Sell in addition to / combined with solar panels

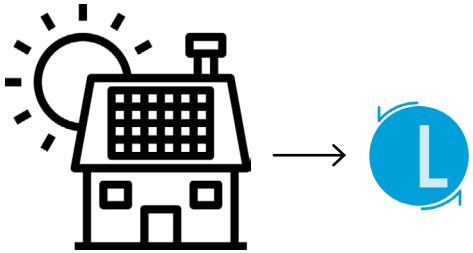

Household has (enough) **panels**

Contact user and check if interested in adding LEFt via a lease plan

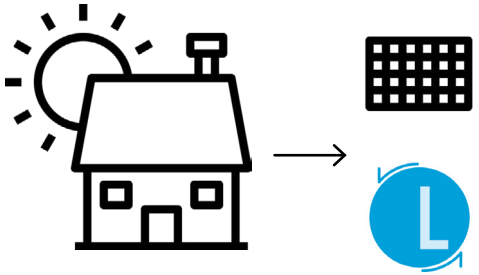

Household has no/insufficient panels

Combination lease

Conclusion

The best way to sell LEFt is to collaborate with companies that are selling solar panels via a lease construction. An estimated retail price of €10.600 for the slender type LEFt results in a periodic payment, for example a yearly €530 over 20 years. It will be interesting to buy in addition to an existing or a new set of solar panels since storing excess electricity virtually increases their efficiency.

4.3 Sustainability Assessment

Introduction

Via a short track sustainability assessment, based on the methodology adapted from the course Sustainable Design Engineering, an expertise area of the project Advanced Embodiment Design. This method, which uses theory from the book "Materials and Sustainable Development" (Ashby, 2015)[119]
LEFt will be compared to the alternative that is currently available on the market; the Tesla Powerwall. The assessment is based on the triple P-analysis, where People, Planet and Profit are considered. The product impacts all three aspects differently, and the analysis resulted in several recommendations to the design.

To be able to understand the biggest downside of lithium ion batteries, this chapter starts by addressing the problems that are occurring during production.

4.3.1. Li-ion problems

The most commonly used rechargeable chemical battery, the lithium ion type, has promising performance in terms of energy density, safety and price. However, as mentioned in the introduction of this paper, social political and environmental problems are caused during production. This paragraph elaborates on these problems. Most of these are caused by mining three important materials for battery production: Lithium, cobalt and graphite.

Lithium - Argentina

An important material for production of the battery is lithium, the ions transport positive electric charge through the battery's medium, hence the name of the battery type. For one Tesla Powerwall, an estimated amount of 9 kg lithium is needed. (Frankel & Whoriskey, Washington Post, 2016)[120] This element is available in the salt flats of South America, and is mined in the so called 'lithium triangle' in Argentina, Chile and Bolivia. In Argentina, the Washington Post stumbled upon the following problems:
The indigenous people feel left out when it comes to lithium mining. Economic benefits of providing jobs only help a little, since it brings even more worries. Jobs are uncertain since companies are fighting for what is theirs, and little respect is being paid to the conditions of living. Drinking water supplies are being depleted, because mining requires large amounts. All this brings disrespect and a lack of trust between the indigenous people and the mining companies. All in all, social, political and environmental problems occur when mining lithium.

Cobalt - Congo

Tesla's Powerwall contains an estimated 1.6 kg of cobalt, which is used for the cathode part. (Frankel, Washington Post, 2016)[121] Cobalt is mined in Congo, in mines where the Washington Post also went to see the working conditions.
The problems that occur here are mainly social, since people here are not treated very well. Not only unsafe working conditions are part of the problems, child labor is seen in the mines as well. As for water resources, just as in Argentina, these are depleted by the mining itself. Companies have promised to source their materials in an ethical way, but the people of Congo show the opposite.

Graphite - China

Northeastern China is the location where many of the well know electronics companies source their graphite, a material that is used in Li-ion batteries in the anode part. Whoriskey of the Washington Post saw that the conditions of living were heavily affected by mining this material. (Whoriskey, Washington Post, 2016)[122]
An estimated 5 kg of graphite is used in Tesla's Powerwall (Battery University, 2019)[123], causing social and ecological problems.

According to the same set of research trips by the Washington Post, graphite mining causes the following problems:
According to the people that live in the mine's surroundings, "Particles of graphite dust are everywhere." These particles cause all laundry to turn dark gray and the water to become undrinkable. In addition, people are getting respiratory problems and trees are being killed. A persistent chemical smell is present, making the environment very unpleasant to live. The problems caused by graphite mining can be defined as social and environmental.

For comparison

Obtaining all of the materials needed for the lithium ion battery means that problems are being created. The rest of this analysis will consider the negative impact of producing a Tesla Powerwall and will use this to compare it to LEFt.
Figure 73 shows the most important problematic material sources for both Tesla's Powerwall and LEFt.
Steel, the most impactful material used in LEFt, will be considered later in this chapter. It is produced in China and displayed in the figure with a yellow color.

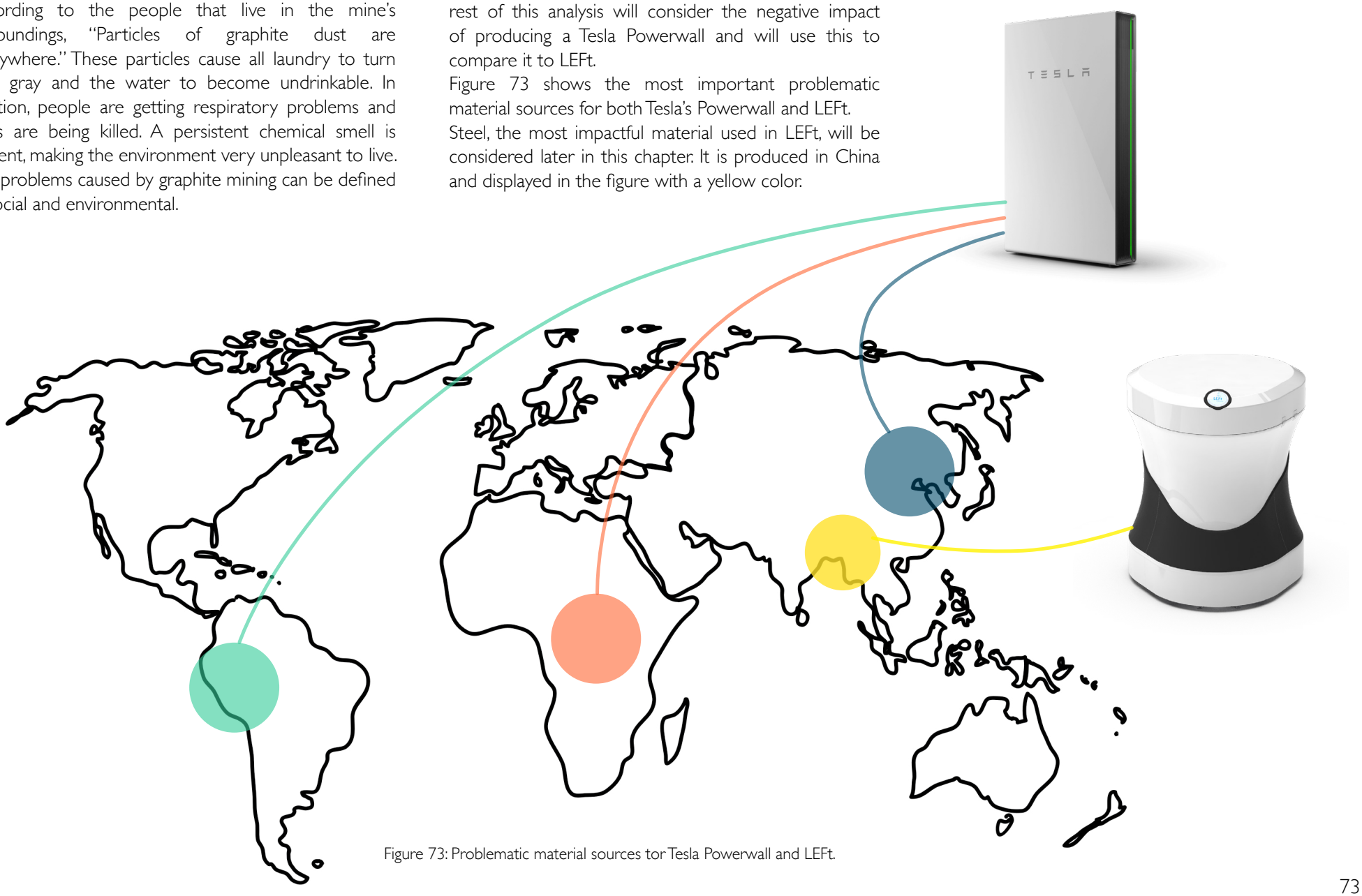

Figure 73: Problematic material sources tor Tesla Powerwall and LEFt.

4.3.2. Environmental impact

The assessment that has been done can be read into further detail in Appendix I, in this paragraph the results are summarized.

Most importantly, the hypothetical effect of using a mechanical storage system is that the environmental problems in addition to CO_2 emissions are reduced. The previously described problems caused by mining lithium, cobalt and graphite are prevented.
The envisioned effects of LEFt are formulated by the following statements:

Prime objective

Reducing the amount of wasted renewable energy due to a lack of residential energy storage without introducing sustainability problems.

Articulation

Increasing energy awareness by communicating the equivalent capacity of mechanically stored electricity.

Concluding from the full impact analysis, LEFt will achieve the desired effect with the user, but production causes CO_2-emissions that are undesirably large.

4.3.3. Recommendations to design

Lowering the amount of steel that is used in the product will drastically lower the environmental impact. When considering the rotor, which is the part with the largest amount of steel, this can be altered in one simple way. Making the rotor hollow, as described in chapter 2.1, Subsystem 1, requires a redesign of several components but lowers the amount of steel needed.

Actual impact

In addition to the triple P analysis (People, Planet, Profit), it is useful to look into the impact of the different materials in both LEFt and the Tesla Powerwall. In the introduction of this thesis, in paragraph 1.1, was stated that mining of lithium, cobalt and graphite causes political, social and ecological problems and a mechanical alternative might prevent these. LEFt does not contain lithium and cobalt, which are considered high impact materials. It does however contain large amounts of steel, of which the impact is analyzed to determine whether the new product has environmental advantages over the old.

4.3.4. Eco Audit

The Eco Audit in Cambridge Engineering Selector (Edupack) (Granta Design, 2019)[6] resulted in the following interesting differences between Tesla's Powerwall and LEFt:

- Steel is the most impactful material in LEFt, making the impact of the production phase higher than that of the Powerwall.
- Increasing the percentage of steel that is recycled decreases the impact up to a point where the environmental impact of the two products becomes similar.

The comparison between two versions of LEFt (solid and hollow rotor) and Tesla's Powerwall is visualized in Figure 74. In this figure, one will notice that changing to a hollow rotor does not make an enormous difference. This is due to the fact that a large percentage of the steel that is used is recycled (up to 80%). The full settings of the Eco Audit can be viewed in Appendix I.

Lifetime

LEFt was designed to have a lifetime of 20 years, which is a rough estimate considering all components (see BoM in Appendix H). Most of these are frictionless, which means no wear will occur. Two components where this will occur are the motor/generator and the vacuum pump. Depending on the intensity of use, these components might need replacement within the product's lifetime.

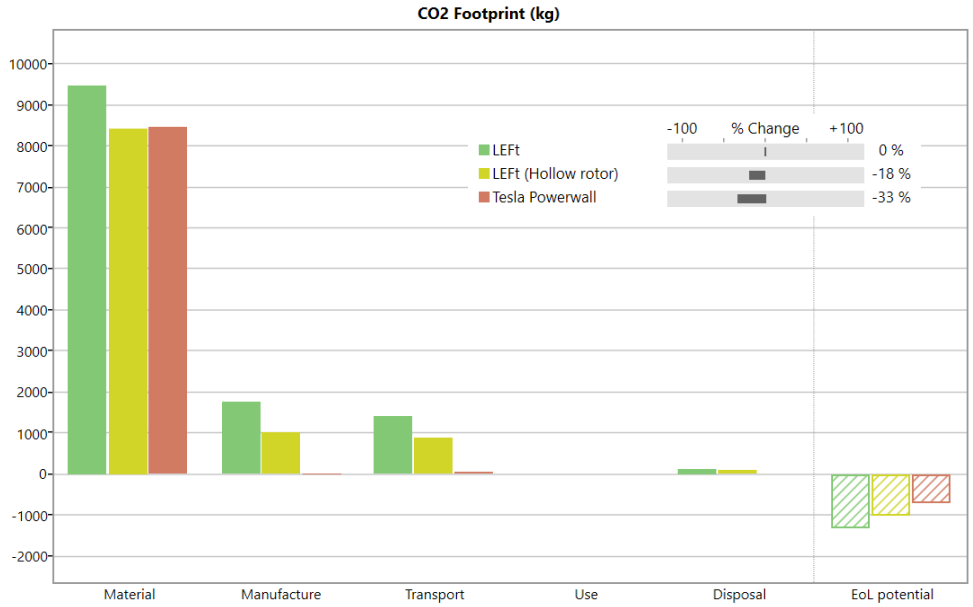

Figure 74: CO_2 footprint comparison from CES Eco Audit.

Tesla Powerwall		LEFt
Lithium (9 kg, 0% recycled) **Cobalt** (1.6 kg, 0% recycled) **Graphite** (5 kg, 0% recycled)	*Impactful materials*	**Steel** (2000 kg, 80% recycled) **HDPE** (80 kg, 100% recycled)
8200 kg CO_2-eq	*CO_2 footprint*	**9500 kg** CO_2-eq
10+ years	*Lifetime*	**20+ years**
-	*Increased environmental awareness*	**+**

Figure 75: Environmental comparison between Tesla Powerwall and LEFt.

4.3.5. Uncertainties in analysis

A first analysis of the environmental effects was done according to the current design. However, this was done with the current design in mind. This version of the product needs further development in some aspects, and production methods of various parts have not been derermined. In a further stage of development, this sustainability assessment will be more accurate.

Recycled percentage

In addition, estimated percentages of recycled material have been added in the Eco Audit. A percentage of 80% for the steel that is used significantlly influences the impact by producting LEFt. In reality, it might not be possible to use this portion of recycled material and therefore a higher impact might be caused.

Maintenance

When looking at the lifetime estimation of 20 years, there are uncertainties when it comes to the amount of maintenance that is needed. The magnetic suspension system is expected to have no significant resistances, which makes it easy to assume that no wear will occur. In reality, wear might occur in some cases, and in some parts where physical contact is present. This should be taken into account regarding a new lifetime estimation.

Footprint

In Figure 75, the environmental comparison between the Tesla Powerwall and LEFt has been visualized. The difference in the CO_2 footprints of both products is relatively small, but is caused by different materials. In addition, the lifetime of LEFt is estimated to be twice as long, spreading the similar CO_2 footprint over 20 years instead of 10.

Conclusion

The overall environmental impact of LEFt was compared to that of Tesla's Powerwall. From the analysis can not be concluded that LEFt has lower environmental impacts in general. However, the materials that are used are different and are responsible for different types of problems.
What can be said with confidence is that the problems that are involved with the production of lithium ion batteries are not present when manufacturing LEFt.

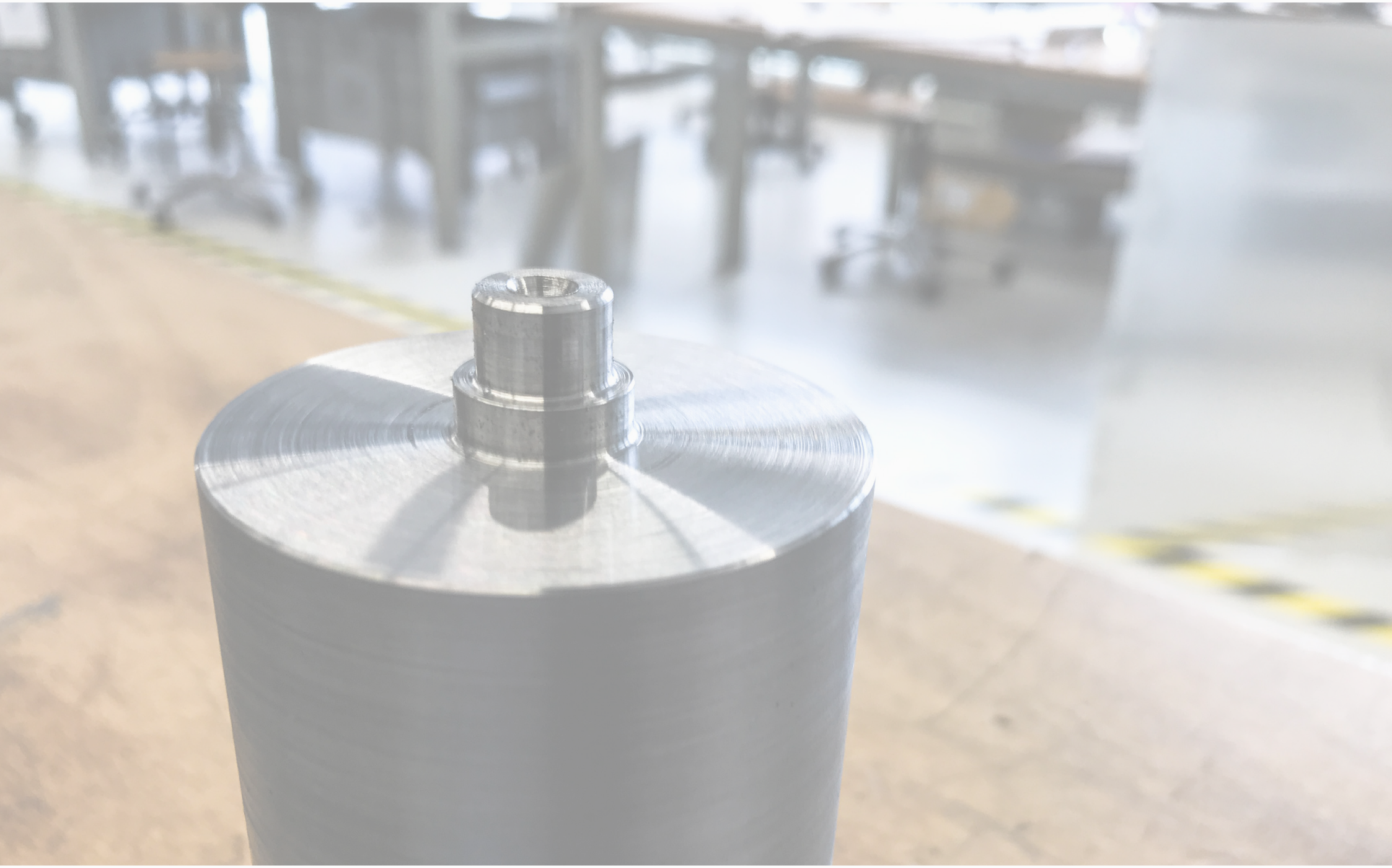

5. Conclusion, Recommendations & Reflection

To conclude this thesis, after checking up to which extent the requirements have been met, some final remarks are made. This final chapter contains considerations of the final design, as well as an evaluation and lessons that were learned during the process.

5.1 Conclusion

Introduction

Determining whether the designed product can be seen as an acceptable outcome for the project, will be done using the list of requirements (Appendix B) that was set up during the early phases. In the case a requirement has not been met, a recommendation followed and is included in the next chapter.

5.1.1. Evaluation of requirements

Below, the list of requirements has been included, of which each has been marked with one of the following three symbols:

✓ *Requirement has been met*

~ *More work is needed before meeting the requirement*

✗ *Requirement has not been met*

Energy storage

✓ The system is capable of **mechanically storing** an **excess** of electrical energy produced by a **renewable source** during an average summer day in The Netherlands.

✓ The system is capable of **supplying** the stored energy **to the household** during a period when renewable energy is **not being generated**.

Storage period

~ The system does **not lose more than half** of the stored energy in a period of **10 hours**, when no energy is demanded by the household.

System size

✓ The complete system falls within the boundaries of **2 m^3**.

✓ The room to place the system does **not need to be modified** for placement.

Environmental impact

✓ The system **does not produce CO_2** emission during the use phase.

✓ **Sourcing materials** for production does not cause political, social or economical problems in the country of origin.

✓ The system has a minimum lifespan of **10 years**.

~ The system **does not require professional maintenance** during its lifespan.

Use

✓ The system does **not require** any **user input** to operate.

✓ The system **communicates** its amount of stored electricity to the user and encourages responsible utilization of electricity.

Costs

✗ The **annual costs** for the consumer are **less than two times** the annual costs of a comparable li-ion alternative.

5.1.2. Overall design conclusion

From the list of requirements on the left hand page, it can be concluded that most of these have been met and therefore the design can be called largely successful.

Technology readiness levels

From paragraph 4.1.4, the conclusion can be drawn that the technologies used in the subsystems of the product are at a low maturity level. As the conclusion of chapter 4.1 already stated, a significant amount of development is needed before LEFt is ready for production.

5.1.3. Adjusted requirements

The requirement for the energy storage period has been met partially. Since the final design consists of a family of products with different specifications of which some meet the requirement of storage period. The Extra Slender version does not meet this particular requirement, since it is meant for scenarios in which only small peaks of energy are stored and used within a short period of time.

Another requirement that obtained the rating "unsure" is about the need of professional maintenance. Since it is not known how the subsystems will behave exactly and a motor/generator is used that might have a limited lifetime.

The only requirement that has not been met is the costs restriction. Because the existing Tesla Powerwall is the only system that was used for a reference price and no market research has been done, determining a maximum allowable retail price was difficult. The requirement that was set has not been met, but is has not been determined whether this is critical for the product to succeed.

5.1.4. Answering research questions

The two research questions that were asked at the start of the project, can now be answered.

Can mechanical battery be a feasible alternative to lithium ion batteries, when using it to store an excess of sustainably generated energy, within the house?

During the analysis of storage methods it became clear that flywheel energy storage is currently mainly used for short-term storage. This project has proven that this type of storage is likely to be applicable to residential storage scenarios. Especially for the scenario where the excess of solar power from midday and afternoon is stored for usage during the evening.
However, some residential storage scenarios require longer storage times, in these cases a lithium ion battery can still be the better choice. Living off-the-grid sometimes means that there is insufficient solar power for multiple days. Flywheel energy storage is not yet capable of storing energy for this long.
Developing the system into a version that can compete with the storage times of multiple days or even weeks, will make it a better alternative in most of the analyzed scenarios and might even make it applicable for living off-the-grid.
In conclusion, it can be said that LEFt can be a feasible alternative for lithium ion batteries, but currently only in specific scenarios of use and if further development shows that the expectations become reality.

How can an energy storage system be designed, that is suitable to the company Amstel Engineering BV and their expertise?

By designing LEFt in a way that it consists out of subsystems, these subsystems can be taken on as separate projects that suit the various interests among engineers. Since the subsystems are mostly mechanical and contain challenging aspects like a dynamic magnetic coupler, it asks for knowledge and skills that are present within the company. On the other hand, experience with electrical drives, bearing systems and heavy duty constructions will be useful during further development. Finally, the design of a fully functional flywheel energy storage system can be used to show external parties what the company Amstel Engineering BV is capable of.

5.2 Recommendations

Introduction

This chapter logically follows from the evaluation of requirements and supplements chapter 4.1.4, where the maturity of each of the subsystems was evaluated in terms of Technology Readiness Level (TRL).

5.2.1. Development of subsystems

For each of the four subsystems, a solution was proposed. However, using the TRLs has shown that all of the subsystems need further development before they are ready to be implemented in the final product and produced.
This paragraph contains the recommended steps to take for Amstel Engineering BV, to reach the desired development level and make LEFt ready for production.

Rotor

The technology for energy storage was proven, but the final shape and magnitude of the differently sized rotors for the LEFt family will have to be determined. This requires extensive testing of multiple versions of rotors at prototyping size (Scale 1:10) and full size.

Aerodynamic effects are present, this can be concluded from the Matlab-script and validation tests that were done with the prototype. However, the magnitude and the exact behavior of these effects are unclear. Various tests in controlled pressure environments are needed for further clarification.
Currently, Amstel Engineering does not have any employees who specialize in aerodynamics. It is therefore suggested to get in contact with one, to discuss the validation of the programmed aerodynamic effects.

Suspension

LEFt contains a suspension system that consists of a passive and an active magnetic part. The Halbach Array that was proposed for vertical support might not be able to fully support the relatively high mass of the flywheel rotor.
The Active Magnetic Bearing system requires complicated control mechanics, which have not been designed. Although studies have shown that this method is applicable to suspension of a high speed flywheel, the exact application should be tested.

Motor/Generator

A standard type single phase motor has been chosen, but integration within a household's specific power system will need to be analyzed. In addition, the magnetic coupling system for driving the rotor externally is currently included in the design as a "black box". The basic version of the magnetic coupler that was used in the prototype has proven the concept of a magnetic drive system, but its manual coupling and decoupling will have to be developed in an automatic version.
It is suggested that Amstel Engineering will look into the automatic magnetic coupling as a separate system. Creative sessions might result in a clever alternative that requires a less complicated control mechanism and is therefore a better option for full development within the company.

Vacuum housing

The housing itself is similar to vacuum chambers that are currently on the market, which means the technology is at a higher readiness level than other subsystems. However, tests at full scale will need to be conducted to determine whether the prospected and calculated effects are valid. Even though this subsystem is essential for the functionality of the system, it is recommended to start detailing it after all other subsystems have been proven and are fully developed.

5.2.2. Script & prototype

Writing the Matlab-script started with a few simple calculations regarding size, rotational speed and stored energy. During the technological analysis, it was extended up to a relatively complicated program. However, not every aspect of the program could be verified.
Building the prototype and executing the tests for the validation of losses has focused on one important aspect of the calculations, but there are still many other aspects that need confirmation.
It is recommended that all of the code that was written is analyzed and verified, before using it for final calculations.

5.2.3. Regeneration of electricity

This project has focused on the storage step of the process; converting electricity into kinetic energy. However, regenerating electricity is at least as important. Unfortunately, the limited timespan of a graduation assignment has not allowed me to analyze this part. Currently, the motor/generator subsystem is assumed to be reversible and function with similar efficiency in regeneration mode as in storage mode. Naturally, this should be verified with in-depth analysis and tests.

5.2.4. Future vision

With the right investments of time and money, I think Amstel Engineering BV can succeed in developing LEFt into a production-ready energy storage system.
To achieve this, a project of at least one year needs to be set up. Led by one engineer who works on it during one or two days a week and supported by others who spend a few hours a week on the project.
It is interesting to hear how solar panel suppliers think about collaboration. Contacting different companies and discussing possibilities will clarify the potential of the current market implementation plan.

As a goal, a full scale prototype should be manufactured and tested for an extended period of time. After this, the product might be ready for the market and the market strategy of chapter 4.2 can be implemented. Perhaps under a new company name.

Amstel Energy

A simplified version of a roadmap that could be used for the internal project is given in Figure 76.

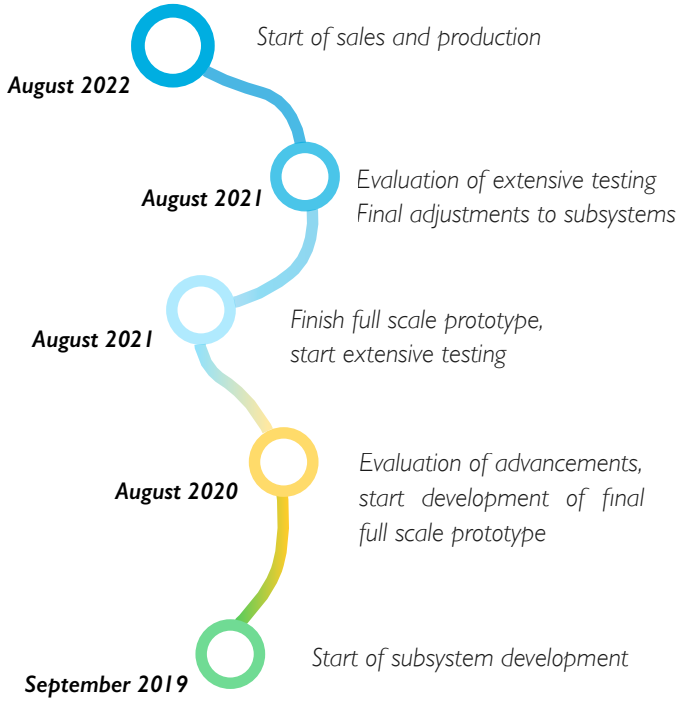

Figure 76: Simplified roadmap to production of LEFt

5.3 Personal Reflection

Introduction

This graduation project has been a big challenge for me, that started before even writing the project brief. This final chapter reflects on my personal experiences while working on the development of a mechanical storage system.

5.3.1. Project structure

Although the results of the project are satisfactory to me, I would suggest a few changes to help a future project run smoother and might reach even higher goals.

Limited scope

Although it was very interesting to analyze all of the energy storage methods and checking their applicability to the scenario, it might have been useful to limit the time that was reserved for this part. This would have left more time for prototyping and testing and might have resulted in the final results to be more useful.

Company involvement

Executing this project mainly at the office of Amstel Engineering has allowed me to communicate directly, it was always possible to discuss something without having to plan official meetings in advance. The involvement and enthusiasm of Robert and Niels, but also of other engineers at the office have continuously motivated me to deliver the best results possible.
This has confirmed the image of working for a company as a design engineer. I recommend anyone doing a similar project to make use of the available resources like knowledge but also use enthusiasm as a driver.

5.3.2. Mechanical vs Design

Before choosing this project as my graduation assignment, I was unsure about the focus on product design. Considering the mechanical background of Amstel Engineering, my own bachelor's degree in mechanical engineering and the goal of the project seemed to ask for in-depth mechanical analysis.
After finishing my bachelor's, I chose to continue with the master Integrated Product Design to learn how to develop full products from "fuzzy front-end" to actual production. The methods I have learned to use have proven to be very useful to create a project structure to hold on to.
On the other hand, my basis as a mechanical engineer have provided me with the skills to analyze one aspect in-depth. Writing the Matlab-script would have been more difficult without programming experience and building the prototype probably would have entailed more technical difficulties.
I have encountered multiple situations in which previous projects during the master, where the team would have accepted the underdeveloped status of a technical aspect. During this project, I was able to work out some of these technical aspects into more detail. Again, taking the Matlab-script as an example.

All in all, I think my study background has made me the right person for this project. I have worked on it with constant enthusiasm and would enjoy doing similar work in the future.
In the future, I can see myself working somewhere in between mechanical engineering and product design. A company like Amstel Engineering suits this in terms of available projects and expertise.

Figure 77: Me, working on the prototype in the workshop at the faculty of Industrial Design Engineering.

References

1 NOS.nl (2018). Zonnepanelen zijn blij met de zon, niet met de hitte. Retrieved from https://nos.nl/artikel/2243431-zonnepanelen-zijn-blij-met-de-zon-niet-met-de-hitte.html [Accessed 23 Jul. 2019]

2 Blanc, P., Remund, J., & Vallance, L. (2017). Short-term solar power forecasting based on satellite images. In Renewable Energy Forecasting (pp. 179-198). Woodhead Publishing.

3 Dutch Government (1998). Artikel 31c Elektriciteitswet 1998. Retrieved from https://wetten.overheid.nl/jci1.3:c:BWBR0009755&hoofdstuk=3&paragraaf=5&artikel=31c&z=2019-01-01&g=2019-01-01 [Accessed 19 Mar. 2019]

4 Tesla Powerwall (2019). https://www.tesla.com/powerwall [Accessed 18 Mar. 2019]

5 United States Environmental Protection Agency (2013). Application of Life-Cycle Assessment to Nanoscale Technology: Lithium-Ion Batteries for Electric Vehicles.

6 Granta Design Limited (2018). Cambridge Engineering Selector EduPack 2018. Version 18.1.1

7 Olivetti, E.A., Ceder, G., Gaustad, G.G., Fu, X. (2017). Lithium-Ion Battery Supply Chain Considerations: Analysis of Potential Bottlenecks in Critical Metals.

8 Erdmann, L., Graedel, T.E. (2011). Criticality of Non-Fuel Minerals: A Review of Major Approaches and Analyses

9 International Electrotechnical Commission (2011). Electrical Energy Storage, White Paper.

10 Chen, H., Cong, T.N., Yang, W., Tan, C., Li, Y., Ding, Y. (2009). Progress in electrical energy storage system: A critical review

11 Defize, N. , de Graaff, R. (2019). Portfolio Amstel Engineering BV.

12 Tesla, Powerwall (2019). Retrieved from https://www.tesla.com/tesla_theme/assets/img/energy/solar/powerwall@2x.png?20180111 [23 Apr. 2019]

13 Aneke, M., Wang, M. (2016). Energy storage technologies and real life applications – A state of the art review

14 Meyer, F. (2007). Compressed air energy storage power plants. BINE Informationsdienst

15 Amber Kinetics (2019), Longer Duration, Lower Cost Energy Storage. https://amberkinetics.com/products-2/ [Accessed 11 Mar. 2019]

16 Nederlandse Aardolie Maatschappij (NAM) (2018). Storelectric wint NAM70 challenge. Retrieved from https://www.nam.nl/nieuws/2018/storelectric-wint-nam70-challenge.html [Accessed 01 Apr. 2019]

17 Budt, M., Wolf, D., Span, R., Yan, J. (2016). A review on compressed air energy storage: Basic principles, past milestones and recent developments

18 CleanTechnica (2019). Surun Brightbox, schematic. Retrieved from https://cleantechnica.com/files/2016/03/surun_brightbox.png [23 Apr. 2019]

19 Dobber, T. (2018). Amstel Innovatie Project

20 KNMI (2019). Hourly data of the weather in the Netherlands. Retrieved from http://projects.knmi.nl/klimatologie/uurgegevens/selectie.cgi [06 Apr. 2019]

21 JA Solar (2019). JAM6 (BK) 60/245 - 265. Retrieved from https://www.zonnepanelen.net/nl/pdf/panels/20150212131952-fjhnnm-2.pdf

22 U.S. Department of Energy (2013). Commercial and Residential Hourly Load Profiles. https://openei.org/doe-opendata/dataset/commercial-and-residential-hourly-load-profiles-for-all-tmy3-locations-in-the-united-states [Accessed 05 Apr. 2019]

23 SMA Solar Technology AG (2019). Sunny Portal App 1.15.1.R. Retrieved from https://itunes.apple.com/nl/app/sunny-portal/id375717023?l=en&mt=8 [Downloaded Apr. 2019]

24 Qu, L., & Qiao, W. (2011). Constant power control of DFIG wind turbines with supercapacitor energy storage. IEEE Transactions on Industry Applications, 47(1), 359-367.

25 Ali, M. H., Wu, B., & Dougal, R. A. (2010). An overview of SMES applications in power and energy systems. IEEE transactions on sustainable energy, 1(1), 38-47.

26 Lu, L., Han, X., Li, J., Hua, J., & Ouyang, M. (2013). A review on the key issues for lithium-ion battery management in electric vehicles. Journal of power sources, 226, 272-288.

27 Battke, B., Schmidt, T. S., Grosspietsch, D., & Hoffmann, V. H. (2013). A review and probabilistic model of lifecycle costs of stationary batteries in multiple applications. Renewable and Sustainable Energy Reviews, 25, 240-250.

28 Steinweg, T. (2011). The Electric Car Battery: Sustainability in the Supply Chain.

29 Lambert, F. (2018). Mercedes-Benz kills its 'Tesla Powerwall killer' energy storage device. https://electrek.co/2018/04/30/mercedes-benz-kills-tesla-powerwall-killer-energy-storage-device/ [Accessed 5 Apr. 2019]

30 LG Chem (2018). ESS Battery catalogue. https://www.lgchem.com/upload/file/product/LGChem_Catalog_Global_2018.pdf [Accessed 5 Apr. 2019]

31 Schoenung, S. M. (2001). Characteristics and technologies for long-vs. short-term energy storage. United States Department of Energy.

32 Mori, D., & Hirose, K. (2009). Recent challenges of hydrogen storage technologies for fuel cell vehicles. International journal of hydrogen energy, 34(10), 4569-4574.

33 Miao, B., & Chan, S. H. (2019). The economic feasibility study of a 100-MW Power-to-Gas plant. International Journal of Hydrogen Energy.

34 Walker, S. B., Mukherjee, U., Fowler, M., & Elkamel, A. (2016). Benchmarking and selection of Power-to-Gas utilizing electrolytic hydrogen as an energy storage alternative. International Journal of Hydrogen Energy, 41(19), 7717-7731.

35 de Gracia, A., & Cabeza, L. F. (2015). Phase change materials and thermal energy storage for buildings. Energy and Buildings, 103, 414-419.

36 Bolund, B., Bernhoff, H., & Leijon, M. (2007). Flywheel energy and power storage systems. Renewable and Sustainable Energy Reviews, 11(2), 235-258.

37 Gurumurthy, S. R., Sharma, A., Sarkar, S., & Agarwal, V. (2013, July). Apportioning and mitigation of losses in a Flywheel Energy Storage system. In 2013 4th IEEE International Symposium on Power Electronics for Distributed Generation Systems (PEDG) (pp. 1-6). IEEE.

38 Kascak, P. E., Kenny, B. H., Dever, T. P., Santiago, W., & Jansen, R. H. (2001). International space station bus regulation. NASA glenn research center flywheel energy storage system development unit, IECEC.

39 Li, X., Erd, N., & Binder, A. (2016, June). Evaluation of flywheel energy storage systems for residential photovoltaic installations. In 2016 International Symposium on Power Electronics, Electrical Drives, Automation and Motion (SPEEDAM) (pp. 255-260). IEEE.

40 Liu, H., & Jiang, J. (2007). Flywheel energy storage—An upswing technology for energy sustainability. Energy and buildings, 39(5), 599-604.

41 Dominion Corporate, (2012). Bath County Pumped Storage Station. https://web.archive.org/web/20120103080341/http://www.dom.com/about/stations/hydro/bath-county-pumped-storage-station.jsp [Accessed 5 Apr. 2019]

42 Gravity Power, (2017). Grid Scale Energy Storage. http://www.gravitypower.net/technology-gravity-power-energy-storage/ [Accessed 5 Apr. 2019]

43 Succar, S., & Williams, R. H. (2008). Compressed air energy storage: theory, resources, and applications for wind power. Princeton environmental institute report, 8, 81.

44 Energy Storage Sense. (2018) LightSail – Another setback for thermo-mechanical energy storage. http://energystoragesense.com/uncategorized/lightsail-another-setback-for-thermo-mechanical-energy-storage/ [Accessed 5 Apr. 2019]

45 Hartmann, N., Vöhringer, O., Kruck, C., & Eltrop, L. (2012). Simulation and analysis of different adiabatic compressed air energy storage plant configurations. Applied Energy, 93, 541-548.

46 Grazzini, G., & Milazzo, A. (2008). Thermodynamic analysis of CAES/TES systems for renewable energy plants. Renewable energy, 33(9), 1998-2006.

47 Guo, C., Xu, Y., Zhang, X., Guo, H., Zhou, X., Liu, C., ... & Chen, H. (2017). Performance analysis of compressed air energy storage systems considering dynamic characteristics of compressed air storage. Energy, 135, 876-888.

48 Maia, T. A., Barros, J. E., Cardoso Filho, B. J., & Porto, M. P. (2016). Experimental performance of a low cost micro-CAES generation system. Applied energy, 182, 358-364.

49 Kumagai, J. (2014). Hydrostor Wants to Stash Energy in Underwater Bags. https://spectrum-ieee-org.tudelft.idm.oclc.org/energy/renewables/hydrostor-wants-to-stash-energy-in-underwater-bags [Accessed 5 Apr. 2019]

50 Pimm, A. J., Garvey, S. D., & de Jong, M. (2014). Design and testing of energy bags for underwater compressed air energy storage. Energy, 66, 496-508.

51 Highview Power, (2018) https://www.highviewpower.com/wp-content/uploads/2018/07/Highview-Power-Pilsworth-Launch-Press-Release.pdf [28 Mar. 2019]

52 Ameel, B., T'Joen, C., De Kerpel, K., De Jaeger, P., Huisseune, H., Van Belleghem, M., & De Paepe, M. (2013). Thermodynamic analysis of energy storage with a liquid air Rankine cycle. Applied Thermal Engineering, 52(1), 130-140.

53 Benato, A., & Stoppato, A. (2018). Pumped thermal electricity storage: A technology overview. Thermal Science and Engineering Progress, 6, 301-315.

54 Morgan, R., Nelmes, S., Gibson, E., & Brett, G. (2015). Liquid air energy storage–analysis and first results from a pilot scale demonstration plant. Applied energy, 137, 845-853.

55 Letcher, T. M., Law, R., & Reay, D. (2016). Storing energy: with special reference to renewable energy sources (Vol. 86). Oxford: Elsevier.

56 Liu, H., He, Q., Borgia, A., Pan, L., & Oldenburg, C. M. (2016). Thermodynamic analysis of a compressed carbon dioxide energy storage system using two saline aquifers at different depths as storage reservoirs. Energy conversion and management, 127, 149-159.

57 National Energy Technology Laboratory. Carbon Storage FAQs. https://www.netl.doe.gov/coal/carbon-storage/faqs/carbon-storage-faqs#stored/ [28 Mar. 2019]

58 Kipor Power Products. Kipor KDE3500X. http://www.kipor.nl/winkel/kippor-diesel/kipor-kde3500x/ [4 Apr. 2019]

59 IOR Energy. Fuel Energy Density. https://web.archive.org/web/20100825042309/http://www.ior.com.au/ecflist.html [4 Apr. 2019]

60 Mousavi, S., Faraji, F., Majazi, A., & Al-Haddad, K. (2017). A comprehensive review of Flywheel Energy Storage System technology. Renewable and Sustainable Energy Reviews, 67, 477-490.

61 Van Boeijen, A., Daalhuizen, J., van der Schoor, R., & Zijlstra, J. (2014). Delft design guide: Design strategies and methods.

62 Germen. (2012). Lost perslucht ons energieprobleem op? https://www.visionair.nl/wetenschap/lost-perslucht-ons-energieprobleem-op/ [Accessed 8 Apr. 2019]

63 Kohari, Z., Nadudvari, Z., Szlama, L., Keresztesi, M., & Csaki, I. (2011). Test results of a compact disk-type motor/generator unit with superconducting bearings for flywheel energy storage systems with ultra-low idling losses. IEEE Transactions on Applied Superconductivity, 21(3), 1497-1501.

64 Skinner, M. A. (2017). Characterization of passive discharge losses in a flywheel energy storage system.

65 Schulz, A., Hartl, S., Sima, H., Hinterdorfer, T., & Wassermann, J. (2015). Innovative Schwungradspeicher mit hoher Energieeffizienz und Zuverlässigkeit. e & i Elektrotechnik und Informationstechnik, 132(8), 481-490.

66 Nuclear-Power.net. Brayton gas turbine. https://www.nuclear-power.net/nuclear-engineering/thermodynamics/thermodynamic-cycles/brayton-cycle-gas-turbine-engine/thermal-efficiency-brayton-cycle/ [Accessed 11 Apr. 2019]

67 Park, J. D. (2010, November). Simple flywheel energy storage using squirrel-cage induction machine for DC bus microgrid systems. In IECON 2010-36th Annual Conference on IEEE Industrial

Electronics Society (pp. 3040-3045). IEEE.

68 Watt-Logic (2017). Electricity storage on the fly. Retrieved from http://watt-logic.com/2017/06/07/flywheel-energy-storage/ [Accessed 23 July 2019]

69 Velkess. Low Cost, High Performance, Non-Toxic, Safe Energy Storage. http://www.velkess.com/flywheel.html [Accessed 11 Apr. 2019]

70 Vycon energy, Runtimes & Specifications. Available at https://vyconenergy.com/products/ups/run-times-specs/ [Accessed 11 Apr. 2019]

71 Beacon Power Brochure, 2019. Retrieved from http://beaconpower.com/wp-content/themes/beaconpower/inc/beacon_power_brochure_081414.pdf [Accessed 11 Apr. 2019]

72 Active Power, Flywheel Technology. Available at http://www.activepower.com/en-US/5059/flywheel-technology [Accessed 11 Apr. 2019]

73 Active Power Systems Inc., 2017. CleanSource HD675 UPS. Retrieved from http://www.activepower.com/en-US/documents/3970/60hz-cleansource-hd675-en.pdf [Accessed 11 Apr. 2019]

74 Molina, M. G. (2009). Dynamic modelling and control design of advanced energy storage for power system applications. In Dynamic Modelling. IntechOpen.

75 Bakay, L., Viarouge, P., Dubois, M., & Ruel, J. (2010). Losses in hybrid and active magnetic bearings applied to long term flywheel energy storage. 5th IET International Conference on Power Electronics, Machines and Drives (PEMD 2010).

76 Brobeck, W.M. & Associates, United States. Department of Energy, & Sandia Laboratories. (1979). Conceptual Design of a Flywheel Energy Storage System. Department of Energy, Sandia Laboratories.

77 Takemoto, M., Chiba, A., Akagi, H., & Fukao, T. (2002, October). Radial force and torque of a bearingless switched reluctance motor operating in a region of magnetic saturation. In Conference Record of the 2002 IEEE Industry Applications Conference. 37th IAS Annual Meeting (Cat. No. 02CH37344) (Vol. 1, pp. 35-42). IEEE.

78 Jiang, L., Zhang, W., Ma, G. J., & Wu, C. W. (2017). Shape optimization of energy storage flywheel rotor. Structural and Multidisciplinary Optimization, 55(2), 739-750.

79 Kress, G. R. (2000). Shape optimization of a flywheel. Structural and Multidisciplinary Optimization, 19(1), 74-81.

80 Sanders, S., Sun, E., He, M., Senesky, M., & Chiao, E. Y. (2019). U.S. Patent Application No. 10167925B2. Washington, DC: U.S. Patent and Trademark Office. https://patents.google.com/patent/US10167925B2/en [Accessed 5 Apr. 2019]

81 Toh, C. S., & Chen, S. L. (2016). Design, modeling and control of magnetic bearings for a ring-type flywheel energy storage system. Energies, 9(12), 1051.

82 Yulong, P., Cavagnino, A., Vaschetto, S., Feng, C., & Tenconi, A. (2017, June). Flywheel energy storage systems for power systems application. In 2017 6th International Conference on Clean Electrical Power (ICCEP) (pp. 492-501). IEEE.

83 Ryder G.H. (1969) Rotating Discs and Cylinders. In: Strength of Materials. Palgrave, London

84 Merritt, B.T., Post, R. F., Dreifuerst, G. R., & Bender, D. A. (1994). Halbach array motor/generators: A novel generalized electric machine (No. UCRL-JC-119050; CONF-950261-2). Lawrence Livermore National Lab., CA (United States).

85 Miles, A. L. (2011). An experimental study of windage due to rotating and static bolts in an enclosed rotor-stator system (Doctoral dissertation, University of Sussex), 157.

86 Gurumurthy, S. R., Sharma, A., Sarkar, S., & Agarwal, V. (2013, July). Apportioning and mitigation of losses in a Flywheel Energy Storage system. In 2013 4th IEEE International Symposium on Power Electronics for Distributed Generation Systems (PEDG) (pp. 1-6). IEEE.

87 Ghaemi, E., & Mirsalim, M. (2017). Design and prototyping of a new flywheel energy storage system. IET Electric Power Applications, 11(9), 1517-1526.

88 Dugas, P. J. (2018). U.S. Patent Application No. 10103600B2. Washington, DC: U.S. Patent and Trademark Office. https://patents.google.com/patent/US10103600B2/en [Accessed 09 Apr. 2019]

89 Schweitzer, G., & Maslen, E. (2009). Magnetic bearings: Theory, design, and application to rotating machinery. Berlin: Springer.

90 M7000 motors catalogue, Nord Drivesystems. (2019) https://www.nord.com/cms/media/documents/bw/M7000_IE1_IE2_IE3_EN_0219.pdf [Accessed 11 Apr. 2019]

91 Gabrys, C. W. (2004). U.S. Patent No. 6,710,489. Washington, DC: U.S. Patent and Trademark Office. https://patents.google.com/patent/US6710489B1/ [Accessed 11 Apr. 2019]

92 Oxford Dictionary of Sports Science & Medicine, 2007. Poisson Effect. Retrieved from http://www.oxfordreference.com/view/10.1093/oi/authority.20110803100333756 [Accessed 11 Apr. 2019]

93 Earnshaw, S. (1842). On the nature of the molecular forces which regulate the constitution of the luminferous ether. Trans. Camb. Phil. Soc., 7, 97-112.

94 Smolinski, M., Perkowski, T., Mystkowski, A., Dragašius, E., Eidukynas, D., & Jastrzebski, R. P. (2017). AMB flywheel integration with photovoltaic system for household purpose–modelling and analysis. Eksploatacja i Niezawodność, 19(1).

95 Amiryar, M., & Pullen, K. (2017). A review of flywheel energy storage system technologies and their applications. Applied Sciences, 7(3), 286.

96 Santiago, J., Oliveira, J. G., Lundin, J., Larsson, A., & Bernhoff, H. (2008, September). Losses in axial-flux permanent-magnet coreless flywheel energy storage systems. In 2008 18th International Conference on Electrical Machines (pp. 1-5). IEEE.

97 Smirnov, A., Uzhegov, N., Sillanpää, T., Pyrhönen, J., & Pyrhönen, O. (2017). High-speed electrical machine with active magnetic bearing system optimization. IEEE Transactions on Industrial Electronics, 64(12), 9876-9885.

98 Combrinck, A. (2010). Adaptive control of an active magnetic bearing flywheel system using neural networks (Doctoral dissertation, North-West University).

99 Technical University of Denmark, DTU. Magfly: Magnetic flywheels for energy storage. http://

www.flywheel.dk/research [Accessed 08 Apr. 2019)

100 Gammelby, P.F. (2006). Renewable energy to be stored in floating flywheels. Aarhus University, Science and Technology. http://scitech.au.dk/en/about-science-and-technology/current-affairs/news/show/artikel/vedvarende-energi-skal-lagres-i-svaevende-svinghjul/ [Accessed 08 Apr. 2019)

101 Yuan, Y., Sun, Y., & Huang, Y. (2015). Design and analysis of bearingless flywheel motor specially for flywheel energy storage. Electronics Letters, 52(1), 66-68.

102 Sun, Y., Yang, F., Yuan, Y., Yu, F., Xiang, Q., & Zhu, Z. (2018). Analysis of a hybrid double stator bearingless switched reluctance motor. Electronics Letters, 54(24), 1397-1399.

103 David, I. B., Zohar, N., & Pincu, D. (2017). U.S. Patent No. 9667117B2. Washington, DC: U.S. Patent and Trademark Office. https://patents.google.com/patent/US9667117B2/en [Accessed 09 Apr. 2019]

104 Skinner, M. A. (2017). Characterization of passive discharge losses in a flywheel energy storage system.

105 M7000 motors catalogue, Nord Drivesystems. (2019) Retrieved from https://www.nord.com/cms/media/documents/bw/M7000_IE1_IE2_IE3_EN_0219.pdf [Accessed 11 Apr. 2019]

106 Sanders, S. (2019) U.S. Patent No. 10167925B2. Washington, DC: U.S. Patent and Trademark Office. https://patents.google.com/patent/US10167925B2, [Accessed 05 Apr. 2019].

107 Sanders, S. (2018) U.S. Patent No. 20180006539A1. Washington, DC: U.S. Patent and Trademark Office. https://patents.google.com/patent/US20180006539A1/, [Accessed 05 Apr. 2019].

108 Evans, M.A., and Pei, E. (2010), iD Cards, Loughborough University.

109 Ahrens, M., Kucera, L., & Larsonneur, R. (1996). Performance of a magnetically suspended flywheel energy storage device. IEEE Transactions on control systems technology, 4(5), 494-502.

110 SKF Group (2019). SKF Bearing Select, version 1.0.36. https://www.skfbearingselect.com/ [Accessed 28 May 2019]

111 Tollig, F. (2019, July 11). Phone conversation concerning applicable bearing types.

112 IsaacPhysics (2019). Lenz's Law, Physics Concept. Retrieved from https://isaacphysics.org/concepts/cp_lenzs_law [Accessed 17 Jul. 2019]

113 Wikipedia, The Free Encyclopedia (2019). Eddy current. Retrieved from https://en.wikipedia.org/wiki/Eddy_current [Accessed 17 Jul. 2019]

114 Thuy Mai, NASA (2012). Technology Readiness Levels (TRLs). Retrieved from https://www.nasa.gov/directorates/heo/scan/engineering/technology/txt_accordion1.html [Accessed 31 Jul 2019]

115 Overstappen.nl (2019). Energietarieven 2019. Retrieved from https://www.overstappen.nl/energie/leveranciers/essent-tarieven/ [Accessed 31 Jul 2019]

116 CBS (2019). Rendementen en CO2-emissie elektriciteitsproductie 2017. Retrieved from https://www.cbs.nl/nl-nl/maatwerk/2018/04/rendementen-en-co2-emissie-elektriciteitsproductie-2017 [Accessed 31 July 2019]

117 Kals, H.J.J., Buiting-Csikós, Cs., van Luttervelt, C.A., Moulijn, K.A., Ponsen, J.M., Streppel, A.H. (2007). Industriële Productie. Het voortbrengen van mechanische producten. 4e herziene druk.

118 Essent (2019). Zonnepanelen: Leasen of huren. Retrieved from https://www.essent.nl/kennisbank/zonnepanelen/wat-zijn-de-voordelen-van-zonnepanelen/zonnepanelen-leasen-of-huren [Accessed 18 Jul. 2019]

119 Ashby, M. F. (2015). Materials and sustainable development. Butterworth-Heinemann.

120 Frankel, T.C., Whoriskey, P. (2016). Tossed aside in the 'White Gold' rush. Washington Post. Available at https://www.washingtonpost.com/graphics/business/batteries/tossed-aside-in-the-lithium-rush/ [Accessed 02 Jul. 2019]

121 Frankel, T.C. (2016). The Cobalt Pipeline. Washington Post. Available at https://www.washingtonpost.com/graphics/business/batteries/congo-cobalt-mining-for-lithium-ion-battery/ [Accessed 03 Jul. 2019]

122 Whoriskey, P. (2016). In your Phone, in their Air. Washington Post. Available at https://www.washingtonpost.com/graphics/business/batteries/graphite-mining-pollution-in-china/ [Accessed 02 Jul. 2019]

123 Battery University (2019). How does Graphite work in Li-ion? Available at https://batteryuniversity.com/learn/article/bu_309_graphite [Accessed 03 Jul. 2019]

124 Nadeem, F., Hussain, S. S., Tiwari, P. K., Goswami, A. K., & Ustun, T. S. (2018). Comparative review of energy storage systems, their roles, and impacts on future power systems. IEEE Access, 7, 4555-4585.

125 Medved, D., Kvakovsky, M., Sklenarova, V. (2010). Latent Heat Storage Systems. Intensive Programme "Renewable Energy Sources". University of West Bohemia, Czech Republic.

126 Thomassen, E.W. (2013). Excel workbook Kostprijsopbouw.

127 Kals, H.J.J., Buiting-Csikós, Cs., van Luttervelt, C.A., Moulijn, K.A., Ponsen, J.M., Streppel, A.H. (2007). Industriële Productie. Het voortbrengen van mechanische producten. 4e herziene druk.

128 Centraal bureau voor Statistiek (2019). Zonnestroom; vermogen zonnepanelen woningen, wijken en buurten, 2017. Retrieved from https://opendata.cbs.nl/statline/#/CBS/nl/dataset/84517NED/table?ts=1563972772122 [Accessed 22 Jul. 2019]

129 Liaoning Borui Machinery Co.,LTD (2019) Cast Steel Price Calculator. Retrieved from http://www.iron-foundry.com/cast-steel-price-calculator.html [Accessed 04 Jul. 2019]

Appendix

Contents

Appendix A. Methods of Energy Storage (continued) 90

Appendix B. List of Requirements 98

Appendix C. Matlab Script FlywheelCalc 100

Appendix D. Morphological Chart 114

Appendix E. Technical Drawings Prototype 116

Appendix F. Cover Design Sketches 122

Appendix G. Cost Price Calculation 124

Appendix H. Bill of Materials 126

Appendix I. Sustainability Assessment 128

Appendix J. Project Brief 132

Appendix A.

Methods of Energy Storage (continued)

Electrical

Electrical

Electrical energy can be stored it in its usable state, without the need for any conversion. With this in mind, storage systems that are making use of supercapacitors were developed and can be used as power buffer in the electricity grid (Qu & Qiao, 2011)[24] . A capacitor is able to store fairly large amounts of electricity and can quickly release it, making them useful for reducing loads on chemical batteries and extending their lifetime.

Next to supercapacitors, Superconducting Magnetic Energy Storage (SMES) is being widely used in the USA and has multiple applications including load leveling, dynamic stability, frequency regulation, power quality improvement and uninterrupted power supplies (USP's) (Ali et al. 2010)[25] . SMES systems make use of superconducting coils which are inductively charged or discharged by adjusting the average voltage across the coil, this way energy is stored in the coil's magnetic field.

Both of the methods described unfortunately have their downsides. Supercapacitors are very costly, have a high self-discharge and a low energy density. SMES is very efficient (round-trip efficiencies 85-90% (International Electrotechnical Commission, 2011), since the system has a very low internal resistance when cooled. However, cooling naturally requires energy, and additionally a large diameter of the coil(s) and risks of the magnetic field cause problems. Losses mainly occur in the cryogenic refrigeration of the system. Energy densities of supercapacitors lie between 2 and 10 Wh/L and those of SMES lie between 0.2 and 2.5 Wh/L, according to Chen et al., 2009. Both are relatively low, compared to for example lithium ion batteries which will be covered next.

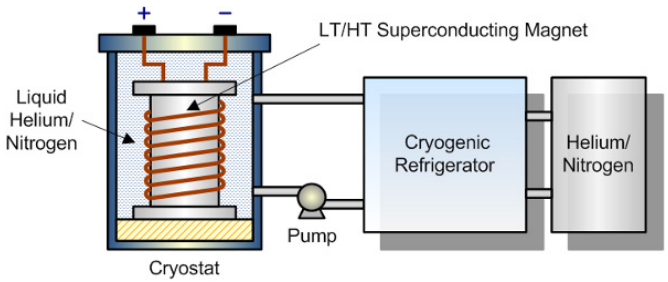

Figure 78: SMES (Nadeem et al. 2019)[124]

Chemical

Chemical

The most widely used method of storing electricity, where electricity is stored as chemical energy. A chemical battery is present in most consumer electronics in the lithium ion form, but many different ways of storing energy in this state are possible.

Batteries

Charging a battery by pushing an electric current through the anode and the cathode ionizes the electrolyte, allowing storage with low losses in idle state below 5% per month (Lu et al, 2013)[26] . Discharging is done by a redox reaction which causes an electric current.

Although development of chemical battery technology continues and is reaching a level where efficiencies range from 85% up to 95% (Battke et al., 2013)[27] , production of any kind of chemical battery causes substantial problems. A commonly used type of battery is the lithium-ion type, making use of production processes that cause political, social and ecological instability (Steinweg, 2011)[28] . Besides these downsides, li-ion has allowed development of interesting products. Electric car company Tesla has developed the Powerwall (Tesla, 2019), a 13.5 kWh battery pack at a size smaller than the average refrigerator. It can be placed indoors or mounted on an outside wall of a house and charges during the day by using the excess of solar energy being charged by solar panels on the roof. During nighttime, or on a day with less solar energy generated, the Powerwall supplies the household with electric power. The system by Tesla is currently amongst the few energy storage systems specifically on the market for households. A small number of other companies also uses Li-ion

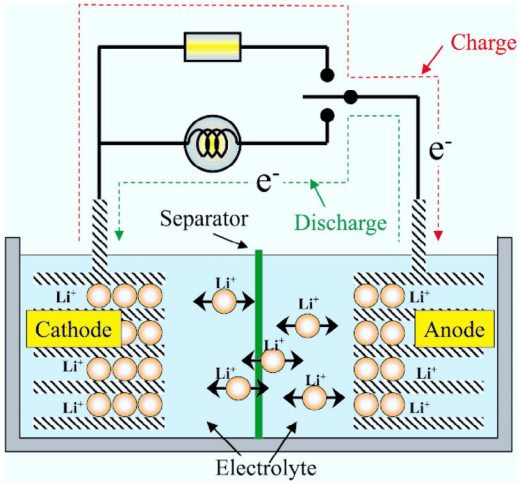

Figure 79: Li-ion battery. (Xu, 2017)

battery packs for residential energy storage but these solutions are eventually discontinued, like Mercedes-Benz's product (Lambert, 2018)[29] or are just not as well-known as the Powerwall like the ESS Battery by LG Chem (LGChem, 2019)[30] .

Looking at the complete system, the energy density of the Tesla Powerwall is calculated at 123 Wh/L, its round trip efficiency is claimed at 90%.

Hydrogen fuel cell

Fuel cell technology makes use of the simple principle of electrolysis. Hydrogen is created from water, by use of electricity and an anode-cathode couple. Reversing the process results in a round-trip efficiency of 59%. (Schoenung et al., 2003)[31]

A hydrogen fuel cell is capable of storage with an energy density of 500 – 3000 Wh/L, which is high in the comparison to other storage methods. The main downside of a hydrogen fuel cell system lies within the pressure that is necessary for storage. When used for hydrogen-powered vehicles, the storage tank is required to withstand high pressures of around 35 MPa (Mori et al., 2008)[32] , which is a challenging factor. This is one of the main reasons why hydrogen cars are not in common technology (yet).

Power-to-gas

When using hydrogen that was generated by electrolysis is not used in a fuel cell, but to fuel a power plant, the process is called power-to-gas. The cycle's efficiency is higher than a standard hydrogen fuel cell, as it lies around 60 percent. (Miao et al., 2019)[33] Three types of power-to-gas reactions are possible, either hydrogen, ammonia or methane can be generated by changing the process. The energy densities of demonstrative power-to-gas systems have reached an energy density of nearly 4500 Wh/L. (Walker et al. 2016)[34]

Thermal

Thermal

This method uses a change in internal energy of a material to store energy. Thermal energy storage (TES) or heat storage can be divided roughly in two different types; sensible heat and latent heat. Sensible heat includes storage in liquids and solids, whereas the latent storage type makes use of a phase change. Phase changes for latent heat storage can be solid to liquid, liquid to gas or the other way around.

The main drawback of this method is that there are losses involved in the conversion from electricity to heat and in the reversed process. This is why the round-trip efficiency of TES systems lies between 30 and 60% (Chen et al., 2009). But the heat cycle itself can be highly efficient, reaching percentages of 70 to 90%. Looking at energy densities, systems typically have energy densities of 80 (Low temperature TES) to 500 Wh/L (High temperature TES).

Studies have been conducted where researchers have attempted to include phase change materials in the wallboards, to be placed onto a building's walls. (Gracia & Cabeza, 2015)[35] This technology however is applicable to store thermal energy, and is not well suited for storing electrical energy.

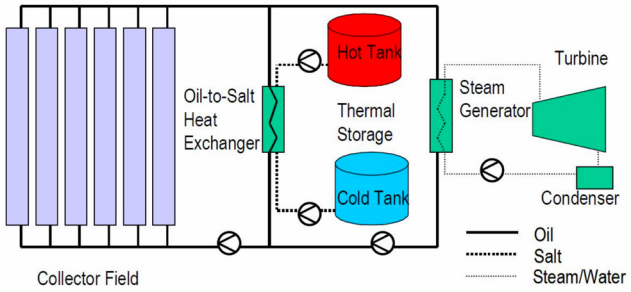

Figure 80: Latent heat thermal energy storage (Medved et al., 2010)[125]

Mechanical

Mechanical - Kinetic

Flywheel

To store energy, electrical power is converted into a rotational movement of a relatively large mass –the flywheel. It is now stored as kinetic energy and can be converted back to electricity by a simple generator. Experiments where different types of flywheel materials are tested have been conducted, and a relatively high energy density can be achieved when applying composite materials (Bolund et al., 2007)[36] . However, the high costs of these materials make this solution less attractive. Another drawback of this energy storage technology is the mechanical resistance which is inevitably present in the system. Magnetic bearings might offer the solution, since less resistance means higher rotational speeds are possible. The next hurdle to overcome within FESS is the occurrence of aerodynamic losses at higher speeds. Systems where the flywheel is enclosed in a low pressure (near vacuum) or helium chamber might be the solution to this.

Roundtrip efficiency of up to 80 percent has been achieved. (Gurumurthy et al., 2013)[37]

NASA has developed a flywheel battery which can store an excess of 15 MJ and can deliver a peak power of more than 4.1 kW (Kascak et al., 2001)[38] . Comparing this to the need of a single household, the system can provide a significant amount of electricity for a normal day of use. However, the timespan over which the system can regenerate electricity is limited to only a few hours. Li et al., 2016[39] , conducted a study into the usability of flywheel energy storage for residential photovoltaic installations, and concluded that internal losses are the main drawback for this application.

Liu & Jiang, 2007[40] , prospected that flywheel systems will have the following performance characteristics: specific energy: 200 Wh/kg and specific power: 30 kW/kg. This last number is mainly depending on prospected reduction of losses, meaning improvements in for example the casing.

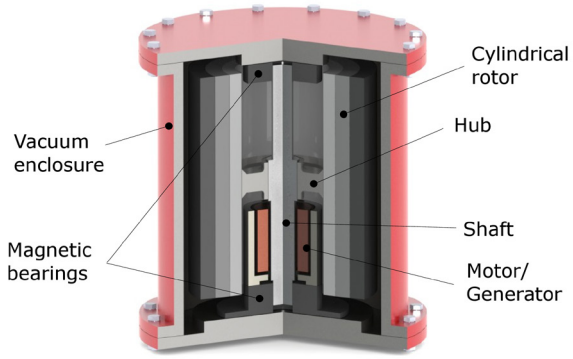

Figure 81: FESS (Toh et al. 2016)[79]

Simple calculations concerning concrete as an affordable material have already been done by Amstel Engineering BV. These calculations result in storage of 0.53 kWh for a system with a diameter of 1 meter and can therefore be classified as having a relatively low power density. Considering shelf parts like a 2400 rpm electric motor, this system is operating at low speeds and is therefore safer than comparable high speed systems. A higher power density can be achieved by increasing the rotor speed.

Mechanical - Potential

Pumped Hydro Storage (PHS)

Electricity is used to drive a pump that transfers water to a higher altitude. Releasing the water and letting it drive turbines regenerates electricity. An efficiency of 70 to 80 percent can be reached, which gives this method high potential for areas where a difference in altitude can easily be realized. PHS has a relatively low energy density of 0.5 to 1.5 Wh/L (Chen et al., 2009), resulting in storage plants of this type that are rather large in size. Bath County Pumped Storage Station[41] , Virginia, USA, currently has the largest pumped hydro storage and is located near a nuclear power plant. The storage plant's capacity lies at 24 GWh, which is many factors higher than the systems that are looked into for this project.

Gravity Energy Storage

One of the simpler methods, which lies closest to basic conversion of potential to electrical, is the gravity method. This is simply based on hoisting a mass by use of an electric motor and releasing it to drive a generator. Although this conversion is not the least efficient type, the energy density of around 0.07 Wh/L, according to a simple calculation is too low for it to be useful. Gravity Power[42] claims a high efficiency of 80% with their Gravity Power Module, which uses a large piston movement in a deep storage shaft. This system could theoretically provide an energy density of 0.5 to 1.5 Wh/l, but will need significant construction to be installed.

Compressed Air Energy Storage (CAES)

Electrical energy can be converted into potential by using it to compress air in a storage medium, this method is called Compressed Air Energy Storage (CAES). It makes use of large underground caverns to store air at high pressures ranging from 45 to 110 bar (Succar & Williams, 2008)[43] . Expanding the air through a turbine generates electricity to be used at the moment when it is needed with reported round-trip efficiencies of over 60%. On a smaller scale, compressed air can be stored in pressure vessels.

Keeping the temperature of the system constant would mean an isothermal system; Isothermal Compressed Air Energy Storage (I-CAES). Systems like these have been designed by startups like Lightsail Energy, but failed due to financial problems[44] .

A significant increase of round-trip efficiency can be achieved by implementing Thermal Energy Storage (TES) in the system. Without any heat or mass transfer, the process becomes adiabatic and is called A-CAES, which increases theoretical efficiency. Heat that is generated by the compressor is used in a recuperator to heat air before entering the turbines. (Hartmann et al., 2012)[45]

Advanced Adiabatic Compressed Air Energy Storage (AA-CAES) systems are reported to reach efficiencies of 67,5%. Which is similar to common electric batteries. (Grazzini et al., 2008)[46]

Energy density of the AA-CAES method is influenced strongly by air storage pressure, according to Guo et al. (2017)[47] . By increasing storage pressure from 8 to 20 MPa, the energy density has increased by a factor of 2.42, reaching a value of 10.73 Wh/L. At the same time, roundtrip efficiency has increased by only 4.5% to 55.5%.

A high efficiency A-CAES system can be built by using large industrial components (Maia et al., 2016)[48] . Tested systems also consist of multi-stage compression as well as multi-stage expansion. Designing a similar system for smaller scale, i.e. domestic or microgrid, requires a considerable reduction of complexity and size.

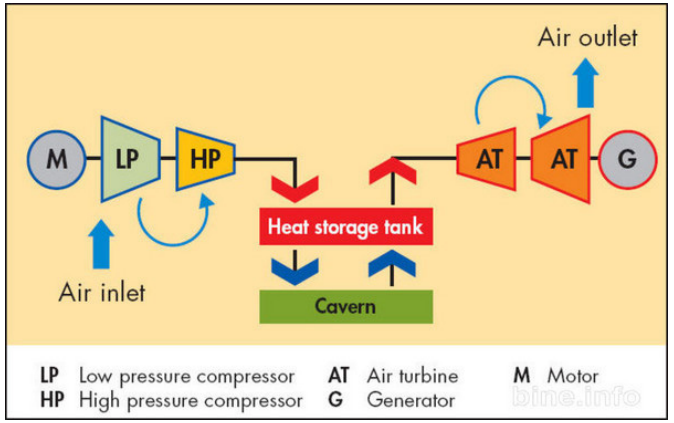

Figure 82: I-CAES (Succar & Williams, 2008)

Mechanical continued

UWCAES (Energy bags)

Professor Seamus Garvey of the University of Nottingham designed "Energy bags"[49], which stores compressed air in underwater balloons. When positioning the bags deeply underwater, air is compressed due to hydrostatic pressure and the same volume can store a larger amount of air than it would on the surface. A round-trip efficiency of 60-70% has been achieved, which is comparable to an above ground cryogenically cooled CAES.

Pimm et al., (2014)[50] determined the energy density of a potential underwater A-CAES, which has high potential especially at larger depths. At 400m below sea level, the energy density was determined at 7.55 Wh/L (=kWh/m^3), which means an energy bag of 1 m^3 could be sufficient for a day's worth of energy storage for a household.

Although energy density and round-trip efficiency of this method look promising, it is not directly applicable to household energy storage. The geographical location of only a few houses would allow installation of bags several hundreds of meters underwater.

Liquid Air Energy Storage (LAES)

This method utilizes a cryogenic liquid to liquefy air and store energy by use of this refrigeration process. A version of this system is being used since June 2018 at a power plant in the UK, made by by Highview Power, where a 15 MWh LAES plant is connected to a landfill gas site[51]. Studies on this storage method have shown round-trip efficiencies around 40% (Ameel et al. 2013)[52], which is significantly lower than CAES efficiencies. On the other hand, energy densities are high with values around 57 Wh/L. A schematic, drawn by Benato & Stoppato (2018)[53] is displayed in Figure 83.

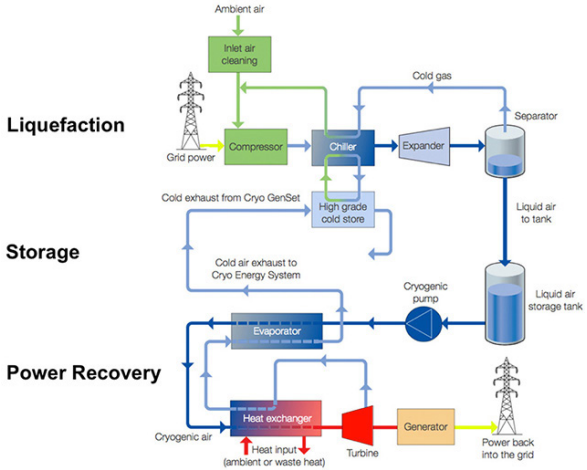

Figure 83: LAES (Benato & Stoppato, 2018)

Unfortunately, scaling this system will be problematic. A study by the University of Brighton (Morgan et al., 2015)[54], showed that a small-scale pilot could only deliver a round-trip efficiency of 8%. This was attributed to the scale of the test and expected to improve by increasing the working pressures and therefore scale.

Compared to other storage technologies like pumped hydro and compressed air, LAES offers the same long discharge time of multiple hours. (Letcher et al. 2016)[55]

Liquid CO2 energy storage (L-CO2)

To store energy in the form of liquid CO2, method similar to CAES can be applied. However to reach phase transition from gas to liquid at room temperature, a pressure of 73.9 bar is required. A round-trip efficiency of 63.35% has been achieved (Liu et al., 2016)[56]. At this temperature and pressure, CO2 becomes a supercritical fluid and absorbs a large amount of energy during condensation. Using CO2 in its transcritical state results in a higher round-trip efficiency but requires a very complicated configuration of the storage system and is therefore not considered an alternative. The energy storage density of a supercritical L-CO2 system was calculated at 255.20 Wh/L, which is significantly higher than that of CAES. However, storing CO2 in its supercritical state requires underground saline storage reservoirs at the right temperature, which are found at depths of around 800m (NETL, 2019)[57]. Above ground vessels for storing large have not been considered since storage temperature has to be kept at the right temperature, which would require energy. Although it seems interesting, developing an above ground storage method for liquid CO2 lies outside the scope of this project.

Fossil (for illustration only)

Diesel generator

One non sustainable method is added for illustrative purposes, namely a diesel generator, which uses the fossil fuel diesel. It is included in this analysis to illustrate how sustainable storage methods compare to traditional ways of generating energy on a small scale. A small diesel generator is a typical way of generating electricity off the. While being available in many sizes, for this comparison a 2.8 kW commercial model by Kipor[58] (Kipor.nl, accessed apr. 2019) has been considered. Diesel as a fuel has a very high energy density of 10,722 Wh/L (IOR energy, 2010)[59] , but since using this to generate electricity cannot be classified as a storage option, this value can be disregarded.

Appendix B.

List of Requirements

Energy storage

The system is capable of **mechanically storing** an **excess** of electrical energy produced by a **renewable source** during an average summer day in The Netherlands.

The system is capable of **supplying** the stored energy **to the household** during a period when renewable energy is **not being generated**.

Storage period

The system does **not lose more than half** of the stored energy in a period of **10 hours**, when no energy is demanded by the household.

System size

The complete system falls within the boundaries of **2 m^3**.

The room to place the system does **not need to be modified** for placement.

Environmental impact

The system **does not produce CO_2** emission during the use phase.

Sourcing materials for production does not cause political, social or economical problems in the country of origin.

The system has a minimum lifespan of **10 years**.

The system **does not require professional maintenance** during its lifespan.

Use

The system does **not require** any **user input** to operate.

The system **communicates** its amount of stored electricity to the user and encourages responsible utilization of electricity.

Costs

The **annual costs** for the consumer are **less than two times** the annual costs of a comparable li-ion alternative.

Appendix C.

Matlab Script FlywheelCalc

Matlab output

The following pages contain a rough output of the script FlywheelCalc. To provide the data, the size of the disc-shaped flywheel was chosen. The graphs that are visible are therefore representative for this version of storage system.

A separate print of the Matlab-script FlywheelCalc.m will be attached here.

Table of Contents

..... 1
Data setup 1
Flywheel setup 2
Settings for initial spindown calculation 3
User settings dialog 3
Basic calculation 5
Output the values 5
calculate theoretically available energy 9
Addition of air friction 13
Include bearing resistance 14
Calculate the available energy after a certain period of passive storage 14
Include regeneration of electricity 16
further visualize the data 18
Hatch the part in the graph where the yield strength was exceeded 19
Table with alternative solutions 20
Plot the spin-down 21
Determine energy stored in the system while simulating a certain scenario 22
Read supply & demand data 24
Define charging the flywheel 28
Include motor torque and maximum angular acceleration 29
Plot the charge/discharge 30
Calculate energy in the system with supply & demand considered 31
Simulate flywheel system in the scenario 34
Passive effects until full charge 36
Plot! 41


```
close all
clear all
clc

% Calculating specific energy in a flywheel energy storage system with
 set
% dimensions and an increasing rotational speed.
```

Data setup

```
% Choose the dataset for supply & demand to use.
% 1 = Supply: IJburg 2025 & PV_setup,              Demand: DNV GL
% 2 = Supply: IJburg 2025 & PV_setup,              Demand: DNV GL
 CORRECTED
% 3 = Supply: KNMI De Bilt during chosen period,   Demand: New York
 yearly average 2013
% 4 = Supply: KNMI De Bilt during chosen period,   Demand: DNV GL
% 5 = Supply: KNMI De Bilt during chosen period,   Demand: DBV GL
 CORRECTED

% dataset = 1;

datasets = {'1','2','3','4','5'};
```



```
[indx,tf] = listdlg('PromptString','Select a dataset:',...
                    'SelectionMode','single',...
                    'ListString',datasets);
dataset = indx;

if isempty(dataset)
    dataset = 3;
end

t_start_h = 12.7; % Time of day when to start, change to make sure
 enough energy stays in the system

% Choose PV panel efficiency: 72 or 80 percent.
Eff_PV = 72;
```

Flywheel setup

```
Type = 2; % Rotor type

% 1 = Hollow, high storage requirement (rim not used)
% 2 = Solid, high storage requirement
% 3 = Hollow, low storage requirement (rim not used)
% 4 = Solid, low storage requirement

p_housing = 40; %Pa the pressure in the housing. Vacuum?

Eff_M = 0.744; % Set motor/generator efficiency
Tau_max = 6.75; % Nm Max torque delivered by the motor/generator
A_max = 11; % A Max current to pass through motor

rout = 0.7; %m                                  Initial: 0.7
rin = 0.6; %m                                   Initial: 0.6
h = 0.3; %m             (thickness of rotor)    Initial: 0.3
omegamax = 1000; %rad/s                             Initial: 1000
Estore_high = 13e3; %Wh                         Initial: 13.5e3
Estore_low = 7.7e3; %Wh                          Initial: 7.7e3

% Increase with steps of 1 rad/s for easier overview of data
omega = 1:1:omegamax;
omegarpm = omega/((2*pi)/60);

poisson = 0.295; % (hss)              Initial: 0.3
rho = 8000; %kg/m3 (hss)            Initial: 8000
Sigma_Yield = 550; %MPa (hss)       Initial: 215

Msolid = rho*pi*h*rout.^2; %kg
Mhollow = rho*pi*h*(rout.^2-rin.^2); %kg

Jsolid = 0.5*Msolid*rout^2; %kg*m^2
Jhollow = ((pi*rho*h)/2)*(rout.^4-rin.^4);

disp(['Chosen flywheel type: ',num2str(Type),'. Chosen dataset:
 ',num2str(dataset),'.']);
```



```
alpha_max_solid = Tau_max/Jsolid; %rad/s^2
alpha_max_hollow = Tau_max/Jhollow; %rad/s^2

Chosen flywheel type: 2. Chosen dataset: 3.
```

Settings for initial spindown calculation

24 hours in a day, split up in seconds.

```
t_day = 1:1:(24*3600);

t_activate_hours = 12; % hours.
% After how many seconds should the system start regenerating
 electricity?

P_used = 1.5e3; % W, power usage by household
```

User settings dialog

```
peaksimul = 0; % Don't include peaks, unless the user chooses to.

if dataset < 3

answer0 = questdlg('How many 300 Wp PV panels are installed?', ...
 'Choice of PV setup', ...
 '12','14','16','14');
% Handle response
switch answer0
    case '12'
        disp('12 Solar panels with 300 Wp are installed.')
        No_PV_1 = 12;
    case '14'
        disp('14 Solar panels with 300 Wp are installed.')
        No_PV_1 = 14;
    case '16'
        disp('16 Solar panels with 300 Wp are installed.')
        No_PV_1 = 16;
end

No_PV_2 = No_PV_1; % To be able to calculate the interia effects later
 in the script.
end

% Let the user choose the period to analyze, when KNMI dataset is
 chosen
if dataset > 2

No_PV_1 = 12; %Just to be able to read demand data from .xlsx

    answer0 = questdlg('How many 250 Wp PV panels are installed?', ...
 'Choice of PV setup', ...
```

```
 '18','20','22','18');
% Handle response
    switch answer0
        case '18'
            disp('18 Solar panels with 250 Wp are installed.')
            No_PV_2 = 18;
        case '20'
            disp('20 Solar panels with 250 Wp are installed.')
            No_PV_2 = 20;
        case '22'
            disp('22 Solar panels with 250 Wp are installed.')
            No_PV_2 = 22;
    end

answer1 = questdlg('Which period should be analyzed?', ...
 'Choice of data', ...
 'Average year','Summer...','Average Winter','Summer...');
% Handle response
switch answer1
    case 'Average year'
        disp('The yearround average solar power will be used for
 calculation.')
        supplydata = 'Year';
    case 'Summer...'
        answer2 = questdlg('More specifically, which period should be
 analyzed?', ...
        'Choice of data', ...
        'Average Summer','Nice day of Summer','Average Summer');
        switch answer2
            case 'Average Summer'
                disp('The average solar power suring the summer months
 will be used for calculation.')
            supplydata = 'Summer';
            case 'Nice day of Summer'
                disp('The data of a nice day during Summertime (July
 8th 2018) will be used for calculation.')
            supplydata = 'Summerday';
        end

        answer3 = questdlg('Should solar power peaks be included in
 the simulation?', ...
        'Peak inclusion', ...
        'Yes','No','No');
        switch answer3
            case 'Yes'
                disp('Occasional peaks in solar power will be included
 in the simulation.')
            peaksimul = 1;
            case 'No'
                disp('The simulation will be done without occasional
 peaks in solar power.')
            peaksimul = 0;
        end
    case 'Average Winter'
```



```
        disp('The average solar power suring the winter months will be
 used for calculation.')
        supplydata = 'Winter';
end
end
```

```
18 Solar panels with 250 Wp are installed.
The average solar power suring the summer months will be used for
 calculation.
The simulation will be done without occasional peaks in solar power.
```

Basic calculation

```
ESolid = 0.5*Jsolid*omega.^2; %J
EHollow = 0.5*Jhollow*omega.^2; %J

EWhSolid = ESolid/3600; %Wh
EWhHollow = EHollow/3600; %Wh

% Maximum tensile stress (Ryder, 1969)

Sigma = (1/1e6)*((3+poisson)/8)*omega.^2*rout.^2*rho; %MPa
```

Output the values

plot the set flywheel dimensions

```
fig0 = figure;
rectangle('Position',[1 1 (2*rout) h],'LineWidth',3,'FaceColor',
[.5 .5 .5])
set(fig0,'Position',[100 100 400 400]);
movegui(fig0,'northwest');
axis([0 3 0 3])
set(fig0, 'NumberTitle', 'off',...
    'Name', sprintf('Flywheel setup'));
if Type == 1
    rectangle('Position',[1+rout-rin 1 (2*rin)
 h],'LineWidth',1,'FaceColor',[1 1 1])
end
rectangle('Position',[1+rout 0.75 0.0001 h+0.5],'Linestyle',':') %
 rotational axis

fig1 = figure;
set(fig1,'Position',[100 100 600 120]);

fig2 = figure;
set(fig2,'Position',[100 100 600 600]);
set(fig2, 'NumberTitle', 'off',...
    'Name', sprintf('Plot of the calculated data'));
hold on;
grid on;
% grid minor;
xlabel('Rotational speed (rpm)');
```



```
ylabel('Energy Stored (kWh)');
movegui(fig1,'northwest');
movegui(fig2,'southwest');
movegui(fig2,[0 50]);

plot(omegarpm,EWhHollow,'Color',
[0/255,189/255,254/255],'Linestyle','--',...
    'Linewidth',2);
plot(omegarpm,EWhSolid,'Color',
[0/255,153/255,216/255],'Linestyle','-',...
    'Linewidth',2);
plot(omegarpm,Estore_low,'.k',...
    omegarpm,Estore_high,'.k','LineWidth',0.5);

txt1 = 'High storage requirement';
text(200,Estore_high+3e2,(txt1));
txt2 = 'Low storage requirement';
text(200,Estore_low+3e2,txt2);

legend({'Ring-shaped rotor','Solid rotor'},'Location','northwest');
set(0,'DefaultLegendAutoUpdate','off');

% If High requirement is desired

if max(EWhHollow) > Estore_high
    potpos1 = find(EWhHollow>Estore_high);
    Esol1 = EWhHollow(potpos1(1));
    omegasol1 = omegarpm(potpos1(1));
    Sigmasol1 = Sigma(potpos1(1));
    plot(omegasol1,Esol1,'ks','Linewidth',4);

    if Sigmasol1 < Sigma_Yield
        Sigma_check1 = true;
    else
        Sigma_check1 = false;
    end

    potpos2 = find(EWhSolid>Estore_high);
    Esol2 = EWhSolid(potpos2(1));
    omegasol2 = omegarpm(potpos2(1));
    Sigmasol2 = Sigma(potpos2(1));
    plot(omegasol2,Esol2,'ks','Linewidth',4);

    if Sigmasol2 < Sigma_Yield
        Sigma_check2 = true;
    else
        Sigma_check2 = false;
    end
else
    msgbox('Did not meet requirements! Please adjust your
 parameters.','Error!');
end

% If Low requirement kWh is desired
```

```
if max(EWhHollow) > Estore_low
    potpos3 = find(EWhHollow>Estore_low);
    Esol3 = EWhHollow(potpos3(1));
    omegasol3 = omegarpm(potpos3(1));
    Sigmasol3 = Sigma(potpos3(1));
    plot(omegasol3,Esol3,'ks','Linewidth',4);

    if Sigmasol3 < Sigma_Yield
        Sigma_check3 = true;
    else
        Sigma_check3 = false;
    end

    potpos4 = find(EWhSolid>Estore_low);
    Esol4 = EWhSolid(potpos4(1));
    omegasol4 = omegarpm(potpos4(1));
    Sigmasol4 = Sigma(potpos4(1));
    plot(omegasol4,Esol4,'ks','Linewidth',4);

    if Sigmasol4 < Sigma_Yield
        Sigma_check4 = true;
    else
        Sigma_check4 = false;
    end
else
    msgbox('Did not meet requirements! Please adjust your
 parameters.','Error!');
end
```

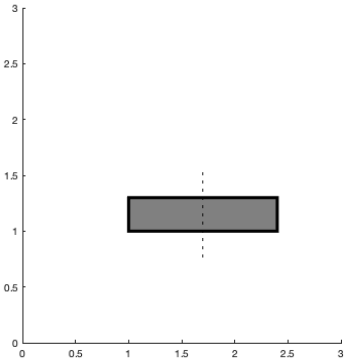

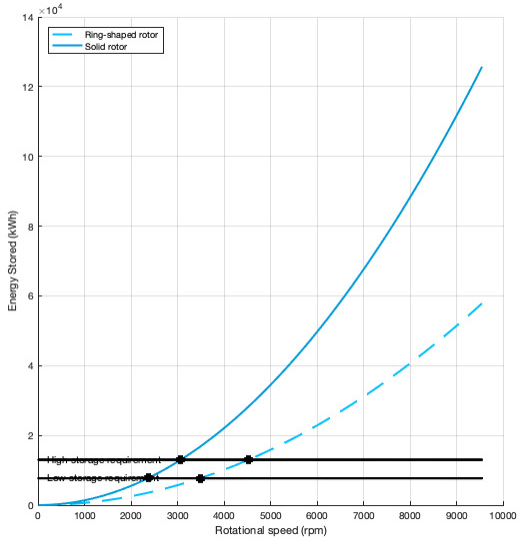

calculate theoretically available energy

when taking into account the fact that electricity can only be regenerated from full speed to half speed

```
halfspeed1 = find(omegarpm<omegasol1/2);
Eleft1 = EWhHollow(max(halfspeed1));
Eeffect1 = Esol1 - Eleft1;

i = 2;
Spec1_1 = false;

if Eeffect1 > Estore_high
    Spec1 = true;
else
    Eeffect1_output = Esol1 - Eleft1;
    while Eeffect1 < Estore_high
        Spec1 = false;
        Esol1_1 = EWhHollow(potpos1(i));
        omegasol1_1 = omegarpm(potpos1(i));
        Sigmasol1_1 = Sigma(potpos1(i));

        halfspeed1_1 = find(omegarpm<omegasol1_1/2);
        Eleft1_1 = EWhHollow(max(halfspeed1_1));
        Eeffect1 = Esol1_1 - Eleft1_1;

        i = i + 1;
        if Eeffect1 > Estore_high
            Spec1_1 = true;
            plot(omegasol1_1,Esol1_1,'s','Color',
[0/255,189/255,254/255],'Linewidth',4);
            Sigma1_1_check = find(omegarpm==omegasol1_1);
            Sigma1_1 = Sigma(Sigma1_1_check);
            Alt1_1 = false;
            if Sigma1_1 < Sigma_Yield
                Alt1_1 = true;
            end
        end
    end
end

halfspeed2 = find(omegarpm<omegasol2/2);
Eleft2 = EWhSolid(max(halfspeed2));
Eeffect2 = Esol2 - Eleft2;

j = 2;
Spec2_1 = false;

if Eeffect2 > Estore_high
    Spec2 = true;
else
    Eeffect2_output = Esol2 - Eleft2;
    while Eeffect2 < Estore_high
    Spec2 = false;
    Esol2_1 = EWhSolid(potpos2(j));
    omegasol2_1 = omegarpm(potpos2(j));
    Sigmasol2_1 = Sigma(potpos2(j));

    halfspeed2_1 = find(omegarpm<omegasol2_1/2);
    Eleft2_1 = EWhSolid(max(halfspeed2_1));
    Eeffect2 = Esol2_1 - Eleft2_1;

    j = j + 1;
        if Eeffect2 > Estore_high
            Spec2_1 = true;
            plot(omegasol2_1,Esol2_1,'s','Color',
[0/255,189/255,254/255],'Linewidth',4);
            Sigma2_1_check = find(omegarpm==omegasol2_1);
            Sigma2_1 = Sigma(Sigma2_1_check);
            Alt2_1 = false;
            if Sigma2_1 < Sigma_Yield
                Alt2_1 = true;
```

```
            end
        end
    end
end

halfspeed3 = find(omegarpm<omegasol3/2);
Eleft3 = EWhHollow(max(halfspeed3));
Eeffect3 = Esol3 - Eleft3;

k = 2;
Spec3_1 = false;

if Eeffect3 > Estore_low
    Spec3 = true;
else
    Eeffect3_output = Esol3 - Eleft3;
    while Eeffect3 < Estore_low
        Spec3 = false;
        Esol3_1 = EWhHollow(potpos3(k));
        omegasol3_1 = omegarpm(potpos3(k));
        Sigmasol3_1 = Sigma(potpos3(k));

        halfspeed3_1 = find(omegarpm<omegasol3_1/2);
        Eleft3_1 = EWhHollow(max(halfspeed3_1));
        Eeffect3 = Esol3_1 - Eleft3_1;

        k = k + 1;
        if Eeffect3 > Estore_low
            Spec3_1 = true;
            plot(omegasol3_1,Esol3_1,'s','Color',
[0/255,189/255,254/255],'Linewidth',4);
            Sigma3_1_check = find(omegarpm==omegasol3_1);
            Sigma3_1 = Sigma(Sigma3_1_check);
            Alt3_1 = false;
            if Sigma3_1 < Sigma_Yield
                Alt3_1 = true;
            end
        end
    end
end

halfspeed4 = find(omegarpm<omegasol4/2);
Eleft4 = EWhSolid(max(halfspeed4));
Eeffect4 = Esol4 - Eleft4;

l = 2;
Spec4_1 = false;

if Eeffect4 > Estore_low
    Spec4 = true;
else
    Eeffect4_output = Esol4 - Eleft4;
    while Eeffect4 < Estore_low
        Spec4 = false;
```



```
        Esol4_1 = EWhSolid(potpos4(l));
        omegasol4_1 = omegarpm(potpos4(l));
        Sigmasol4_1 = Sigma(potpos4(l));

        halfspeed4_1 = find(omegarpm<omegasol4_1/2);
        Eleft4_1 = EWhSolid(max(halfspeed4_1));
        Eeffect4 = Esol3_1 - Eleft3_1;

        l = l + 1;
        if Eeffect4 > Estore_low
            Spec4_1 = true;
            plot(omegasol4_1,Esol4_1,'s','Color',
[0/255,189/255,254/255],'Linewidth',4);
            Sigma4_1_check = find(omegarpm==omegasol4_1);
            Sigma4_1 = Sigma(Sigma4_1_check);
            Alt4_1 = false;
            if Sigma4_1 < Sigma_Yield
                Alt4_1 = true;
            end
        end
    end
end

Sigma_type = eval(strcat('Sigmasol',num2str(Type),'_1'));
omega_type = eval(strcat('omegasol',num2str(Type),'_1'));

Sigma_type_check = find(omegarpm==omega_type);
Sigma_type_value = Sigma(Sigma_type_check);
Yield_check = true;
if Sigma_type_value > Sigma_Yield
    Yield_check = false;
    disp('CAUTION! The yield stress is exceeded! Adjust parameters
 please...');
end
```


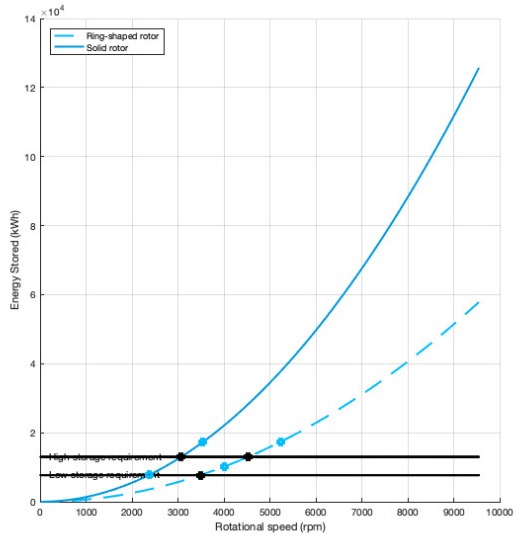

Addition of air friction

Formulas from Skinner (2017), which uses theory set up by Broecker (1959)

```
p_air = p_housing; % Pa, define above according to vacuum/no vacuum
R_air = 8.3144598; % J/mol*K (universal gas constant)
T_air = 293; % Room temperature 20 Celcius in Kelvin
M_air = 28.9647/1000; % kg/mol Molar mass of dry air
mu = 1.825e-5; % kg/m*s

rho_air = (p_air*M_air)/(R_air*T_air); %kg/m^3 Skinner uses M_air, is
 this required???

Re = (rout^2*omega.*rho_air)/mu;

cm = 0.131.*Re.^(-0.186); % Reduced moment coefficient according to
 Bayley & Owen (1969)
```

```
                    % From Miles (2011)

% cm = 0.2; % "Reduced moment coefficient" From graph (Skinner, 2017
 fig 25)
if Type == 1 || Type == 3
    Mt = 0.5.*cm.*rho_air*(rout^(24/5)-rin^(23/5)).*omega.^2;
    tau = Mt./(2*pi*(5/23)*(rout^3-rin^3));
else
    Mt = 0.5.*cm.*rho_air*rout^(24/5).*omega.^2;
    tau = Mt./(2*pi*(5/23)*rout^3);
end

Mb = Mt;
Ms = 2*pi*rout^2*h*tau;

Mtot = Mt + Mb + Ms; % Total drag moment

P_drag = Mtot.*omega; % W losses due to aerodynamic drag
```

Include bearing resistance

```
% According to Gurumurthy et al., 2013
P_bearing = 0.0498244.*omegarpm;

% According to Liu & Jiang, 2007
% P_bearing(1:1000) = 100; %W (Magnetic bearings)
```

Calculate the available energy after a certain period of passive storage

```
Estored1 = Esol1_1 * 3600; %J
Estored2 = Esol2_1 * 3600; %J
Estored3 = Esol3_1 * 3600; %J
Estored4 = Esol4_1 * 3600; %J

Estored_type = eval(strcat('Estored',num2str(Type))); %J Maximum
 energy stored
Eleft = eval(strcat('Eleft',num2str(Type))) * 3600; %J Energy left
 when half speed is left.
Enow = Estored_type;

% 24 hours from the maximum storage capacity. THIS IS A TIMER!
t_stored = 1;
t_stored_max = 120*3600;

Eresidu = zeros(1,t_stored_max); % Fill a vector with zeros
Eresidu(1) = Estored_type; %J Initial energy stored

P_actual = zeros(1,t_stored_max);

if Type == 1 || Type == 3 % Hollow Rotor types
```



```
    Jtype = Jhollow;
    P_increase = gradient(EHollow); % Energy increase per addition of
 1 rad/s (=max storing capability)
    while Enow > Eleft

        pos_now = find(EHollow < Enow,1,'last'); % Energies both in J
        omegarpm_now = omegarpm(pos_now);
        nowcalc = find(omegarpm == omegarpm_now);

        P_now = P_drag(nowcalc) + P_bearing(nowcalc);
        P_actual(t_stored) = P_now;
        for xx = 0:1:1
            Enow = Eresidu(t_stored) - P_now * xx; % J.
                                    % one second of losses is
 subtracted
                                    % every value of t
            Eresidu(t_stored+1) = Enow;
                                    % This value is entered in the
 vector
        end
        t_stored = t_stored + 1;  % evaluate the next second of the
 spin-down
    end
else

    Jtype = Jsolid;
    P_increase = gradient(ESolid); % Energy increase per addition of 1
 rad/s (=max storing capability)
    while Enow > Eleft

        pos_now = find(ESolid < Enow,1,'last'); % Energies both in J
        omegarpm_now = omegarpm(pos_now);
        nowcalc = find(omegarpm == omegarpm_now);

        P_now = P_drag(nowcalc) + P_bearing(nowcalc);
        P_actual(t_stored) = P_now;
        for xx = 0:1:1
            Enow = Eresidu(t_stored) - P_now * xx; % J.
                                    % one second of losses is
 subtracted
                                    % every value of t
            Eresidu(t_stored+1) = Enow;
                                    % This value is entered in the
 vector
        end
        t_stored = t_stored + 1;  % evaluate the next second of the
 spin-down
    end
end

for t_residu = t_stored : t_stored_max
    Eresidu(t_residu) = Eleft;
end
```



```
Eresidu_Wh = Eresidu / 3600; %Wh
Eleft_Wh = Eleft / 3600; %Wh

t_half_type = find((Eresidu_Wh-Eleft_Wh)<10,1)-1;
t_empty_type = find(Eresidu_Wh<10,1) - 1;

E0h = (Eresidu_Wh(1)/1000)-Eleft_Wh/1000; %kWh
if E0h < 0
    E0h = 0;
end

E8h = (Eresidu_Wh(8*3600-1)/1000)-Eleft_Wh/1000; %kWh
if E8h < 0
    E8h = 0;
end

E12h = (Eresidu_Wh(12*3600-1)/1000)-Eleft_Wh/1000; %kWh
if E12h < 0
    E12h = 0;
end

fprintf('\n');
disp(['Passive spin-down of this system, starting at
 ',num2str(omega_type,'%10.0f'),...
    ' rpm, with ',num2str(max(Eresidu_Wh)/1000,'%10.2f'),' kWh
 stored.']);

disp(['At initial rpm, the usable energy left in the system is ',...
        num2str(E0h,'%10.2f'),' kWh.']);

disp(['After ',num2str(t_half_type/3600,'%10.2f'),...
        ' hour(s), the reference rotor is at half speed and holds
 ',...
        num2str(Eresidu_Wh(t_half_type)/1000),' kWh.']);

fprintf('\n')
```

```
Passive spin-down of this system, starting at 3543 rpm, with 17.30 kWh
 stored.
At initial rpm, the usable energy left in the system is 14.09 kWh.
After 65.48 hour(s), the reference rotor is at half speed and holds
 3.2284 kWh.
```

Include regeneration of electricity

```
% Eff_M = 0.744; % Specified motor resistance (Nord Drivesystems 100
 L/4-2)

P_M = 2.4e3; % W, power specification of the motor
```

```
% P_used = 1.5e3; % W, power usage by household
% P_used is defined at the beginning of the script

t_regen = 1; % seconds
t_regen_max = t_stored_max; % seconds, maximum
t_activate = t_activate_hours*3600; % seconds
% t_activate_hours is defined at the beginning of the script

Eresidu_regen = zeros(1,t_regen_max); % Fill a vector with zeros
Eresidu_regen(1) = Eresidu(t_activate+1); %J
% Energy in system when regenerating starts

Enow = Eresidu_regen(1); %J

if Type == 1 || Type == 3 % Hollow Rotor types

    while Enow > Eleft

        pos_now = find(EHollow < Enow,1,'last'); % Energies both in J
        omegarpm_now = omegarpm(pos_now);
        nowcalc = find(omegarpm == omegarpm_now);

        P_now = P_used/Eff_M;
        for xx = 0:1:1
            Enow = Eresidu_regen(t_regen) - P_now * xx; % J.
                                    % one second of losses is
 subtracted
                                    % every value of t
            Eresidu_regen(t_regen+1) = Enow;
                                    % This value is entered in the
 vector
        end
        t_regen = t_regen + 1;  % evaluate the next second of the
 spin-down
    end

else

    while Enow > Eleft

        pos_now = find(ESolid < Enow,1,'last'); % Energies both in J
        omegarpm_now = omegarpm(pos_now);
        nowcalc = find(omegarpm == omegarpm_now);

        P_now = P_used/Eff_M;
        for xx = 0:1:1
            Enow = Eresidu_regen(t_regen) - P_now * xx; % J.
                                    % one second of losses is
 subtracted
                                    % every value of t
            Eresidu_regen(t_regen+1) = Enow;
                                    % This value is entered in the
 vector
        end
```



```
        t_regen = t_regen + 1;  % evaluate the next second of the
 spin-down
    end
end

for t_regen_left = t_regen:t_regen_max
    Eresidu_regen(t_regen_left) = Eresidu_regen(t_regen);
end
```

further visualize the data

```
set(fig1, 'NumberTitle', 'off',...
    'Name', sprintf('Data without consideration of losses'));

d = {'Hollow, High
 req.',omegasol1,Esol1/1000,Sigmasol1,Sigma_check1,Spec1,Eeffect1_output/1000;...
    'Solid, High
 req.',omegasol2,Esol2/1000,Sigmasol2,Sigma_check2,Spec2,Eeffect2_output/1000;...
    'Hollow, Low
 req.',omegasol3,Esol3/1000,Sigmasol3,Sigma_check3,Spec3,Eeffect3_output/1000;...
    'Solid, Low
 req.',omegasol4,Esol4/1000,Sigmasol4,Sigma_check4,Spec4,Eeffect4_output/1000};

table = uitable(fig1,'Data',d,'unit','normalized','Position',[0 0 1
 1]);

table.ColumnName = {'Version and req.','Max. Speed (rpm)','Total
 (kWh)',...
    'Stress (MPa)','<yield?','>spec?','Usable (MPa)'};

% Some visual settings for the "Energy Stored" graph
axis([0 max(omegarpm) 0 ((Esol1_1+Esol2_1)/2)*1.2]);

xticks(0:1000:max(omegarpm)); % One tick every 500 rpm %%%%%

yticks(0:1000:((Esol1_1+Esol2_1)/2)*1.2); % One tick every 2 kWh %%%%%
yt = get(gca, 'YTick');
set(gca, 'YTick',yt, 'YTickLabel',yt/1000) % Display E in kWh
```

	Version and req.	Max. Speed (rpm)	Total (kWh)	Stress (MPa)	<yield?	>spec?	Usable (MPa)
1	Hollow, High req.	4.5359e+03	13.0541	364.2828	☑	☐	9.8043
2	Solid, High req.	3.0749e+03	13.0347	167.4030	☑	☐	9.8164
3	Hollow, Low req.	3.4855e+03	7.7081	215.0984	☑	☐	5.7916
4	Solid, Low req.	2.3682e+03	7.7320	99.3013	☑	☐	5.8301

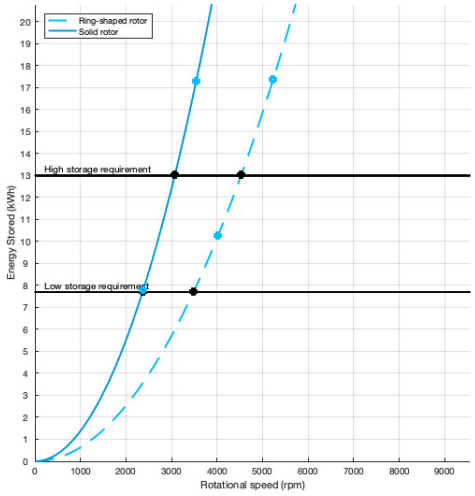

Hatch the part in the graph where the yield strength was exceeded

```
if max(Sigma) > Sigma_Yield
    failpos = find(Sigma > Sigma_Yield,1);
    %plot(omegarpm(failpos),EbWhHollow(failpos),'ro');
    %plot(omegarpm(failpos),EbWhSolid(failpos),'ro');

    xl = [omegarpm(failpos),max(omegarpm)*1.1];
    yl = [0 ((Esol1_1+Esol2_1)/2)*1.3];

    [X,Y] = hatch_coordinates(xl,yl,0.2);
    plot(X,Y,'r');
else
    disp('The yield stress will not be exceeded at the maximum
 rotational speed that was set.');
```



```
end
```

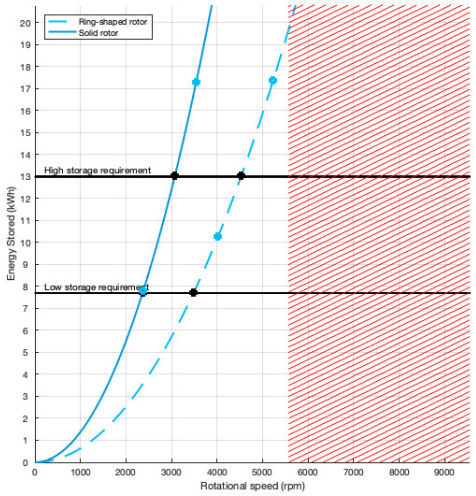

Table with alternative solutions

```
% This could be done in a more beautiful way...
if Type == 1
    Type1 = true;
else
    Type1 = false;
end

if Type == 2
    Type2 = true;
else
    Type2 = false;
end
```

```
if Type == 3
    Type3 = true;
else
    Type3 = false;
end

if Type == 4
    Type4 = true;
else
    Type4 = false;
end

fig3 = figure;
set(fig3,'Position',[100 100 600 120]);
movegui(fig3,'northwest');
movegui(fig3,[0 -240])
set(fig3, 'NumberTitle', 'off',...
    'Name', sprintf('Data with consideration of losses'));

d2 = {'Hollow, High
 req.',omegasol1_1,Eeffect1/1000,Sigmasol1_1,Alt1_1,Spec1_1,Type1;...
    'Solid, High
 req.',omegasol2_1,Eeffect2/1000,Sigmasol2_1,Alt2_1,Spec2_1,Type2;...
    'Hollow, Low
 req.',omegasol3_1,Eeffect3/1000,Sigmasol3_1,Alt3_1,Spec3_1,Type3;...
    'Solid, Low
 req.',omegasol4_1,Eeffect4/1000,Sigmasol4_1,Alt4_1,Spec4_1,Type4};

table2 = uitable(fig3,'Data',d2,'unit','normalized','Position',[0 0 1
 1]);

table2.ColumnName = {'Version and req.','Max. Speed (rpm)',...
    'Usable (kWh)','Stress (MPa)','<yield?','>spec?','Chosen type'};
```

	Version and req.	Max. Speed (rpm)	Usable (kWh)	Stress (MPa)	<yield?	>spec?	Chosen type
1	Hollow, High req.	5.2330e+03	13.0628	484.8558	☑	☑	☐
2	Solid, High req.	3.5428e+03	13.0011	222.2283	☑	☑	☑
3	Hollow, Low req.	4.0203e+03	7.7032	286.1645	☑	☑	☐
4	Solid, Low req.	2.3778e+03	7.7032	100.1037	☑	☑	☐

Plot the spin-down

```
fig4 = figure;
hold on;
grid on;
% grid minor;
set(fig4,'Position',[100 100 600 600]);
movegui(fig4,'southeast');
movegui(fig4,[1350 50]);
xlabel('time (h)');
ylabel('Energy Stored (kWh)');

plot(Eresidu_Wh,'color',[0/255,189/255,254/255],'Linewidth',1);
```

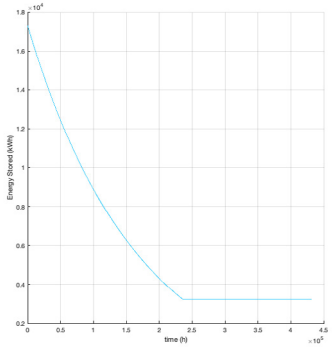

Determine energy stored in the system while simulating a certain scenario

```
Escenario = Eresidu;

t_scenario = 1;
for t_scenario = 1:t_regen_max
    %E_scenario(t_activate+t_scenario) = 0;

    Escenario(t_activate+t_scenario) = Eresidu_regen(t_scenario);
end

Escenario_Wh = Escenario/3600;
```



```
plot(Escenario_Wh,'color',[0/255,153/255,216/255],'Linewidth',2);
plot(t_activate,Escenario_Wh(t_activate),'ks','Linewidth',4);
set(fig4, 'NumberTitle', 'off',...
    'Name', sprintf('Active spin-down of the rotor, aerodynamic &
 bearing losses + regeneration'));

limitx = (t_half_type)*1.3;
% limitx = 60*3600;

axis([0 limitx -500 Escenario_Wh(1)]);
% xticks(0:1*3600:round(limitx)); % One tick every hour %%%%%
xticks(0:4*3600:round(limitx)); % One tick every 4 hours
% xticks(0:6*3600:round(limitx)); % One tick every 6 hours

xt = get(gca, 'XTick');
set(gca, 'XTick',xt, 'XTickLabel',xt/3600) % Display t in hours

xL = xlim;
line(xL, [0 0],'color','k','linewidth',1) %x-axis

yt = get(gca, 'YTick');
set(gca, 'YTick',yt, 'YTickLabel',yt/1000) % Display E in kWh
```

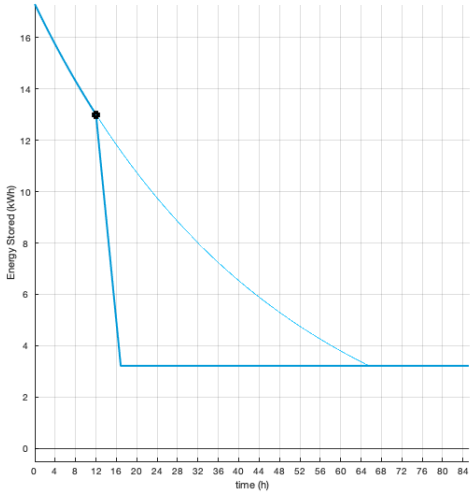

Read supply & demand data

```
PV_setup_1 = strcat(num2str(No_PV_1),'x',num2str(Eff_PV));

% Data from Dobber (2018)
if dataset == 1
    % Excel file contains values for every 1/8 hour
    time = transpose(xlsread('Supply - Demand
 2025.xlsx',num2str(PV_setup_1),...
        'B2:B146'));
    supply = transpose(xlsread('Supply - Demand
 2025.xlsx',num2str(PV_setup_1),...
        'C2:C146'));
    demand = transpose(xlsread('Supply - Demand
 2025.xlsx',num2str(PV_setup_1),...
        'D2:D146'));
```



```
    % Interpolate the data from the Excel file to every second of a
 day
    supply_interp_imp = interp1(time, supply, t_day, 'linear');
    demand_interp_imp = interp1(time, demand, t_day, 'linear');
end

if dataset == 2
% Read alternative demand data
    time = transpose(xlsread('Supply - Demand
 2025.xlsx',num2str(PV_setup_1),...
        'B2:B146'));
    supply = transpose(xlsread('Supply - Demand
 2025.xlsx',num2str(PV_setup_1),...
        'C2:C146'));
    demand = transpose(xlsread('Supply - Demand
 2025.xlsx',num2str(PV_setup_1),...
        'J2:J146'));
    % Interpolate the data from the Excel file to every second of a
 day
    supply_interp_imp = interp1(time, supply, t_day, 'linear');
    demand_interp_imp = interp1(time, demand, t_day, 'linear');
end

if dataset == 3
% Use supply data from KNMI
    time1 = transpose(xlsread('Supply - Demand
 2025.xlsx',num2str(supplydata),...
        'C2:C26'));
    supply = transpose(xlsread('Supply - Demand
 2025.xlsx',num2str(supplydata),...
        'E2:E26'));
% Read New York average demand data and corresponding time
    time2 = transpose(xlsread('Supply - Demand
 2025.xlsx','NYDemand',...
        'B2:B26'));
    demand = transpose(xlsread('Supply - Demand
 2025.xlsx','NYDemand',...
        'D2:D26'));
    % Interpolate the data from the Excel file to every second of a
 day
    supply_interp_imp = interp1(time1, supply, t_day, 'linear');
    demand_interp_imp = interp1(time2, demand, t_day, 'linear');
end

if dataset == 4
% Use supply data from KNMI
    time1 = transpose(xlsread('Supply - Demand
 2025.xlsx',num2str(supplydata),...
        'C2:C26'));
    supply = transpose(xlsread('Supply - Demand
 2025.xlsx',num2str(supplydata),...
        'E2:E26'));
% Read Dobber (2018) average demand data and corresponding time
```

```
    time2 = transpose(xlsread('Supply - Demand
 2025.xlsx',num2str(PV_setup_1),...
        'B2:B146'));
    demand = transpose(xlsread('Supply - Demand
 2025.xlsx',num2str(PV_setup_1),...
        'D2:D146'));
    % Interpolate the data from the Excel file to every second of a
 day
    supply_interp_imp = interp1(time1, supply, t_day, 'linear');
    demand_interp_imp = interp1(time2, demand, t_day, 'linear');
end

if dataset == 5
% Use supply data from KNMI
    time1 = transpose(xlsread('Supply - Demand
 2025.xlsx',num2str(supplydata),...
        'C2:C26'));
    supply = transpose(xlsread('Supply - Demand
 2025.xlsx',num2str(supplydata),...
        'E2:E26'));
% Read CORRECTED Dobber (2018) average demand data and corresponding
 time
    time2 = transpose(xlsread('Supply - Demand
 2025.xlsx',num2str(PV_setup_1),...
        'B2:B146'));
    demand = transpose(xlsread('Supply - Demand
 2025.xlsx',num2str(PV_setup_1),...
        'J2:J146'));
    % Interpolate the data from the Excel file to every second of a
 day
    supply_interp_imp = interp1(time1, supply, t_day, 'linear');
    demand_interp_imp = interp1(time2, demand, t_day, 'linear');
end

if dataset > 2
    Eff_PV_module = 0.1529;
    A_PV_module = 1.47;

    A_PV = A_PV_module * No_PV_2;

    supply_imp_tot = supply_interp_imp * A_PV * Eff_PV_module;
else
    Eff_PV_module = 0.1529;
    A_PV_module = 1.8;

    A_PV = A_PV_module * No_PV_2;

    supply_imp_tot = supply_interp_imp;
end


if peaksimul == 1
    supplypeaks = zeros(1,max(t_day));
    demandpeaks = zeros(1,max(t_day));
```



```
%     % Random peaks
%     randomness1 = randi([-800 500],1,20);
%     time3 = linspace(0,12*3600,20);
%     time4 = 1:12*3600;
%     peakinterpol1 = interp1(time3,randomness1,time4);
%     supplypeaks(7*3600:19*3600-1) = peakinterpol1; %W
%
%     randomness2 = randi([-100 800],1,10);
%     time3 = linspace(0,2*3600,10);
%     time4 = 1:2*3600;
%     peakinterpol2 = interp1(time3,randomness2,time4);
%     demandpeaks(7*3600:9*3600-1) = peakinterpol2; %W

    % Set peaks
    % Supply
    semirandom = [0, 1000, 1200, 0];
    time3 = linspace(0,3.5*3600,4);
    time4 = 1:3.5*3600;
    peakinterpol = interp1(time3,semirandom,time4);
    supplypeaks(6.5*3600:10*3600-1) = peakinterpol; %W

    semirandom = [0, 1000, 0];
    time3 = linspace(0,1*3600,3);
    time4 = 1:1*3600;
    peakinterpol = interp1(time3,semirandom,time4);
    supplypeaks(10.1*3600:11.1*3600-1) = peakinterpol; %W

    semirandom = [0, -200, 0];
    time3 = linspace(0,1*3600,3);
    time4 = 1:1*3600;
    peakinterpol = interp1(time3,semirandom,time4);
    supplypeaks(11.5*3600:12.5*3600-1) = peakinterpol; %W

    semirandom = [-1000, 1300, -100];
    time3 = linspace(0,1*3600,3);
    time4 = 1:1*3600;
    peakinterpol = interp1(time3,semirandom,time4);
    supplypeaks(13*3600:14*3600-1) = peakinterpol; %W

    semirandom = [0, -800, 0];
    time3 = linspace(0,2*3600,3);
    time4 = 1:2*3600;
    peakinterpol = interp1(time3,semirandom,time4);
    supplypeaks(15.5*3600:17.5*3600-1) = peakinterpol; %W

    % Demand
    semirandom = [0, 400, 200, -200, 0];
    time3 = linspace(0,1*3600,5);
    time4 = 1:1*3600;
    peakinterpol = interp1(time3,semirandom,time4);
    demandpeaks(8*3600:9*3600-1) = peakinterpol; %W

    semirandom = [0, 400, 900, -200, 0];
```



```
    time3 = linspace(0,1*3600,5);
    time4 = 1:1*3600;
    peakinterpol = interp1(time3,semirandom,time4);
    demandpeaks(19*3600:20*3600-1) = peakinterpol; %W

    % Add these peaks to the imported data
    supply_interp = supply_imp_tot + supplypeaks; %W
    demand_interp = demand_interp_imp + demandpeaks; %W
else
    supply_interp = supply_imp_tot;
    demand_interp = demand_interp_imp;
end
```

Define charging the flywheel

```
P_charge = zeros(1,max(t_day));
P_charge_real = zeros(1,max(t_day));

% Including realistic motor/generator efficiency of 74,4% (Nord
 Drivesystems)
for t_charge = 1:1:max(t_day)
    P_charge_real(t_charge) = supply_interp(t_charge)*0.744 -
 demand_interp(t_charge)/0.744; %W
end

% Including motor/generator efficiency that was set at the beginning
 of the script
for t_charge = 1:1:max(t_day)
    P_charge(t_charge) = supply_interp(t_charge)*Eff_M -
 demand_interp(t_charge)/Eff_M; %W
end

E_demand_Wh = sum(demand_interp)/3600; %Wh

disp(['The total demand by the simulated household is ',...
    num2str(E_demand_Wh/1000,'%10.2f'),' kWh.']);

fprintf('\n');

% How much excess solar power is available to charge the system?
P_positive = P_charge; %W
P_positive(P_positive < 0) = 0;

E_available_Wh = sum(P_positive)/3600; %Wh

disp(['The total excess of solar power that can be used for charging
 is ',...
    num2str(E_available_Wh/1000,'%10.2f'),' kWh.']);

fprintf('\n');
```

```
The total demand by the simulated household is 13.50 kWh.
```

The total excess of solar power that can be used for charging is 5.51 kWh.

Include motor torque and maximum angular acceleration

```
k_t = Tau_max/A_max; % Nm/A Motor constant

I_irr = 0.0088; % Current induced by solar panels at certain
 irradiance

if dataset > 2
    I_PV = P_charge ./ A_PV ./ Eff_PV_module .* I_irr .* No_PV_2; %
 The output current from all PV panels added (parallel)
else
    I_PV = P_charge ./ A_PV ./ Eff_PV_module .* I_irr .* No_PV_1;
end

Tau_actual = I_PV .* k_t; % Nm

Tau_actual_lim = Tau_actual; % Nm

Tau_actual_lim(Tau_actual_lim > Tau_max) = Tau_max; % Nm

alpha_actual_lim = Tau_actual_lim ./ Jtype; % rad/s^2

figure
hold on;
plot(t_day/3600,Tau_actual,'color',
[248/255,171/255,148/255],'Linewidth',1)
plot(t_day/3600,Tau_actual_lim,'color',
[255/255,102/255,51/255],'Linewidth',2)
xL = xlim;
line(xL, [0 0],'color','k','linewidth',1) %x-axis
xlabel('time of day (h)');
ylabel('Tau (Nm)');
```


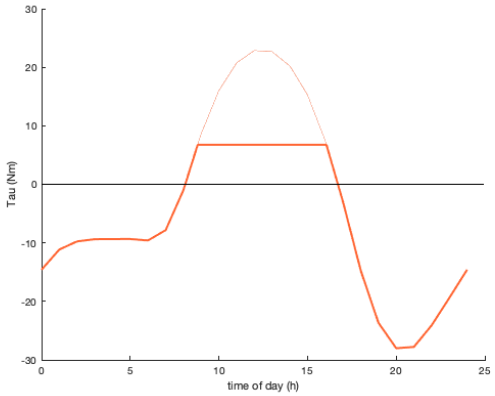

Plot the charge/discharge

```
fig5 = figure;
hold on;
grid on;
set(fig5,'Position',[100 100 500 450]);
movegui(fig5,'southeast');
movegui(fig5,[1450 700]);
xlabel('time of day (h)');
ylabel('Power (kW)');

plot(t_day,supply_interp,'color',
[255/255,226/255,42/255],'Linewidth',2);
plot(t_day,demand_interp,'color',
[255/255,102/255,51/255],'Linewidth',2);
plot(t_day,P_charge,'color',[51/255,204/255,102/255],'Linewidth',2);

set(fig5, 'NumberTitle', 'off',...
    'Name', sprintf('Supply & demand during 24h'));

limitx = max(t_day);

xticks(0:3600:round(limitx)); % One tick every hour
axis([0 limitx min(P_charge)-500 max(supply_interp)+500]);
```



```
xt = get(gca, 'XTick');
set(gca, 'XTick',xt, 'XTickLabel',xt/3600) % Display t in hours

xL = xlim;
line(xL, [0 0],'color','k','linewidth',1) %x-axis

yt = get(gca, 'YTick');
set(gca, 'YTick',yt, 'YTickLabel',yt/1000) % Display P in kW
```

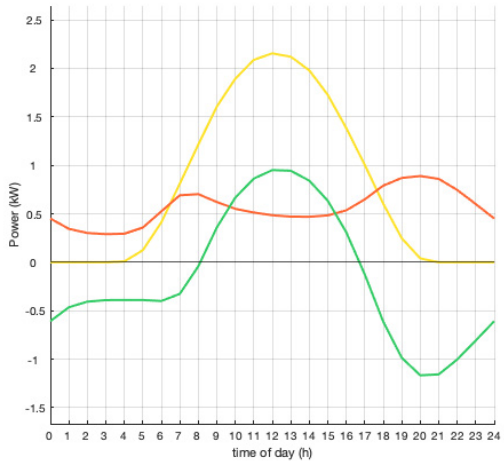

Calculate energy in the system with supply & demand considered

```
Ecurrent = zeros(1,max(t_day));
Ecurrent(1) = Eleft;

for t_charge = 1:1:max(t_day)-1

    Enow = Ecurrent(t_charge) + P_charge(t_charge);
```

```
    Ecurrent(t_charge+1) = Enow;
end

Ecurrent_real = zeros(1,max(t_day));
Ecurrent_real(1) = Eleft;

for t_charge = 1:1:max(t_day)-1

    Enow = Ecurrent_real(t_charge) + P_charge_real(t_charge);

    Ecurrent_real(t_charge+1) = Enow;
end

Ecurrent_Wh = Ecurrent/3600;
Ecurrent_Wh_real = Ecurrent_real/3600;

fig6 = figure;
hold on;
grid on;
set(fig6,'Position',[100 100 600 600]);
% set(fig6,'Position',[100 100 500 450]);
% movegui(fig6,'southeast');
movegui(fig6,[0 50]);
xlabel('time of day (h)');
ylabel('Stored Energy (Wh)');

plot(t_day,P_charge,'y','Linewidth',1);

Curplot = plot(t_day,Ecurrent_Wh,'color',
[0/255,189/255,254/255],'Linewidth',2);
plot(t_day,Ecurrent_Wh_real,'--','color',
[0/255,153/255,216/255],'Linewidth',1);

set(fig6, 'NumberTitle', 'off',...
    'Name', sprintf('Supply & demand during 24h'));

Esol_lossless = zeros(1,max(t_day)); %J

Esol_lossless(1) = Ecurrent(1) - min(Ecurrent)+Eleft; %This prevents
 discharge below Eleft

for t_charge = 1:1:max(t_day)-1

    Enow = Esol_lossless(t_charge) + P_charge(t_charge);

    Esol_lossless(t_charge+1) = Enow;
end

Esol_Mloss = zeros(1,max(t_day)); %J
Esol_Mloss(1) = Ecurrent_real(1) - min(Ecurrent_real)+Eleft; %This
 prevents discharge below Eleft

for t_charge = 1:1:max(t_day)-1
```



```
    Enow = Esol_Mloss(t_charge) + P_charge_real(t_charge);

    Esol_Mloss(t_charge+1) = Enow;
end

Esol_lossless_Wh = Esol_lossless/3600; %Wh
Esol_Mloss_Wh = Esol_Mloss/3600; %Wh

Solplot = plot(t_day,Esol_lossless_Wh,'color',
[0/255,189/255,254/255],'Linewidth',2);
plot(t_day,Esol_Mloss_Wh,'--','color',
[0/255,189/255,254/255],'Linewidth',1);

limitx = max(t_day);

xticks(0:3600:round(limitx)); % One tick every hour
axis([0 limitx min(P_charge_real)-500 max(Esol_lossless_Wh)+500]);

xt = get(gca, 'XTick');
set(gca, 'XTick',xt, 'XTickLabel',xt/3600) % Display t in hours

xL = xlim;
line(xL, [0 0],'color','k','linewidth',1) %x-axis

xL = xlim;
line(xL, [Eleft_Wh Eleft_Wh],'color',
[51/255,204/255,0/255],'linewidth',1) % Minimum charge level

xL = xlim;
line(xL, [Esol_lossless_Wh(max(t_day))
 Esol_lossless_Wh(max(t_day))],'color',...
    'c','linewidth',1,'Linestyle',':') % Charge level check end of the
 day

axis([0 limitx min(P_charge)-500 max(Esol_lossless_Wh)+500]);

disp('For the system to be capable of storing the desired amount of
 energy, ');
disp(['it should be designed to store at least ',...
    num2str(max(Esol_lossless_Wh)/1000),' kWh.']);

fprintf('\n');

% Check if additional power is needed
if Esol_lossless_Wh(max(t_day)) < Esol_lossless_Wh(min(t_day))
    disp('The lossless system will need additional power to provide
 the household.');
    disp([num2str((Esol_lossless_Wh(min(t_day))-
Esol_lossless_Wh(max(t_day)))/1000,'%10.2f'),' kWh',...
        ' of electricity is needed to sustain the daily cycle.'])
else
    disp('Without aero- and bearing losses, no need for additional
 power to provide the household!');
end
```



```
% Bring the important graphs to the front
uistack(Curplot,'top');
uistack(Solplot,'top');
```

For the system to be capable of storing the desired amount of energy, it should be designed to store at least 9.3314 kWh.

The lossless system will need additional power to provide the household.
3.69 kWh of electricity is needed to sustain the daily cycle.

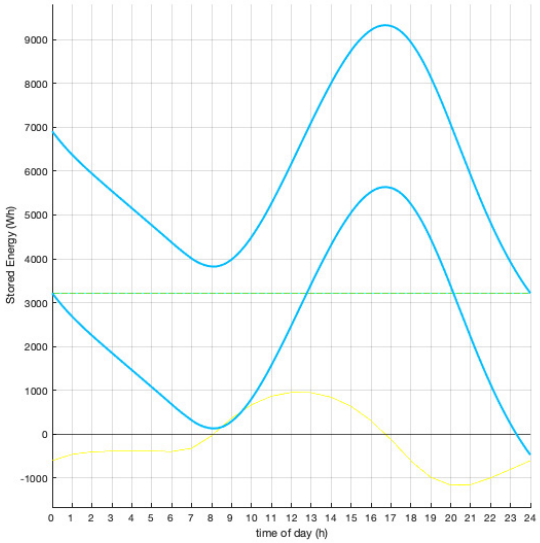

Simulate flywheel system in the scenario

```
t_full = find(Esol_lossless_Wh==max(Esol_lossless_Wh)); % Time when
 full charge is reached
```

```
% At which point does the system store enough energy to supply at
 maximum need?
t_Ereq = find(Eresidu_Wh>max(Esol_lossless_Wh),1,'last');

if isempty(t_Ereq)
    fprintf('\n')
    disp('Simulation ended. The system is not able to store the
 required amount of energy.')
    disp('Please adjust flywheel dimensions!')
    return
end

% Check how much is stored at that point
Eresidu_Wh_simul = Eresidu_Wh(t_Ereq);

% % Optional margin
% t_margin = 0*3600; % Look at the energy 2 hours before. For more
 margin
% t_Emaxcharge = t_Ereq - t_margin;

% To analyze spindown from max charge to end of day
% Evaluate only the hours of passive spin down until midnight
t_spindown = 24*3600 - t_full;

% When does the (lossless) simulation its minimum?
t_empty = find(Esol_lossless_Wh==min(Esol_lossless_Wh));

% Simulate the system including spindown lossses
Esimul = zeros(1,max(t_day)); %J

% Start the day with the amount of energy left after spindown to
 midnight
Esimul(1) = Eresidu(t_Ereq+t_spindown); %J

% Or start the day with just enough to keep above Eleft (wild guess)
t_start = t_start_h*3600; % Choose the hour of day at which initial
 energy will be taken
Esimul(1) = Esol_lossless(t_start); %J

P_loss_simul = zeros(1,max(t_day));

% Simulate losses from day start to full charge
P_loss_simul(1:t_full) = P_actual(t_start+t_spindown:t_start
+t_spindown+t_full-1); %W

% Losses increasing while charging should be included for equal
 comparison!

for t_simul = 1:1:t_full

%     Enow = Eresidu(t_simul+t_Emaxcharge+t_max_plot) +
 P_charge(t_simul);
    for xx = 0:1:1
```



```
            Enow = Esimul(t_simul) + (P_charge(t_simul)-
P_loss_simul(t_simul))*xx; % J.
                                    % one second of charge is added
                                    % every value of t
            Esimul(t_simul+1) = Enow;
                                    % This value is entered in the
 vector
    end
    Esimul(t_simul+1) = Enow;
end

% Values up until full charge
Esimul_Wh = Esimul/3600;

% % Testplot
% plot(t_day,Esimul_Wh,'r','Linewidth',1);
```

Passive effects until full charge

```
t_Estart = find(Eresidu_Wh>Esimul_Wh(1),1,'last');

Epassive_Wh = zeros(1,max(t_day));
Epassive_Wh(1:t_empty) = Eresidu_Wh(t_Estart:t_Estart+t_empty-1);

% According to charging the system, what is the maximum energy that it
 will store?
t_Emax = find(Eresidu_Wh>max(Esimul_Wh),1,'last');

if isempty(t_Emax)
    fprintf('\n')
    disp('Simulation ended. The system is not able to store the
 required amount of energy.')
    disp('Please adjust flywheel dimensions!')
    return
end

Epassive_Wh2 = zeros(1,max(t_day));
Epassive_Wh2(t_full:max(t_day)) = Eresidu_Wh(t_Emax:t_Emax
+t_spindown);

% Losses from full charge to end of day
P_loss_simul(t_full:max(t_day)) = P_actual(t_Emax:t_Emax
+t_spindown); %W

for t_simul = t_full:1:max(t_day)-1

%     Enow = Eresidu(t_simul+t_Emaxcharge+t_max_plot) +
 P_charge(t_simul);
    for xx = 0:1:1
            Enow = Esimul(t_simul) + (P_charge(t_simul)-
P_loss_simul(t_simul))*xx; % J.
                                    % one second of charge is added
                                    % every value of t
```



```
            Esimul(t_simul+1) = Enow;
                                    % This value is entered in the
 vector
    end
    Esimul(t_simul+1) = Enow;
end

% Values for entire day
Esimul_Wh_no_inertia = Esimul/3600; %Wh

% Rotational speed for every moment of day
omega_actual = sqrt(Esimul/(0.5*Jtype)); %rad/s (For every second of
 day)

if omega_actual(max(t_day)) < 1
    disp('The flywheel will stop rotating, please adjust t_start_h.')
end

omegamax_day_rpm = max(omega_actual)/((2*pi)/60);

fprintf('\n')
disp(['The maximum rotational speed of the system during a day like
 this is ',...
    num2str(omegamax_day_rpm),' rpm.'])

% How many rad/s should the speed increase to cause the wanted energy
 increase?
alpha_desired = gradient(omega_actual);

% % % % The power needed at a certain point in time to increase omega
 by 1 rad/s
% % % % So, what if: on any moment a day, 1 rad/s has to be added?
% % % P_increase_actual = P_increase(round(omega_actual)); %W

P_charge_increase = gradient(P_charge); %W/s

% % % P_percentage = P_charge_increase./P_increase_actual;

t_inert = alpha_desired./alpha_actual_lim; %s time needed to add 1
 rad/s of speed
% If this is smaller than 1, there is enough time to increase the
 speed of the rotor

% If this is larger than 1:
t_inert_fail = t_inert;

% Only include positive values for charging the flywheel
t_inert_fail(t_inert_fail < 0) = 0;
t_inert_fail(P_charge < 0) = 1;
% Set all values where motor is capable of accelerating enough to 1
t_inert_fail(t_inert_fail < 1) = 1;
% Set the values where charge changes to regeneration and backwards to
 1
t_inert_fail(P_charge < 100) = 1;
```

```
fraq_stored = 1./t_inert_fail;


% The part of the charging power that van be transfered to the system
 with max motor torque considered
P_inert_lim = P_charge .* fraq_stored;

% P_inert_lim(1:8*3600) = 0;
% P_inert_lim(14*3600:end) = 0;

% P_torqueloss = P_charge - P_inert_lim;
P_torqueloss = P_charge - P_inert_lim;

figure
hold on;
grid on;
movegui('northwest')
plot(t_day/3600,P_charge,'color',
[248/255,171/255,148/255],'Linewidth',1)
plot(t_day/3600,P_inert_lim,'color',
[255/255,102/255,51/255],'Linewidth',2)
xlabel('time of day (h)');
ylabel('Limited charge power vs charge power (kW)');
axis([0 max(t_day)/3600 min(P_charge)*1.2 max(P_charge)*1.2]);
xL = xlim;
line(xL, [0 0],'color','k','linewidth',1) %x-axis

xticks(0:1:24); % One tick every hour
% xt = get(gca, 'XTick');
% set(gca, 'XTick',xt, 'XTickLabel',xt/3600) % Display t in hours

yt = get(gca, 'YTick');
set(gca, 'YTick',yt, 'YTickLabel',yt/1000) % Display E in kWh

figure
movegui('southwest')
plot(t_day/3600,fraq_stored,'color',
[255/255,102/255,51/255],'Linewidth',2)
xlabel('time of day (h)');
ylabel('time to increase rad/s step (s)');

for t_simul = 1:1:t_full

%     Enow = Eresidu(t_simul+t_Emaxcharge+t_max_plot) +
 P_charge(t_simul);
    for xx = 0:1:1
            Enow = Esimul(t_simul) + (P_charge(t_simul)-
P_torqueloss(t_simul)-P_loss_simul(t_simul))*xx; % J.
                                % one second of charge is adde
                                % every value of t
            Esimul(t_simul+1) = Enow;
                                % This value is entered in the
 vector
```



```
    end
    Esimul(t_simul+1) = Enow;
end

% Values for entire day
% Esimul_Wh = Esimul/3600; %Wh

for t_simul = t_full:1:max(t_day)-1

%     Enow = Eresidu(t_simul+t_Emaxcharge+t_max_plot) +
 P_charge(t_simul);
    for xx = 0:1:1
            Enow = Esimul(t_simul) + (P_charge(t_simul)-
P_loss_simul(t_simul))*xx; % J.
                                % one second of charge is added
                                % every value of t
            Esimul(t_simul+1) = Enow;
                                % This value is entered in the
 vector
    end
    Esimul(t_simul+1) = Enow;
end

% Values for entire day
Esimul_Wh = Esimul/3600; %Wh

% According to charging the system, when does the system store its
 maximum amount of energy?
t_Emax =
 find(Eresidu_Wh>Esimul_Wh(find(islocalmax(Esimul_Wh)>0,1,'last')),1,'last');

if isempty(t_Emax)
    fprintf('\n')
    disp('Simulation ended. The system is not able to store the
 required amount of energy.')
    disp('Please adjust flywheel dimensions!')
    return
end

Epassive_Wh2 = zeros(1,max(t_day));
Epassive_Wh2(t_full:max(t_day)) = Eresidu_Wh(t_Emax:t_Emax
+t_spindown);

The flywheel will stop rotating, please adjust t_start_h.

The maximum rotational speed of the system during a day like this is
 2226.3406 rpm.
```


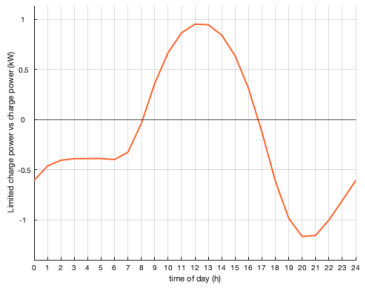

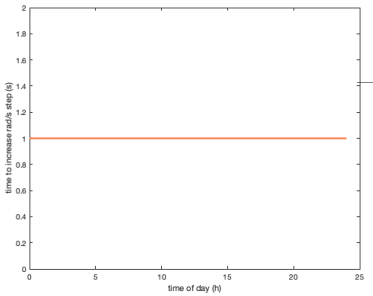

Plot!

```
fig7 = figure;
hold on
grid on
set(fig7,'Position',[100 100 600 600]);
movegui(fig7,'southwest');
movegui(fig7,[10 50]);
xlabel('time of day (h)');
ylabel('Stored Energy (kWh)');

% plot(t_day,P_charge,'y','Linewidth',1);

Simplot_no_inertia = plot(t_day,Esimul_Wh_no_inertia,'color',
[0/255,153/255,216/255],'Linewidth',1);

% Solution for a system that will continue working over daily cycles
if Esimul_Wh(max(t_day)) > Esimul_Wh(1)
    Simplot = plot(t_day,Esimul_Wh,'color',
[0/255,189/255,254/255],'Linewidth',3);

    % % Plot the passive discharges to check (discharge from t=0 only
    % happens when system contains usable energy at that moment)
    plot(t_day,Epassive_Wh,'--','color',
[248/255,171/255,148/255],'Linewidth',1);
end

% Passive discharge effects from maximum charge level
plot(t_day,Epassive_Wh2,'--','color',
[248/255,171/255,148/255],'Linewidth',1);

plot(t_day,Esol_lossless_Wh,'color',
[51/255,255/255,255/255],'Linewidth',1);

set(fig7, 'NumberTitle', 'off',...
    'Name', sprintf('Simulation over 24h'));

xL = xlim;
line(xL, [0 0],'color','k','linewidth',1) %x-axis

% line(xL, [Eleft_Wh Eleft_Wh],'color',
[51/255,204/255,102/255],'linewidth',1,...
%     'linestyle',':') % Minimum charge level

Eleft_Wh_simul = max(Esimul_Wh)/4; %Wh
Eleft_simul = Eleft_Wh_simul*3600; %J

line(xL, [Eleft_Wh_simul Eleft_Wh_simul],'color',
[51/255,204/255,0/255],'linewidth',1)
   % Minimum charge level when taking simulation max speed into
 account

line(xL, [Esimul_Wh(max(t_day)) Esimul_Wh(max(t_day))],'color',...
```

```
    [0/255,189/255,254/255],'linewidth',1,...
    'linestyle',':') % Extra power check

limitx = max(t_day);
xticks(0:3600:round(limitx)); % One tick every hour
xt = get(gca, 'XTick');
set(gca, 'XTick',xt, 'XTickLabel',xt/3600) % Display t in hours

if max(Esimul_Wh) > max(Esol_lossless_Wh)
%     axis([0 limitx min(P_charge)-500 max(Esimul_Wh)+500]); % When
 plotting P_charge
    axis([0 limitx -5 max(Esimul_Wh)+500]); % Not plotting P_charge
    yticks(0:2000:max(Esimul_Wh)); % One tick every 2 kWh
    yt = get(gca, 'YTick');
    set(gca, 'YTick',yt, 'YTickLabel',yt/1000) % Display E in kWh
else
%     axis([0 limitx min(P_charge)-500 max(Esol_lossless_Wh)+500]); %
 When plotting P_charge
    axis([0 limitx -5 max(Esol_lossless_Wh)+500]); % Not plotting
 P_charge
    yticks(0:2000:max(Esol_lossless_Wh)); % One tick every 2 kWh
    yt = get(gca, 'YTick');
    set(gca, 'YTick',yt, 'YTickLabel',yt/1000) % Display E in kWh
end

fprintf('\n');

if Esimul_Wh_no_inertia(max(t_day)) < Esimul_Wh_no_inertia(min(t_day))
    Egrid_no_inertia = (Esimul_Wh_no_inertia(min(t_day))-
Esimul_Wh_no_inertia(max(t_day)))/1000; %kWh

    disp('Including losses but excluding inertia, the system will need
 additional power to provide the household.');
    disp([num2str(Egrid_no_inertia,'%10.2f'),' kWh',...
        ' of electricity is needed to sustain the daily cycle.'])
else
    Egrid_no_inertia = (Esimul_Wh_no_inertia(min(t_day))-
Esimul_Wh_no_inertia(max(t_day)))/1000;
    disp('With losses included, the system does not need additional
 power to provide the household!');
end

fprintf('\n');

if Esimul_Wh(max(t_day)) < Esimul_Wh(1)
    Egrid = (Esimul_Wh(1)-Esimul_Wh(max(t_day)))/1000; %kWh

    disp('With losses and inertia included, the system will need
 additional power to provide the household.');
    disp([num2str(Egrid,'%10.2f'),' kWh',...
        ' of electricity is needed to sustain the daily cycle.'])

    t_min = find(islocalmin(Esimul) == max(islocalmin(Esimul)),1);
```



```
    for t_simul = 1:1:t_min
        Esimul(t_simul) = Esimul(t_min);
    end

    t_min2 = find(Esimul < Esimul(t_min)-1);
    t_min2(t_min2 < t_full) = [];

    for t_simul = min(t_min2):1:max(t_min2)
        Esimul(t_simul) = Esimul(t_min);
    end

    % Values for entire day
    Esimul_Wh_min = Esimul/3600; %Wh

    % Solution for a system that is kept at minimum speed by grid/
battery power
    Simplot_min = plot(t_day,Esimul_Wh_min,'color',
[0/255,189/255,254/255],'Linewidth',3);


    for t_simul = t_full:1:max(t_day)-1

%     Enow = Eresidu(t_simul+t_Emaxcharge+t_max_plot) +
 P_charge(t_simul);
    for xx = 0:1:1
            Enow = Esimul(t_simul) + (P_charge(t_simul)-
P_loss_simul(t_simul))*xx; % J.
                                    % one second of charge is added
                                    % every value of t
            Esimul(t_simul+1) = Enow;
                                    % This value is entered in the
 vector
    end
    Esimul(t_simul+1) = Enow;
    end

    t_empty_sim = find(Esimul_Wh < Eleft_Wh_simul,1);

    if t_empty_sim > 0
        for t_simul = t_empty_sim:1:max(t_day)-1
            Esimul(t_simul) = Eleft_Wh_simul;
        end
    end

else
    Egrid = (Esimul_Wh(min(t_day))-Esimul_Wh(max(t_day)))/1000;
    disp('With losses and inertia included, the system does not need
 additional power to provide the household!');
end

Eloss_inertia = Egrid - Egrid_no_inertia;

fprintf('\n');
```



```
disp(['Losses due to limited motor torque and inertia of the flywheel
 are ',num2str(Eloss_inertia),' kWh.'])

% %
```

Including losses but excluding inertia, the system will need additional power to provide the household.
8.50 kWh of electricity is needed to sustain the daily cycle.

With losses and inertia included, the system will need additional power to provide the household.
8.50 kWh of electricity is needed to sustain the daily cycle.

Losses due to limited motor torque and inertia of the flywheel are 0 kWh.

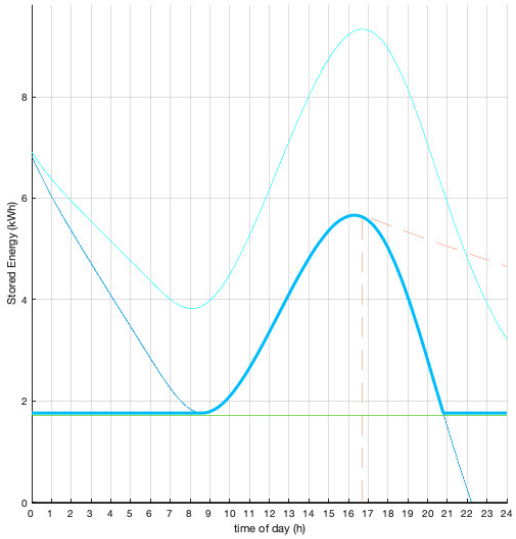

Published with MATLAB® R2017b

Appendix D.

Morphological Chart

Solutions to FESS subsytems

As mentioned in paragraph 2.3, the three potential system solutions are based on morphological sketches, which summarize all potential solutions. On the following pages, these sketches are displayed.
The different colors correspond with the colors given to the potential solutions on page 38 and page 39.

Stacked multi-flywheel, multi-EM

Co-axial merged, single fixed EM

Multi-flywheel array, movable single EM

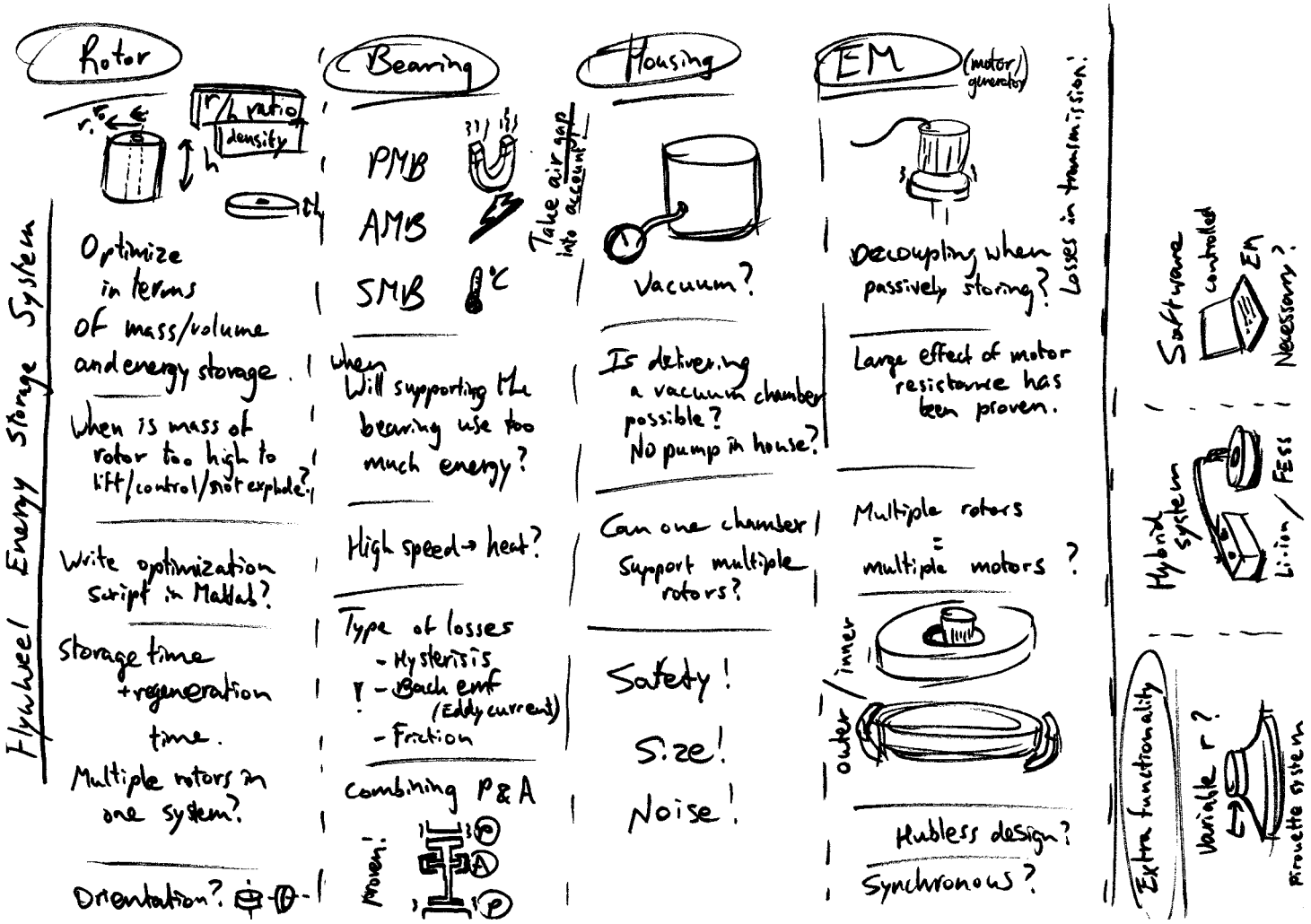

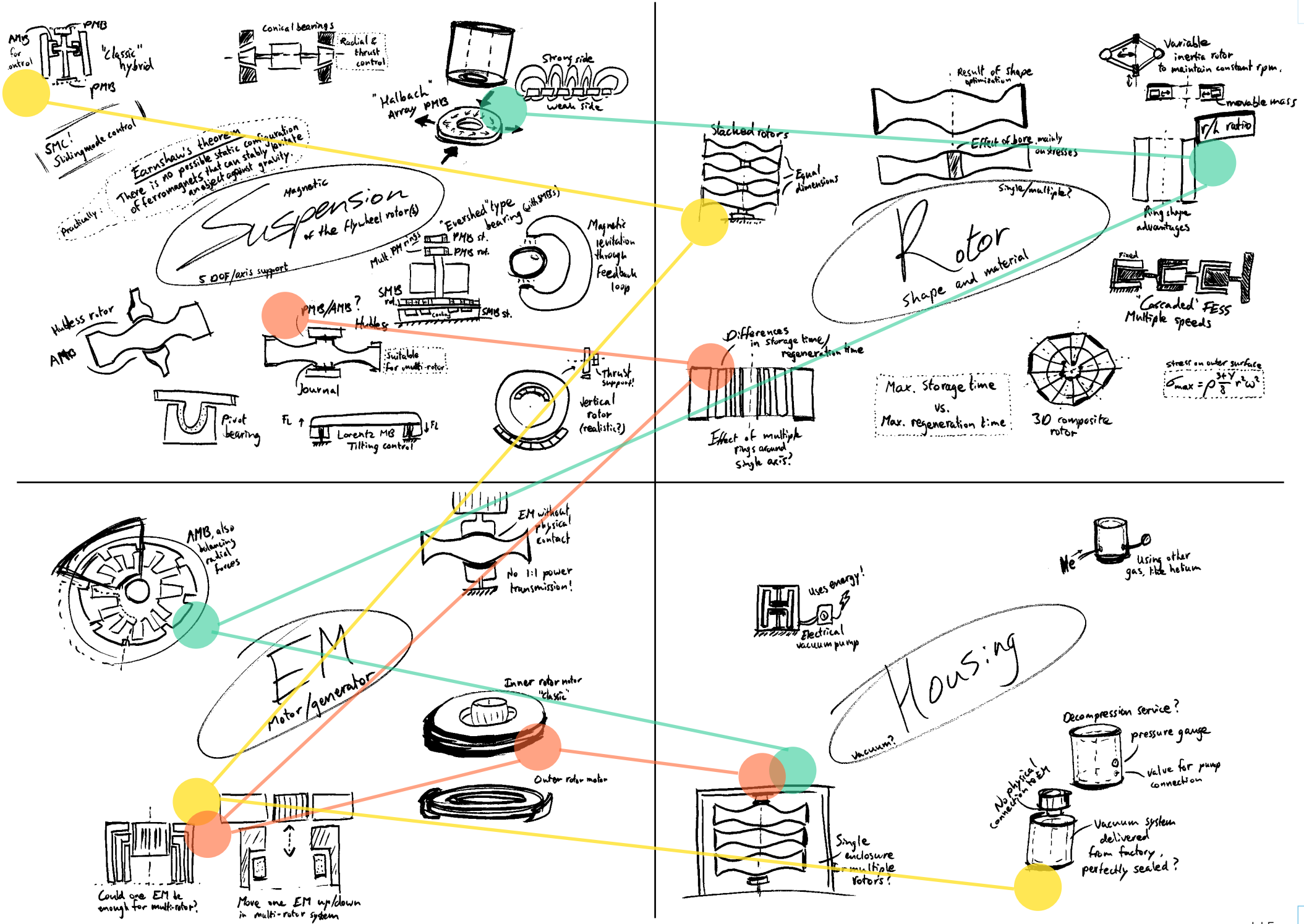
AMB for control
PMB
"Classic" hybrid
PMB
SMC! Sliding mode control
Practically:
Earnshaw's theorem
There is no possible static configuration of ferromagnets that can stably levitate an object against gravity.
Magnetic Suspension of the flywheel rotor(s)
5 DOF/axis support
Conical bearings
Radial & thrust control
"Halbach" Array PMB
Strong side
Weak side
"Evershed" type bearing (with SMBs)
Mult. PM rings
PMB st.
PMB rot.
SMB rot.
SMB st.
Contact
Magnetic levitation through feedback loop
Hubless rotor
AMB
PMB/AMB?
Hubless
Journal
Suitable for multi-rotor
Pivot bearing
Fl
Lorentz MB Tilting control
Thrust support!
Vertical rotor (realistic?)
Stacked rotors
Equal dimensions
Result of shape optimization
Effect of bore, mainly on stresses
Single/multiple?
Rotor
Shape and material
Variable inertia rotor to maintain constant rpm.
movable mass
r/h ratio
Ring shape advantages
Fixed
"Cascaded" FESS
Multiple speeds
Differences in storage time/ regeneration time
Effect of multiple rings around single axis?
Max. Storage time
vs.
Max. regeneration time
3D composite rotor
stress on outer surface
$\sigma_{max} = \rho \frac{3+\nu}{8} r^2 \omega^2$
AMB, also balancing radial forces
EM without physical contact
No 1:1 power transmission!
EM
Motor/generator
Inner rotor motor "classic"
Outer rotor motor
Could one EM be enough for multi-rotor?
Move one EM up/down in multi-rotor system
Uses energy!
Electrical vacuum pump
He
Using other gas, like helium
Housing
Vacuum?
Decompression service?
pressure gauge
valve for pump connection
No physical connection to EM
Vacuum system delivered from factory, perfectly sealed?
Single enclosure multiple rotors?

Appendix E.

Technical Drawings Prototype

Lathe and CNC milled parts

The following pages contain the technical drawings that were used to manufacture the rotors and the enclosing plates of the prototype.
The rotors were lathed out of SJ235 steel in the PMB workshop of the faculty of Industrial Design Engineering at TU Delft. In the same workshop, the CNC milling machine was used to make the bottom, top and seal plate.

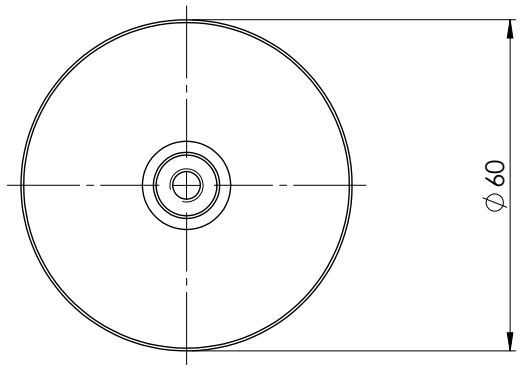

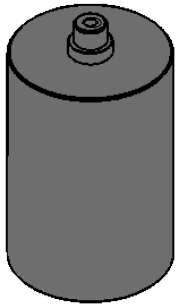

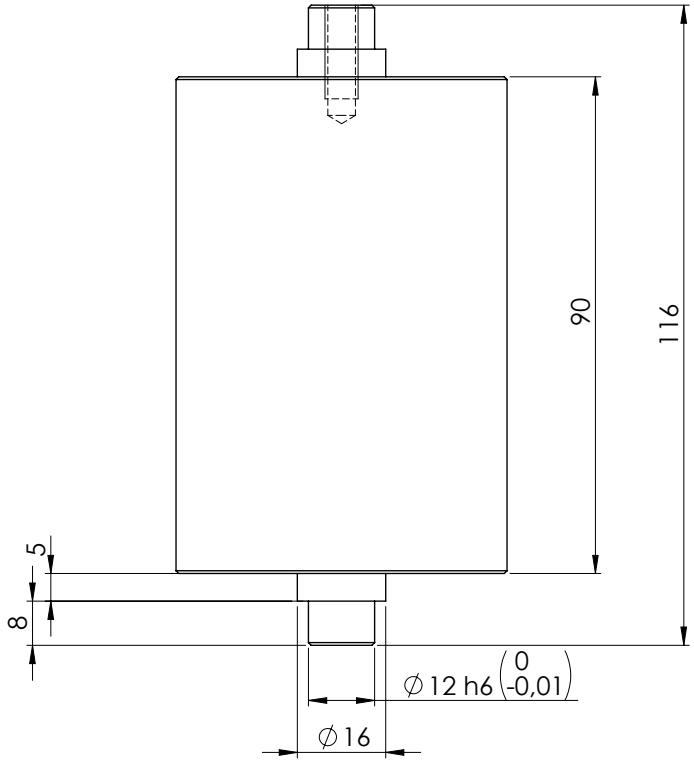

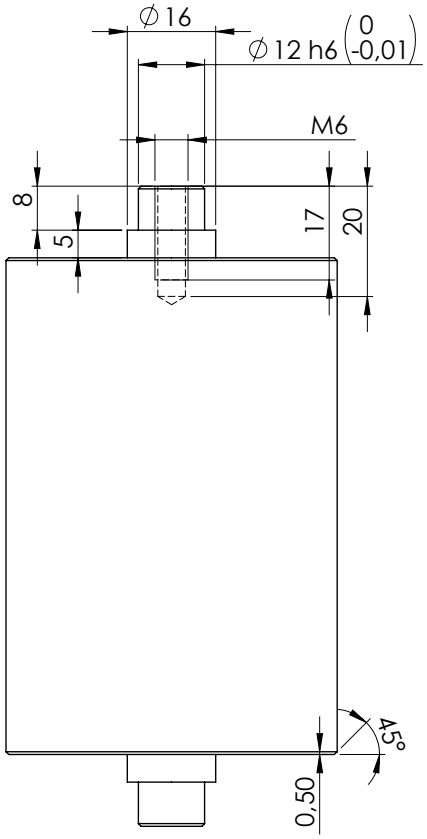

See STEP file: 12-005-Rotor - Slender.STEP

UNLESS OTHERWISE SPECIFIED: DIMENSIONS ARE IN MILLIMETERS GENERAL TOLERANCES: ISO 2768 MK	FINISH:		DEBURR AND BREAK SHARP EDGES		DO NOT SCALE DRAWING	REVISION
	NAME	SIGNATURE	DATE		TITLE: FESS Prototype	
DRAWN	Stefan Lorist					
CHK'D						
APPV'D						
MFG						
Q.A				MATERIAL: SJ235	DWG NO. 12-005-Rotor - Slender	A3
				WEIGHT:	SCALE:1:1	SHEET 1 OF 1

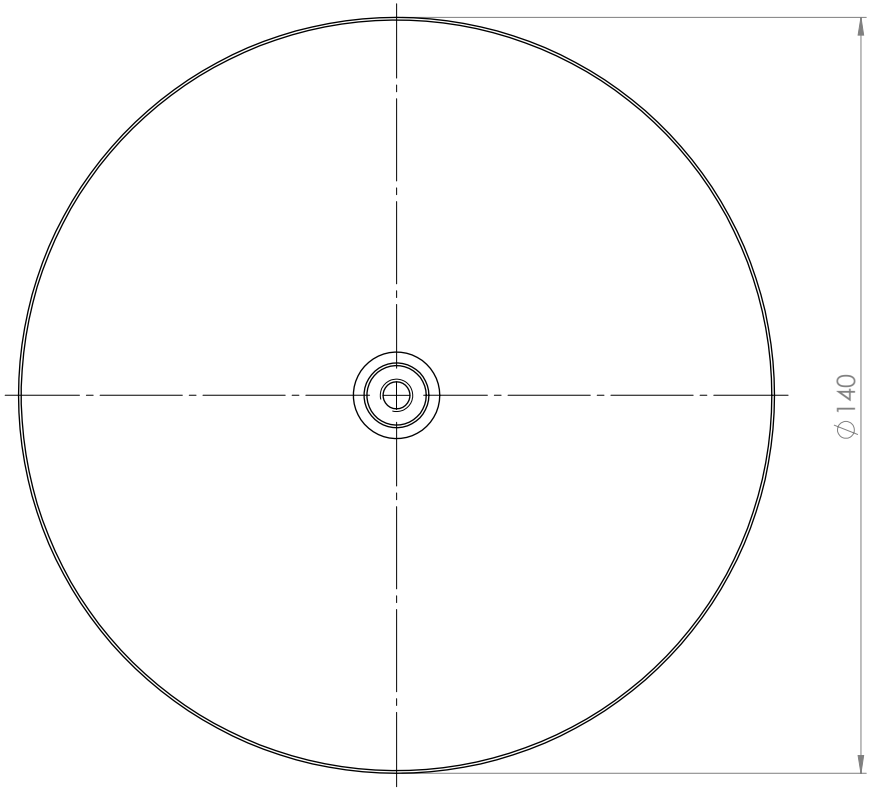

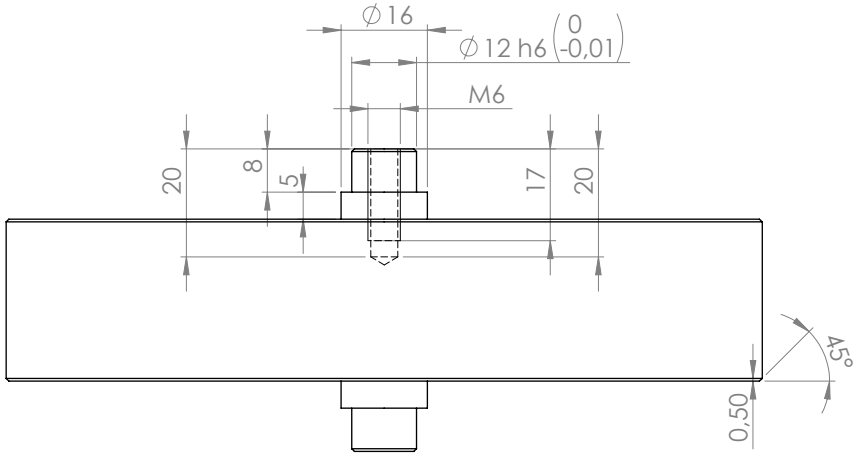

See STEP file: 12-004-Rotor - Disc.STEP

UNLESS OTHERWISE SPECIFIED: DIMENSIONS ARE IN MILLIMETERS GENERAL TOLERANCES: ISO 2768 MK	FINISH:		DEBURR AND BREAK SHARP EDGES			DO NOT SCALE DRAWING	REVISION
	NAME	SIGNATURE	DATE			TITLE: FESS Prototype	
DRAWN	Stefan Lorist						
CHK'D							
APPV'D							
MFG							
Q.A				MATERIAL: SJ235		DWG NO. 12-004-Rotor - Disc	A3
				WEIGHT:		SCALE:1:2	SHEET 1 OF 1

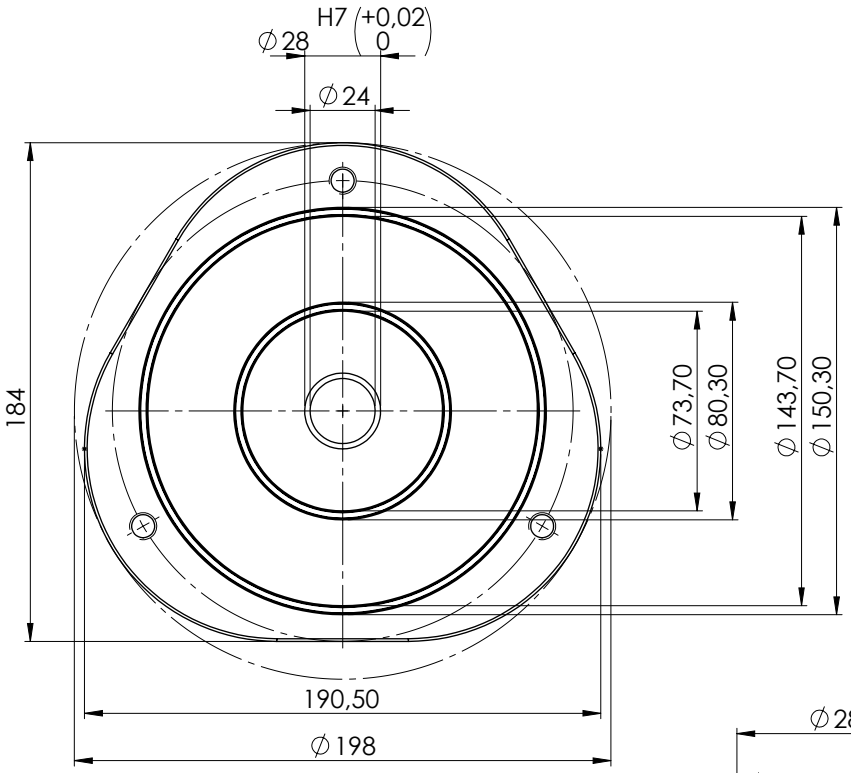

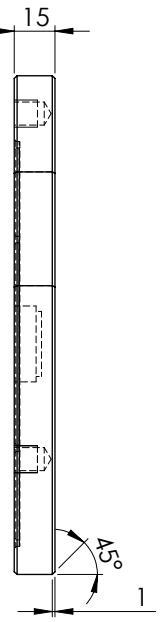

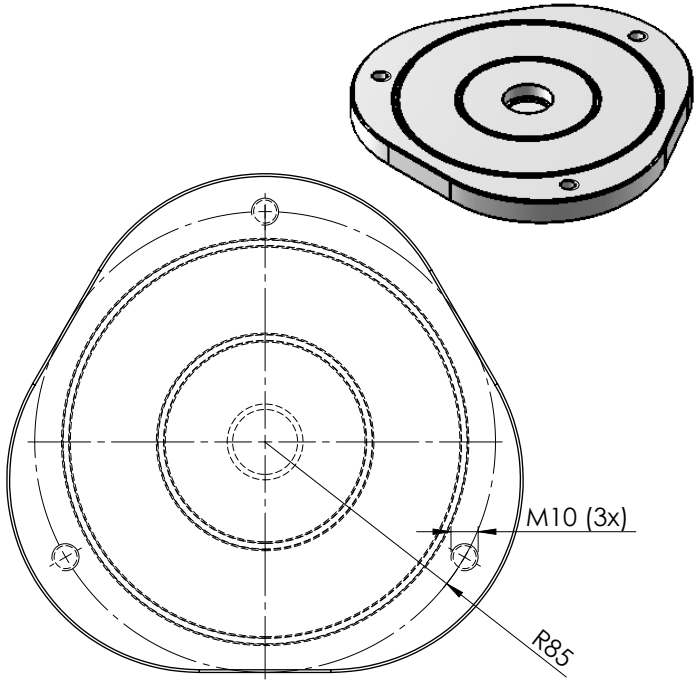

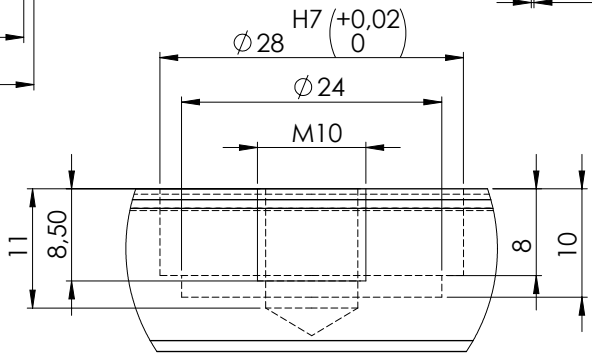

DETAIL C
SCALE 2 : 1

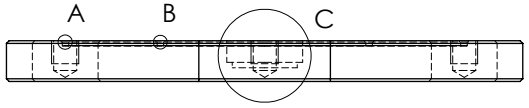

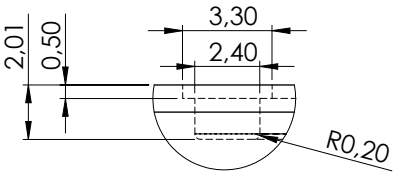

DETAIL A
SCALE 5 : 1

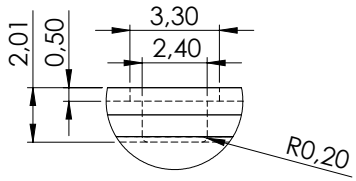

DETAIL B
SCALE 5 : 1

See STEP file: 12-001-Bottom Plate - 200mm rod.STEP

UNLESS OTHERWISE SPECIFIED: DIMENSIONS ARE IN MILLIMETERS GENERAL TOLERANCES: ISO 2768 MK	FINISH:			DEBURR AND BREAK SHARP EDGES	DO NOT SCALE DRAWING		REVISION
	NAME	SIGNATURE	DATE		TITLE: FESS Prototype		
DRAWN	Stefan Lorist						
CHK'D							
APPV'D							
MFG							
Q.A							
				MATERIAL: ACP5080 Toolingplate	DWG NO. 12-001-Bottom Plate - 200mm rod		A3
				WEIGHT:	SCALE:1:2	SHEET 1 OF 1	

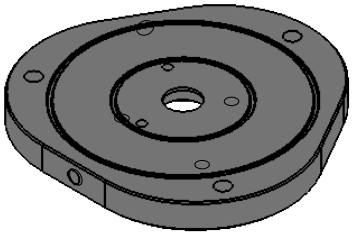

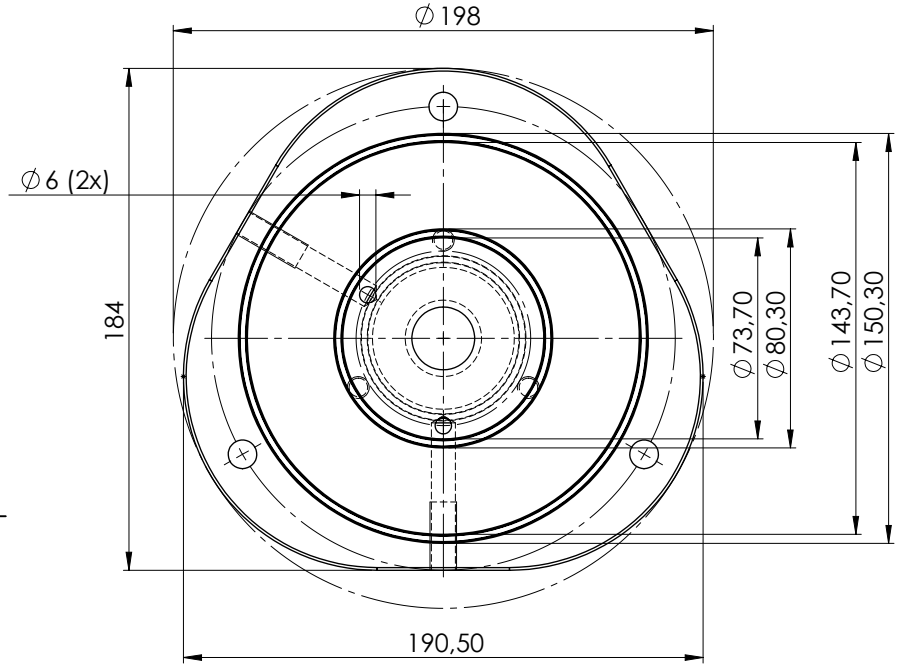

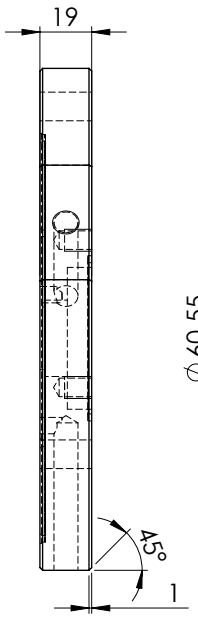

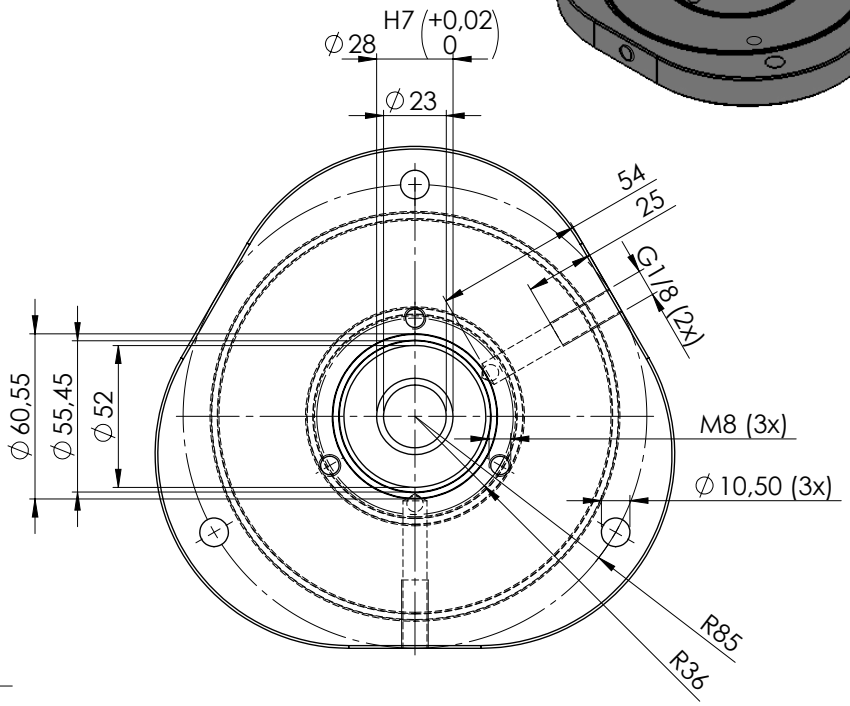

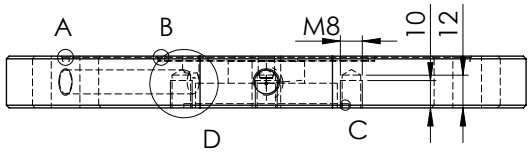

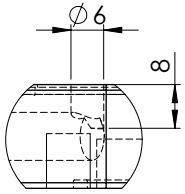

DETAIL D
SCALE 1 : 1

See STEP file: 12-002-Top Plate - 200mm rod.STEP

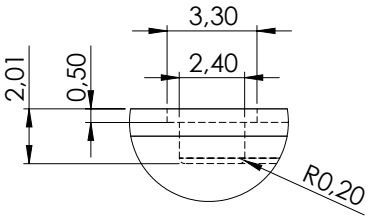

DETAIL A
SCALE 5 : 1

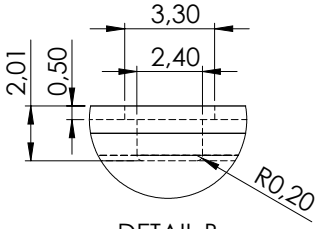

DETAIL B
SCALE 5 : 1

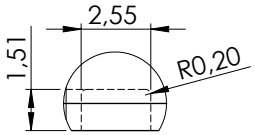

DETAIL C
SCALE 5 : 1

UNLESS OTHERWISE SPECIFIED: DIMENSIONS ARE IN MILLIMETERS GENERAL TOLERANCES: ISO 2768 MK	FINISH:				DEBURR AND BREAK SHARP EDGES	DO NOT SCALE DRAWING / REVISION
	NAME	SIGNATURE	DATE			TITLE: FESS Prototype
DRAWN	Stefan Lorist					
CHK'D						
APPV'D						
MFG						
Q.A				MATERIAL: ACP5080 Toolingplate		DWG NO. 12-002-Top Plate - 200mm rod / A3
				WEIGHT:		SCALE:1:2 / SHEET 1 OF 1

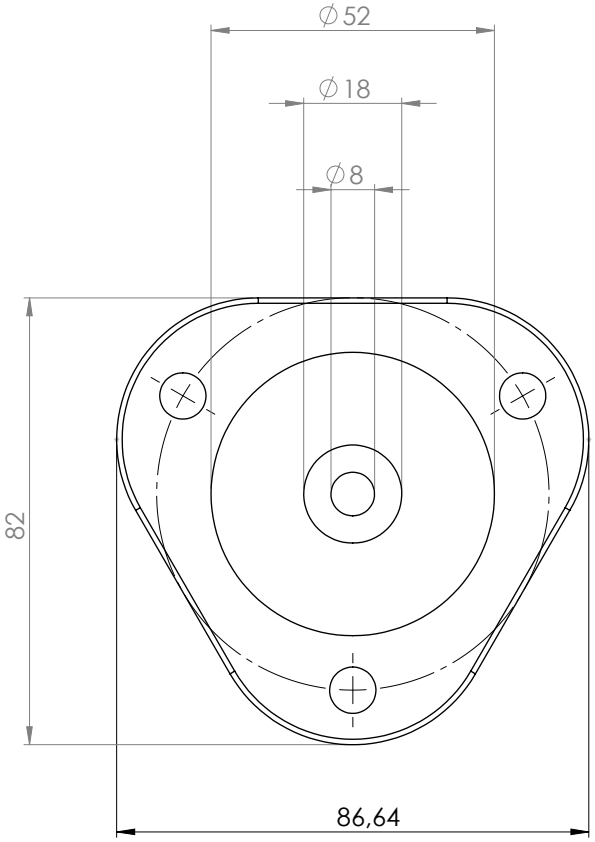

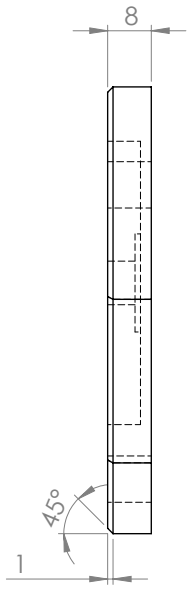

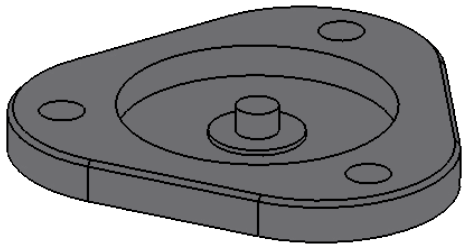

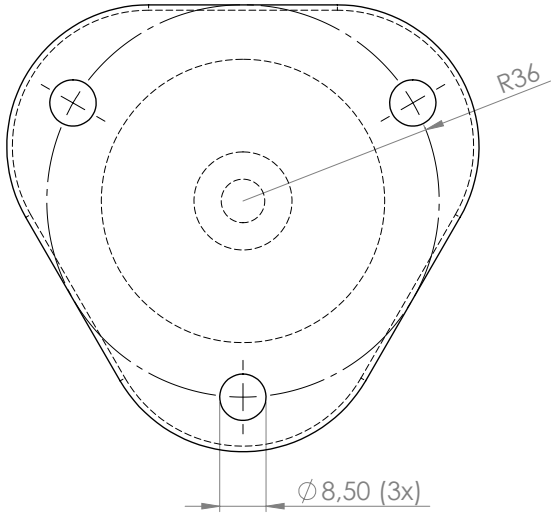

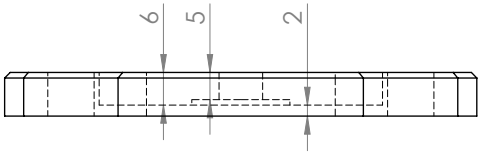

See STEP file: 12-003-Seal Plate - milled.STEP

UNLESS OTHERWISE SPECIFIED: DIMENSIONS ARE IN MILLIMETERS GENERAL TOLERANCES: ISO 2768 MK		FINISH:		DEBURR AND BREAK SHARP EDGES			DO NOT SCALE DRAWING	REVISION
	NAME	SIGNATURE	DATE				TITLE: FESS Prototype	
DRAWN	Stefan Lorist							
CHK'D								
APPV'D								
MFG								
Q.A				MATERIAL: ACP5080 Toolingplate			DWG NO. 12-003-Seal plate - milled	A3
				WEIGHT:			SCALE:1:1	SHEET 1 OF 1

Appendix F.

Cover Design Sketches

On these pages, sketches of the cover design are displayed. Some of these were made during individual sketching sessions, others during a creative session that was held with Robert and Niels from Amstel Engineering. The bottom half of the sketches on the right hand page is made by them.

Rotate motor 90°?
125

Appendix G.

Cost Price Calculation

Introduction

Whether LEFt is an interesting alternative for excess electricity storage is mainly determined by its functionality. However, people will only install it in their houses when the market price is acceptable.
A cost price calculation, based on the bill of materials (BoM) and manufacturing costs was done, from which a retail price followed.

Estimation method

A handy spreadsheet (Thomassen, 2013)[126] which was based on the methods by Kals et al. (2007)[127] , was used to estimate the cost price of the various custom parts in LEFt.

Parts structure

To keep manufacturing costs to a minimum, LEFt was designed with as many standard shelf parts as possible. However, the unique way of suspending the rotor and operation in a vacuum requires custom parts to be made. The bill of materials, with all essential parts and their cost estimation is included in Appendix H.

Custom parts

The core part of LEFt is the steel flywheel rotor, storing the energy.

Suspending the flywheel rotor is unique to the application, and cannot be realized with bearings that are commercially available. Therefore, a set of custom bearings should be developed. The principle parts were included in the cost analysis, with an estimation of the costs for the required engineering.
The magnet coupler that ensures frictionless coupling and decoupling from outside the vacuum, needs to be actively controlled. Therefore, a control system needs to be designed. Included in the cost price of this part are estimated material costs and engineering costs.

Production quantity

The version of LEFt that was analyzed is the Slender type. Households with an average consumer profile are most likely to have recommended a storage system of this type. It is therefore the type that will be produced in the largest quantities.
Based on the number of households in the Netherlands that have a set of solar panels installed and an estimation of the likeliness to be interested in a flywheel energy storage system, the production quantity is set to 10,000 products.
According to the Central bureau of Statistics (CBS, 2019)[128], in 2017 over half a million households had solar panels installed. Considering a continuing increase of this number, and a (pessimistic) percentage of interested households of 5%; 25,000 households, was estimated. Of this number, around half of the customers will be buying the Slender version of LEFt, this lead to the number 10,000 that was used for the calculation.

Rotor costs

As can be seen from the pie charts in Figure 84, manufacturing the system's rotor is responsible for a significant amount of the costs.
To make sure the estimation is realistic, two different methods for calculating the rotor costs are used. The first method was a cast steel calculator provided by the Chinese website Iron-Foundry.com (Liaoning Borui, 2019)[129]. This utility allows definition of the castable product into little detail. The material composition, weight, machining and surface finish can be set, as well as an order quantity. Setting the weight at 2000 kg (obtained from the CAD-drawn part) results in a price of €7,660 per rotor.
Using the calculation method provided by Kals et al., the same weight of steel and additional machining costs results in a much lower price of €1,940 per rotor.
Since it cannot be said with confidence that one

LEFt - Slender
Solid rotor - Iron Foundry

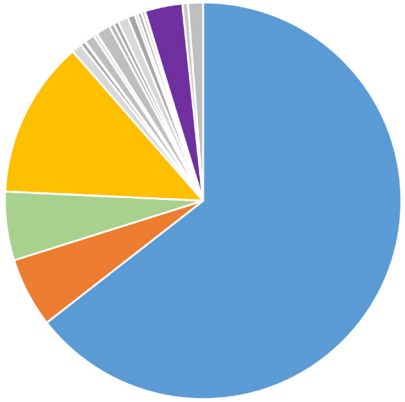

Unit cost price: €11,910.-

Rotor:	**€7,660.-**	**64%**
Top plate:	€ 660,-	6%
Bottom plate:	€ 670,-	6%
Vacuum enclosure:	€1,510,-	13%
Permanent magnets:	€ 360,-	3%

LEFt - Slender
Solid rotor - Kals

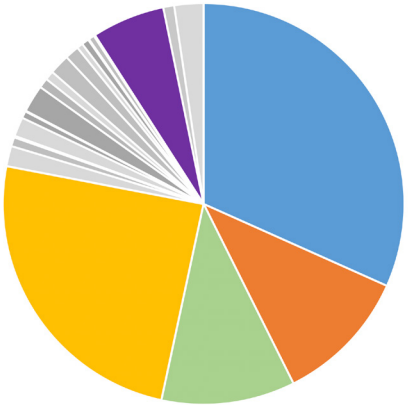

Unit cost price: €6,250.-

Rotor:	**€1,940.-**	**31%**
Top plate:	€ 660,-	11%
Bottom plate:	€ 670,-	11%
Vacuum enclosure:	€1,510,-	24%
Permanent magnets:	€ 360,-	6%

LEFt - Slender
Hollow rotor - Kals

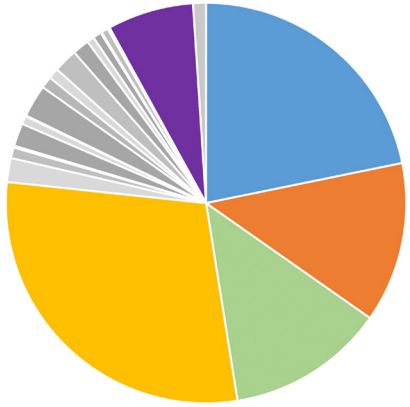

Unit cost price: €5,300.-

Rotor:	**€1,130.-**	**21%**
Top plate:	€ 660,-	13%
Bottom plate:	€ 670,-	12%
Vacuum enclosure:	€1,510,-	29%
Permanent magnets:	€ 360,-	7%

Figure 84: Cost price breakdown of LEFt using different methods, highlighting the most influential parts

calculation is more accurate than the other, the retail price will be calculated for the worst-case scenario, where the rotor costs are maximized.

Retail price

An estimation of the consumer price of LEFt-Slender is made by simply multiplying the cost price with a factor 2. This is in line with the estimation method that is normally used at Amstel Engineering BV.
In the worst-case scenario, this comes down to €23,820. With an estimated product lifetime of 20 years, the annual costs are €1,191.

Comparison

Comparing to Tesla's Powerwall is useful to get an indication of the market positioning when price is considered. Please note that the functionality of this product is not exactly equal to that of LEFt since it is able to store more energy for a longer period. The Powerwall has a warranty period of 10 years and a retail price of €8.240, which results in annual costs of €824.

Price reduction

When calculating the rotor's cost price with Kals's method, it becomes clear that still 31% of the product's cost price (€6.250 from this calculation) is caused by this part. Reducing the costs can be done most effectively by reducing the amount of material used for the rotor. One of the alternative rotor designs that was proposed in chapter 2.1 is the hollow rotor type, or ring-shaped rotor. According to the FlywheelCalc-script, this rotor type is applicable and results in a mass reduction of 1000 kg. Considering this, the rotor's manufacturing costs are reduced to €1,130, bringing the total cost price down to €5,300. and the retail price to €10,600. Spread over 20 years, this results in an annual price of €530.

Conclusion

The best-case scenario for cost price calculation shows an annual consumer price of €530, which is slightly lower than the Powerwall at €824 per year.
However, this comparison relies on the product functionality to be equal, wich is not exactly true. The Powerwall is still capable of storing a higher percentage of the excess power, potentially making it more cost-effective for the user.

Appendix H.

Bill of Materials

Introduction

As mentioned in chapter 4.2, the cost price is calculated using three different approaches.
On the right hand page, the Bill of Materials for the Slender model of LEFt, with a hollow rotor is displayed.

Costs of the parts are calculated according to Kals et al. (2013). In the screen shot below, the spreadsheet used for estimation of the hollow rotor's cost price is displayed.

Opbouw van de fabricagekostprijs van een compleet product (vgl. Kals opgave 15.3)

Benaming	**Rotor (Slender, hol)**		**Productieserie**	**10.000**	**stuks**	**per onderdeel**
Materiaalkosten		**bruto hoeveelheid/product**	**eenheid**	**prijs/eenheid**	**bedrag**	
halffabrikaat	Gietstaal	1000	kg	€ 0,70	€ 700,00	
				totaal materiaalkosten	**€ 700,00**	**€ 700,00**
Bewerkingskosten	**capaciteit [stuks/u]**	**machineuren**	**machine-uurtarief**	**machine-kosten**		
Gieten	1	10000,00	€ 43,33	€ 433.300,00		
CNC frees	0,5	20000,00	€ 80,00	€ 1.600.000,00		
etc.	1000	10,00	€ 0,00	€ 0,00		
nabewerking	1000	10,00	€ 0,00	€ 0,00		
				totaal machinekosten	**€ 2.033.300,00**	
machines als bovenstaand	**mens/machine-bezetting**	**arbeidsuren**	**mensuurtarief**	**arbeidskosten**		
Gieten	1	10.000,00	€ 18,00	€ 180.000,00		
CNC frees	1	20.000,00	€ 24,00	€ 480.000,00		
etc.	1	10,00	€ 0,00	€ 0,00		
nabewerking	1	10,00	€ 0,00	€ 0,00		
				totaal arbeidskosten	**€ 660.000,00**	
				totaal bewerkingskosten	**€ 2.693.300,00**	**€ 269,33**
Instelkosten serie	**insteltijd [u]**	**uurtarief insteller**	**mach.uurtarief**	**kosten**	**per product**	
Gieten	10	€ 24,00	€ 43,33	€ 673,30	**€ 0,07**	**€ 0,07**
Gereedschapskosten	**aanschafprijs**	**standtijd [stuks]**	**restwaarde**	**prijs/eenheid**		
matrijs A	€ 30.000	10.000	€ 0,00	€ 3,00		
montagemal B		25.000	€ 0,00	€ 0,00		
subtotalen	€ 30.000		€ 0,00			
gemiddelde waarde	€ 15.000					
kapitaalrente	0,0%	rentekosten	€ 0,00	€ 0,00		
				totaal gereedschapskosten	**€ 3,00**	**€ 3,00**
Algemene toeslagen						
uitval-factor*	1,0%	*afgekeurde producten, zie Kals voor percentages			**subtotaal**	**€ 972,40**
overheadfactor**	15,0%	** algemene toeslag voor productiefaciliteiten				
totaal	**16,0%**					**€ 155,58**
		K_{Fi} voor interne calculatie:		**Productiekostprijs Rotor (Slender, hol)**		**€ 1.127,98**

LEFt
Leftover Energy Flywheel technology
by Amstel Engineering

Bill of Materials (based on slender model)

No.	Description	Supplier	Production method	Material	Dimensions	Weight (kg)	Quantity	Unit Price (ex. BTW)	Parts total	% of total
	Custom parts									
1	Rotor		Cast/Lathe	Steel	0.90 x 0.60 m (hxd)	1000	1	€ 1.128,000	€ 1.128,00	21%
2	Bottom plate		CNC Milling	Steel	0.05 x 1.0 m (hxd)	105	1	€ 670,000	€ 670,00	13%
3	Top plate		CNC Milling	Steel	0.05 x 1.0 m (hxd)	100	1	€ 660,000	€ 660,00	12%
4	Vacuum enclosure		CNC Milling	Steel	0.05 x 1.0 m + 0.95 x 0.70 m (hxd)	400	1	€ 1.511,500	€ 1.511,50	29%
5	Magnet coupler		CNC Milling	Aluminium/Neodymium	100 x 200 mm (hxd)	TBD	1	€ 100,000	€ 100,00	2%
6	AMB base		Cast	Steel	30 x 200 mm (hxd)	4,2	2	€ 22,430	€ 44,86	1%
7	Motor bracket		Folding	Steel	5 mm	1,3	1	€ 7,540	€ 7,54	0%
8	Cover bottom 1/3		Vacuum form	Recycled HDPE	1 x 1.05 m (lxb)	9	3	€ 31,770	€ 95,31	2%
9	Cover top		Vacuum form	Recycled HDPE	1.5 x 1.5 m (lxb)	11	1	€ 34,560	€ 34,56	1%
10	Display housing		Injection mold	Recycled HDPE	30 x 500 mm (hxd)	0,05	1	€ 3,870	€ 3,87	0%
	Shelf parts									
11	1-phase 2.1 kW motor	Nord Drivesystems			300 x 200 x 200 mm (lxbxh)		1	€ 135,00	€ 135,00	3%
12	Vacuum pump	TBD			200 x 150 x 150 mm (lxbxh)		1	€ 120,00	€ 120,00	2%
13	AMB coil	TBD		Copper	30 x 30 mm (wound)		12	€ 4,06	€ 48,72	1%
14	Display	TBD		OLED	5 inch diagonal		1	€ 45,00	€ 45,00	1%
15	Control system									
	a. Control box	TBD			250 x 150 x 100 mm (lxbxh)		1	€ 100,00	€ 100,00	2%
	b. Software development	TBD					1	€ 70,00	€ 70,00	1%
	c. Various electronic components	TBD					1	€ 30,00	€ 30,00	1%
16	O-ring	Eriks		NBR	658,88 x 6,99 mm (din x d)		1	€ 35,280	€ 35,28	1%
17	O-ring	Eriks		NBR	202,57 x 6,99 mm (din x d)		1	€ 4,760	€ 4,76	0%
18	Bolt M24	Primex		Stainless steel A2	M24		12	€ 2,380	€ 28,56	1%
19	Nut M24	Primex		Stainless steel A2	M24		12	€ 0,550	€ 6,60	0%
20	Washer M24	Primex		Stainless steel A2	M24		12	€ 0,240	€ 2,88	0%
21	Halbach Array magnet	Supermagnete		Neodymium			12	€ 30,000	€ 360,00	7%
22	Machine foot	TBD		Stainless steel A2	M24		6	€ 9,000	€ 54,00	1%
						Total price (ex. BTW)		€	5.296,44	

Appendix I.

Sustainability Assessment

LEFt - People, Planet, Profit

The primary goal of LEFt is to eliminate the previously described social, political and environmental problems. To determine if this has been achieved, the triple P-model has been used. Via this model, not the direct CO_2-equivalent is calculated, but the potential effects of the design are considered.

To start, the following was defined:

Prime objective

Reducing the amount of wasted renewable energy due to a lack of residential energy storage without introducing sustainability problems.

Articulation

Increasing energy awareness by communicating the equivalent capacity of mechanically stored electricity.

Size of impact

75% of the generated renewable energy within a household that is otherwise wasted can be utilized.

Time scale

Within one year after implementation.

People

Increasing people's energy awareness and motivating to use responsibly.

Planet

Reducing political, social and ecological problems by making use of materials that have low environmental impact.

Profit

Value of residential renewable energy sources is increased because a larger percentage of generated energy can be utilized.

Fact finding

LEFt and the product to which it will be compared, Tesla Powerwall, have the same main functionality: storing an excess of renewable energy within a household. There are two important functional differences; LEFt stores the energy mechanically and adds an increased energy awareness by communicating storage information to the user. The non-functional differences lie in the environmental impact of the two products. A comparison will be made on six aspects: Materials, Energy, Environment, Legislation, Economics and Society. These will be combined into a concluding synthesis for each of the main definitions People, Planet and Profit.

Materials

LEFt does not use any of the high impact materials lithium, graphite and cobalt, of which it is proven that mining causes social, political and environmental problems. (chapter 4.3) However, the large amounts of steel that are used cause high CO_2 emissions during mining and forging.
An Eco Audit in Cambridge Engineering Selector[6] was done to indicate the most impactful materials that are used in the product. More about this in the paragraph Eco Audit on the next page.

Energy

LEFt motivates a more responsible usage of electricity by communicating how much is stored in the system and calculating the equivalent regeneration capacity of easily understandable electricity consuming products (i.e. electric vehicle/watching television). Manufacturing LEFt requires energy, mainly during mining, forging and milling steel.

Environment

Using LEFt increases the feeling of handling renewable energy in a good way. The energy is not wasted but stored for another moment. Additionally, the use

of precious materials that cause social, political and environmental problems is diminished, which is an improvement to the environment.

Legislation

At the end of life, LEFt can be easily disassembled and separate parts can be recycled. Batteries that have to be taken back due to legislations are not present and therefore do not have to be taken back by the producing company.

Economics

The cost price of LEFt is higher than that of Tesla's Powerwall. However, the prospected lifespan is twice as long, which equalizes the annual costs and return of investment time. The goal of both products, which is storing energy, provides the user with the same advantage of not having to pay for electricity that is generated but discarded without using.

Society

LEFt helps increasing the awareness of electricity usage in society, by communicating the stored energy as was mentioned before. By selling the product in large quantities, the overall percentage of renewable energy that is utilized effectively will increase. An overall increase of responsible electricity usage leads to lower losses. Power plants that are dependent on fluctuations of usage will be able to make better estimations and can therefore optimize their electricity generation to be more cost efficient.

Synthesis

When combining the aforementioned aspects of the analysis, the conclusion can be drawn that LEFt has important advantages over the Powerwall to which it was compared. The main advantage lies within the production of the product, where the lack of lithium, graphite and cobalt prevents the increase of social, political and ecological problems that currently occur.
With respect to functionality, it should be noted that LEFt stores a lower amount of energy for a shorter period of time. However, it adds the important functionality of communication to the user and improves the responsible handling of renewable energy.
To summarize, page 130 contains a synthesis matrix.

Stakeholders

The design product is influenced by a number of stakeholders, who in their turn have different interests.

Research institutions

Data produced by for instance KNMI and energy suppliers is used for calculations and therefore directly influences the design of the product.

Government

The fact that net metering will not be continued increases the interest among households with their own renewable energy source in storing their excessive energy.

Energy suppliers

Companies that supply grid power and sell electricity are influential in the design of a residential storage system, since they do not provide a storage possibility. They will not be interested in the product, since it might lower their profit.

Solar panel suppliers

Companies that sell solar panels can increase their product's value by selling a storage system alongside it. This means they will have some interest in the development of the mechanical energy storage system.

Households with renewable energy source

People who already generate their own renewable energy within their household and depend on net metering, to lower their energy bill. This stakeholder influences the design by supplying data of current residential energy generation.

Households without renewable energy source

People who do not have solar panels or another renewable energy source installed, will see the added value of a storage system and have increased interest in installing a combination of the two.

Amstel Engineering BV

The issuing company for the project is highly interested in the potential benefits of a mechanical energy storage system. By steering the development of the product, the company is showing its capabilities when it comes to mechanical design and their motivation to deliver sustainable products.

Synthesis matrix

People, Planet, Profit

LEFt versus Tesla Powerwall, synthesis matrix

	Human Capital - People	Natural Capital - Planet	Manufactured Capital - Profit
Materials	(+) Mining of materials like cobalt, lithium and graphite is not needed and accompanying problems reduced	(+) Both products are depending on rare earth materials, although LEFt uses no Lithium	(-) The large amount of raw materials used to manufacture LEFt limits the profit that can be made
Energy	(+) LEFt motivates responsible use of renewable energy	(-) LEFt does not store all of the available energy and has a limited storage time	(+) LEFt stores renewable energy and increases awareness of electricity usage
Environment	(+) Using LEFt creates a positive feeling with the user, he is not disposing renewable energy	(+) The use of precious materials is decreased	-
Legislation	-	(+) Easier disassembly means easier recycling	(+) Batteries that had to be taken back by the company are not present in LEFt
Economics	(+/-) No differences between both products	-	(+) A higher percentage of renewable energy can be utilized, making renewable sources more valuable
Society	(+) Creates energy usage awareness	(+) A larger percentage of renewable energy is used	(+) An overall increase of responsible electricity usage leads to lower losses
Synthesis	(+) LEFt increases people's energy awareness and motivates to use responsibly	(+/-) Components are made out low impact materials, but also less effective in storing energy	(+) Value of residential renewable energy sources is increased because a larger percentage of generated energy can be utilized.

Eco Audit

In the screen shots on this page, the settings for the Eco Audit in CES Edupack are displayed.

Product information

Name: LEFt (Hollow rotor)

Include cost analysis

Country of manufacture: China

Package dimensions: H: 1,7 m W: 1,2 m D: 1,2 m

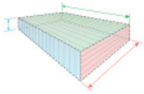

Material, manufacture and end of life

Components

Qty.	Component name	Material	Recycled content	Mass (kg)	Primary process	Length (m)	Secondary process	% removed	End of life	% recovered
1	Rotor	Low alloy steel, SAE 4130...	80,0%	1000	Casting	Not Required	Fine machining	5	Recycle	90
1	Bottom plate	Carbon steel, AISI 1010, a...	50,0%	105	Roll forming	1	Fine machining	10	Recycle	90
1	Top plate	Carbon steel, AISI 1010, a...	50,0%	100	Roll forming	1	Fine machining	10	Recycle	90
1	Vacuum housing	Carbon steel, AISI 1010, a...	50,0%	400	Roll forming	2	Fine machining	10	Recycle	90
1	Cover	PE-HD (general purpo...	100,0%	40	Polymer molding	Not Required	Cutting and trimming	10	Recycle	90
1	Motor	Neodymium magnet...	Virgin (0%)	10	Forging	Not Required	Fine machining	10	Recycle	80
1	Vacuum pump	Neodymium magnet...	Virgin (0%)	5	Forging	Not Required	Fine machining	10	Recycle	80
1	Halbach magnet	Neodymium magnet...	Virgin (0%)	40	Forging	Not Required	Fine machining	10	Recycle	90
1	Electronics	Integrated circuit (la...	Virgin (0%)	10	Incl. in material value	Not Required		0	Downcycle	80

Joining and finishing

Name	Process	Amount	Unit
Final assembly	Fasteners, small	40	
Vacuum housing assembly	Welding, gas	6,5	m
		0	

The specifications for LEFt with a hollow rotor are displayed in this screen shot. The version of LEft with a solid rotor was analyzed by similar settings, the only difference being the rotor weight which is double the weight at 2000 kg.

Product information

Name: Tesla Powerwall

Include cost analysis

Country of manufacture: China

Package dimensions: H: 1,4 m W: 1 m D: 0,4 m

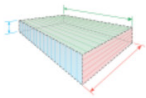

Material, manufacture and end of life

Components

Qty.	Component name	Material	Recycled content	Mass (kg)	Primary process	Length (m)	Secondary process	% removed	End of life	% recovered
1	Battery	Li-Ion battery (for s...	Virgin (0%)	100	Incl. in material value	Not Required		0	Reuse	30
1	Case	PE-HD (general purpo...	50,0%	20	Polymer molding	Not Required	Cutting and trimming	10	Recycle	100
1	Electronics	Integrated circuit (la...	Virgin (0%)	10	Incl. in material value	Not Required		0	Downcycle	80

Joining and finishing

Name	Process	Amount	Unit
Assembly	Fasteners, small	20	

The environmental impact of the Tesla Powerwall is estimated to be mainly dependent on the battery itself. In CES Edupack, a Li-ion battery can be picked and scaled by its weight. According to the total weight of a Powerwall, which is given in the specifications, the weight of the battery itself was estimated at 100 kg.

Amstel Engineering

TU Delft

Stefan Henrico Lorist
stefanlorist@gmail.com
+31 6 83350531